

Loughborough University Institutional Repository

In-line technology for assessment of pulmonary drug delivery

This item was submitted to Loughborough University's Institutional Repository by the/an author.

Additional Information:


- A Doctoral Thesis. Submitted in partial fulfilment of the requirements for the award of Doctor of Philosophy of Loughborough University.

Metadata Record: <https://dspace.lboro.ac.uk/2134/12923>

Publisher: © Olga Evgenievna Kusmartseva

Please cite the published version.

This item was submitted to Loughborough University as a PhD thesis by the author and is made available in the Institutional Repository (<https://dspace.lboro.ac.uk/>) under the following Creative Commons Licence conditions.




CC creative commons
COMMONS DEED


Attribution-NonCommercial-NoDerivs 2.5


You are free:

- to copy, distribute, display, and perform the work

Under the following conditions:

 **Attribution.** You must attribute the work in the manner specified by the author or licensor.

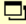
 **Noncommercial.** You may not use this work for commercial purposes.

 **No Derivative Works.** You may not alter, transform, or build upon this work.

- For any reuse or distribution, you must make clear to others the license terms of this work.
- Any of these conditions can be waived if you get permission from the copyright holder.

Your fair use and other rights are in no way affected by the above.

This is a human-readable summary of the [Legal Code \(the full license\)](#).

[Disclaimer](#) 

For the full text of this licence, please go to:
<http://creativecommons.org/licenses/by-nc-nd/2.5/>



University Library

Author/Filing Title KUSMARTSEVA, O

Class Mark T

Please note that fines are charged on ALL
overdue items.

REFERENCE ONLY

0403270405





DEPARTMENT OF ELECTRONIC AND ELECTRICAL ENGINEERING

FACULTY OF ENGINEERING

LOUGHBOROUGH UNIVERSITY

**IN-LINE TECHNOLOGY FOR ASSESSMENT OF
PULMONARY DRUG DELIVERY**

BY

OLGA EVGENIEVNA KUSMARTSEVA

A doctoral Thesis

Submitted in partial fulfilment of the requirements for the award of

Doctor of Philosophy of Loughborough University


December 2005

Supervisor: Professor Peter R. Smith

Department of Electronic and Electrical Engineering

©Copyright

OLGA EVGENIEVNA KUSMARTSEVA, 2005

 Loughborough University Pilkington Library
Date SEPT 2006
Class T
Acc No. 0403270405

Abstract

The World Health Organisation estimates that 100 million people worldwide suffer from asthma. Chronic obstructive pulmonary disease (COPD) is the fourth leading cause of death worldwide. Pulmonary drug delivery is widely accepted as the first-choice method for the treatment of respiratory diseases by glucocorticosteroids. Delivering these drugs to the lung by inhalation has many advantages in comparison to the same drug delivered orally. These include *rapid onset of action*, *reduced dose* and *minimised side effects* such as adrenal suppression, electrolyte imbalance, muscle weakness and growth retardation in children. Pulmonary drug delivery is also increasingly used for pain-controlling therapies and for administration of medications which are *difficult to formulate orally* such as proteins and peptides.

The advantages of delivering drugs to the lung are undisputed, however, there are practical challenges still remaining to achieve repeatable and accurate dose delivery to the deep lung. An enabling technology for actuation-by-actuation, in-line measurement of pulmonary drug delivery is part of this greater challenge. The aerosol particles can penetrate into the deep lung only if their aerodynamic size is in the narrow range of 0.5 μm to 5 μm . The larger particles contribute to the oropharyngeal deposition diminishing the pulmonary-delivery advantages, and the smaller particles are exhaled. Particles of this size-range agglomerate easily through adhesion/cohesion interactions. Agglomerates have to disperse in the patient's inspiration flow. Therefore, the respirable dose and therapeutic efficacy depend on the drug formulation, the inhalation device, the ambient conditions and also heavily rely on the patient's inspiratory effort, which is highly variable. An ability to assess the efficacy of the pulmonary delivery in-line with a patient will ultimately improve the effectiveness and efficiency of medical therapy.

This thesis presents a novel optical technology for non-invasive and in-line measurement of the respirable cloud during pulmonary drug delivery. The technology can be used as a stand-alone instrument, in conjunction with standard

laboratory analytic apparatus and ultimately in-line with a patient. It is shown how the technology concept is based on the Mie theory for light scattering by particles and on the Lambert-Beer law for light extinction by a turbid medium. A prototype device is developed to implement this concept and a series of experimental investigations are conducted to evaluate the feasibility of the approach. Comparisons between the novel in-line technology and conventional *in vitro* measurements using physical chemistry apparatus suggest that the approach can become a useful enabling technology in pulmonary drug delivery assessment.

Acknowledgements

It is a pleasure to acknowledge the continuing and major contribution from my supervisor Professor P.R. Smith. I am grateful for his initial suggestion of this work, his guidance and support throughout the duration of my research. I would also like to thank all the other members of the Optical Engineering Group for their companionship and numerous scientific discussions.

I am very thankful to the technicians and other staff from Loughborough University for their advice and assistance in realisation of this project. Thanks also to Howard Billam for proofreading the manuscript.

Finally I wish to thank the Engineering and Physical Sciences Research Council who have provided financial backing for this project.

CONTENTS

ABSTRACT.....	i
ACKNOWLEDGEMENTS.....	iii
CONTENTS.....	iv
1. Chapter 1 – INTRODUCTION.....	1
1.1. Thesis overview.....	2
1.2. Pulmonary drug delivery.....	4
1.2.1. Physiology of the lung.....	5
1.2.1.a. Lung structure.....	5
1.2.1.b. Lung ventilation.....	7
1.2.2. Pulmonary drug formulations.....	11
1.2.3. Delivery devices.....	12
1.2.3.a. Pressurised metered dose inhalers.....	12
1.2.3.b. Dry powder inhalers.....	13
1.2.3.c. Nebulisers.....	13
1.3. Efficacy evaluation.....	15
1.3.1. Introduction.....	15
1.3.2. <i>In vivo</i> assessments.....	16
1.3.2.a. Gamma (γ)- scintigraphy.....	16
1.3.2.b. Physiological characterisation.....	16
1.3.3. <i>In vitro</i> assessments.....	17
1.3.3.a. Aerodynamic size distribution.....	17
1.3.3.b. Inertial impaction method.....	18
1.3.3.c. Limitations of cascade impactors.....	20
1.3.3.d. Link to humans.....	20
1.3.4. <i>Needs</i> for a fast, non-invasive, patient-related assessment.....	21
1.4. Methods for particle characterisation.....	23
1.4.1. Overview.....	23
1.4.1.a. Equivalent sphere theory.....	23
1.4.1.b. Common methods of size analysis.....	24
1.4.2. Optical methods for in-line measurement.....	25
1.4.2.a. Particle imaging.....	26
1.4.2.b. Laser diffraction.....	27

1.4.2.c. Turbidity measurements.....	29
1.5. Conclusions.....	31
2. Chapter 2 – The MODEL.....	33
2.1. Model description.....	34
2.1.1. Aims of the model.....	34
2.1.2. Applicability.....	34
2.2. Particle distribution in a moving cloud.....	36
2.2.1. Spatial distribution.....	37
2.2.2. Interpretation of the temporal and spatial variation.....	38
2.3. Theory of light extinction.....	39
2.3.1. Lambert-Beer law.....	39
2.3.2. Mie theory method.....	40
2.3.2.a. Mie coefficients.....	41
2.3.2.b. Extinction coefficient.....	42
2.4. Light extinction by a cloud of particle.....	44
2.4.1. Stationary mono-dispersed clouds.....	44
2.4.2. A dynamic cloud containing two species.....	46
2.4.3. Multi-species clouds and NGI measurements.....	48
2.4.3.a. Model equations and further assumptions.....	49
2.4.3.b. Concentration issue.....	51
2.4.3.c. A dynamic cloud and fine particles.....	53
2.5. Summary.....	57
3. Chapter 3 – METHOD for in-line ASSESSMENT.....	59
3.1. Prototype device.....	60
3.1.1. Essential equipment.....	61
3.1.2. Measurement volume.....	61
3.1.3. Sensor position.....	63
3.2. Data Acquisition.....	64
3.2.1. Acquisition frequency.....	65
3.2.2. Attenuation value.....	65
3.2.2.a. A spectral variation of the light obscuration.....	66
3.2.3. Triggering issues.....	67
3.2.3.a. Software control.....	67

3.3. Data Analysis	67
3.3.1. Mathematical fit to an obscuration profile.....	68
3.3.2. Aerosol characterisation.....	70
3.3.2.a. Cloud homogeneity.....	71
3.3.2.b. Fine particle dose.....	71
3.3.2.c. Wall residue.....	72
3.3.2.d. Time related parameters.....	73
3.4. Spectral sensitivity	76
3.4.1. Spectrum of the illuminating beam.....	76
3.4.2. Spectral behaviour of obscuration profiles.....	77
3.5. Summary	81
4. Chapter 4 – EXPERIMENTAL EVALUATION	82
4.1. Turbohaler® dose variation	83
4.1.1. Experimental set.....	83
4.1.2. Inhalation profile.....	84
4.1.3. Results.....	85
4.1.3.a. Issues of the wall residue.....	85
4.1.3.b. Dose variation.....	89
4.1.3.c. Quick check on an inhaler routine.....	91
4.1.4. Conclusions.....	91
4.2. Calibration of VariDose against TSI	92
4.2.1. Experimental set-up.....	92
4.2.2. Results.....	93
4.2.2.a. Fine particle dose.....	94
4.2.2.b. Cloud homogeneity.....	97
4.2.3. Conclusions.....	99
4.3. Comparing in-line optical and NGI measurements	100
4.3.1. Experimental set-up.....	100
4.3.2. Results.....	101
4.3.2.a. NGI data.....	102
4.3.2.b. VariDose data.....	104
4.3.2.c. Comparing the model with the observed obscuration.....	105
4.3.2.d. Value of the FPD.....	107
4.3.3. Conclusions.....	109

4.4. Summary.....	110
5. Chapter 5 – CONCLUSIONS and DISCUSSION.....	112
5.1. Conclusions.....	113
5.2. Suggestions for future research.....	115
5.2.1. Technology modernisation.....	115
5.2.2. Technology applications.....	116
5.2.3. Technology exploration.....	118
REFERENCES.....	120
Appendix – Notation and Glossary.....	127

Chapter 1

Introduction

The recent proliferation in the use of pulmonary drug delivery has been fuelled by the success of biomedical research on inhaled systemic drugs and global concern over the sharp rise in respiratory conditions such as asthma and chronic obstructive pulmonary disease. The advantages of delivering drugs to the lung are well known, however, there are practical challenges still remaining to achieve repeatable and accurate dose delivery to the deep lung. An enabling technology for actuation-by-actuation, in-line measurement of pulmonary drug delivery is part of this greater challenge. In this chapter we consider the complex nature of drug formulations for pulmonary delivery. The physiology of the human lung and standard methods for the efficacy evaluation are briefly introduced. The methods for particle characterisation have been researched to find a simple, in-line, non-invasive method for assessing an inhaler aerosol actuation.

1.1. Thesis overview

Heightened interest in innovative pulmonary drug delivery is fuelled by the emergence of inhaled systemic drugs and global concern over the sharp rise in respiratory conditions such as asthma and chronic obstructive pulmonary disease. The principal factor limiting the accuracy of the pulmonary delivered dose is an indirect assessment of the efficiency of the pulmonary delivery. The lack of an in-line assessment means that an individual actuation cannot be measured and the patient inhalation effort is not taken into account. The aim of this thesis is to explore the possibility of an enabling technology for actuation-by-actuation, in-line measurement of a pulmonary delivery dose.

This first chapter begins by introducing the complexity of pulmonary drug delivery, the standard assessment technologies and includes a discussion about methods for particle characterisation. The chapter concludes by stating the objectives and basic requirements for the possible in-line technology.

In chapter 2 a model is developed that describes an aerosol cloud released by an inhaler and propagating through a cylindrical conduit for the purposes of measuring the optical density of the cloud. Numerical calculations using the Mie theory have examined the optical density 'signatures' for aerosol clouds of different particle distributions. The main principles for the technology are proposed in the chapter summary. The author has previously published some of these principles in the paper:

Smith, P.R., Kusmartseva, O.E., Conway, J., Price, R., Morton, David A.V., Conway, P.P. and Summers, R., "E-Medic: Linking Informatics to a Dry Powder Inhalation System", *Drug Delivery to the Lungs XIV*, The Aerosol Society, DDL14, London, December 2003, pp. 4-7.

Chapter 3 deals with practical issues of the proposed technology. At this early stage of the technology development, the major objective was to prove the concept rather than to optimise the measurement parameters. The chapter describes a prototype measurement device, data acquisition and analytical routine for the characterisation of the efficiency of the pulmonary delivery in-line with a user. For the first time a specific technical arrangement and analytical method have been developed and

tested. The methods described in this chapter are both previously published and filed at the U.K. Patent Office:

O.E. Kusmartseva, A.S. Kattige, R. Prise, P.R. Smith, "In-line assessment of pulmonary drug delivery using light obscuration", *Biosensors and Bioelectronics* **20** (2004), pp. 468-474.

A patent application for "Pulmonary Drug Delivery" was filed on 15th April 2003 and is expected to be granted soon.

Chapter 4 compiles the experimental results supporting the technology concept. For the first time it has been shown that the temporal profile of the light obscuration by an aerosol cloud provides an indicator for the amount of particles, which are regarded as fine particles for the pulmonary delivery and can reach the respiratory zone of the human lung. Strong correlation has been established between the novel and standard ways of assessing the pulmonary delivery efficiency through simultaneous measurements of the drug delivery. Some of these results have also been previously published:

Kusmartseva, O.E., Smith, P.R. and Morton, D.A.V., "Comparing in-line optical and NGI measurements on a drug cloud", *Drug Delivery to the Lungs XV*, The Aerosol Society, DDL15, London, December 2004, pp. 183-186.

Chapter 5 briefly reiterates the major achievements of the work and provides concluding remarks. Recommendations are also made for further studies in this area.

The references are collected in a single section following the main body of the report.

1.2. Pulmonary drug delivery

The potential advantages of delivering a drug to the lung by inhalation have been well known to scientists, physicians and also to drug abusers for many years. For drugs that exert their biological effect in the lung, these advantages include rapid onset of action, reduced dose and minimised side effects in comparison to the same drug delivered orally. Pulmonary drug delivery is widely accepted as the first-choice method for the treatment of obstructive airway diseases such as asthma or chronic obstructive pulmonary disease (COPD) (British Thoracic Society, 2003), because it minimises the problems associated with oral corticosteroids such as adrenal suppression, electrolyte imbalance, muscle weakness and growth retardation in children (Barnes *et al.*, 1993; Geddes, 1992; Lipworth, 1992;). Future applications for pulmonary drug delivery can be in areas of therapeutic peptide/protein drugs (Adji *et al.*, 1997). These drugs are difficult to formulate orally due to either enzymatic instability or non-permeability through the gastrointestinal membrane, and therefore must be injected into the blood stream. The lung's large absorptive area, thin alveolar epithelia and extensive vasculature make it an attractive, non-invasive route for the administration of these systemic drugs.

There are three major patient groups which will benefit from effective pulmonary drug delivery. Namely: 1) asthma patients for symptom-managing therapies; 2) diabetics for a non-invasive insulin treatment and 3) cancer patients and pain-sufferers for pain-controlling therapies.

The therapeutic efficacy of the pulmonary drug delivery is a very complex issue and strongly depends on four major components: 1) the drug itself as an active pharmaceutical ingredient; 2) the drug formulation, which facilitates the drug reaching the targeted part of the respiratory system; 3) the delivery device, which produces an aerosol cloud of the drug formulation and 4) the patient, who is able to use the delivery device correctly. Since pulmonary drug administration is directly related to the human respiratory structure and function and to the approaches of drug formulation being introduced into the lung, any discussion requires a thorough understanding of these fundamentals.

1.2.1. Physiology of the lung

1.2.1.a. Lung structure

The human respiratory system is a complicated organ system of close structure-function relationships. To fully understand the impact of respiratory structure and function on drug delivery, some aspects of the anatomical structure and functional physiology of the respiratory system are set out below.

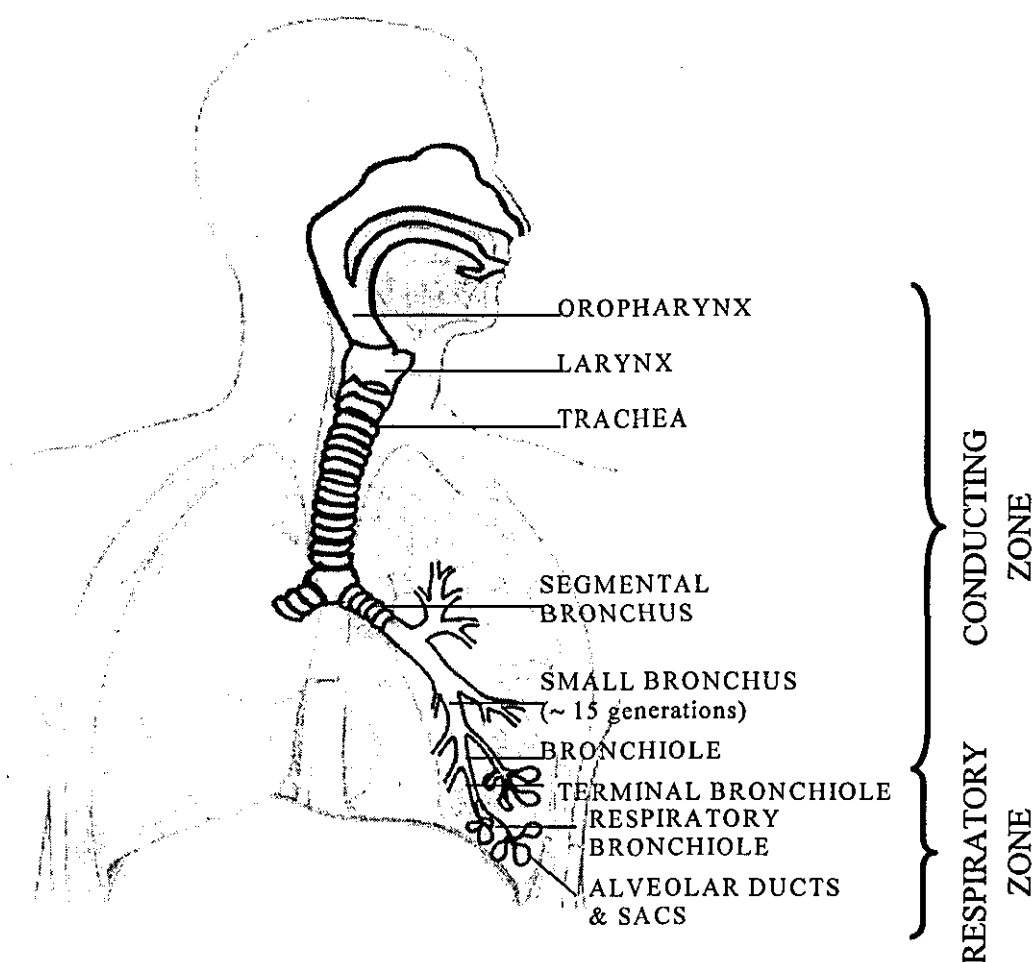


Figure 1.1. Graphical illustration of the human respiratory tract.

The respiratory system (Figure 1.1) is functionally composed of two major regions: the conducting airway and the respiratory region. The conducting airway is composed of the nasal cavity and associated sinuses, mouth, oropharynx, larynx, trachea, bronchi, and bronchioles, including the first 16 generations of airways of

Weibel's tracheobronchial tree (Weibel, 1963). These structures are incapable of performing gas exchange with the venous blood, but are lined with a viscoelastic, gel-like mucus layer (Sanderson, *et al.*, 1981). This protective mucus blanket entraps and removes the inhaled particles from the airway. Before reaching the respiratory region, the true area of gas-exchange, the inspired air is filtered, heated to body temperature and humidified as it passes through the conducting airway. The respiratory region is composed of respiratory bronchioles, alveolar ducts, and alveolar sacs, including generations 17 to 23 of Weibel's tracheobronchial tree. The main function of the respiratory region is to facilitate the rapid gas exchange between the inhaled air and the blood stream.

Table 1.1. Structural characteristics of the human respiratory system.

		N ^a	n ^b	D ^c , [mm]
Conducting zone	Trachea	0	1	18
	Main bronchi	1	2	13
	Lobar bronchi	2 - 3	4 - 8	7 - 5
	Segmental bronchi	4	16	4
	Small bronchi	5 - 11	32 - 2,000	3 - 1
	Bronchioles	12 - 16	4,000-65,000	1 - 0.5
Respiratory zone	Respiratory bronchioles	17 - 19	130,000-500,000	0.5
	Alveolar ducts	20 - 22	1,000,000-4,000,000	0.3
	Alveolar sacs	23	8,000,000	0.3

^{a)} N is the generation of Weibel's tracheobronchial tree; ^{b)} n is the number of structures; ^{c)} D is the diameter of the structures (Weibel, 1963).

The mean diameter of the adult human trachea is about 1.8 cm (Table 1.1). As it branches progressively, its diameter decreases to 1 mm at the 11th generation, corresponding to a dramatic increase in total cross-sectional area (Weibel, 1963). The calibre of following generations of airways is a function of the lung volume, since the forces holding their lumina open are stronger at higher lung volumes. After

the 11th generation, the number of bronchioles increases far more rapidly than the calibre diminishes (Table 1.1). Branching into the respiratory region, airway diameter does not change significantly, however, the enormous increase in the number of alveolar ducts results in an exponential increase in total cross-sectional area and, therefore, a significant decrease in the velocity of airflow. The total surface area of the lung is about 80 square meters, equivalent to the size of a tennis court. Only about 10% of the lung is occupied by solid tissue, whereas the remainder is filled with air and blood. Two circulation processes occur in the lung: the air circulation or ventilation and the blood circulation for perfusion. Pulmonary circulation carries almost the same blood flow, approximately 5 litres per minute, as the whole systemic circulation.

The lung structure makes it a very effective organ for administering a substance into the blood stream since, as soon as this substance can be delivered to the respiratory zone of the lung, it is able to penetrate the air-blood dividing membrane.

1.2.1.b. Lung ventilation

The air circulation is accomplished by a well-coordinated interaction of the lung with the central nervous system, the diaphragm and chest wall musculature. The respiratory cycle consist of an inspiration followed by expiration. It can be presented as a breathing profile describing the flow rate entering the oropharynx as a function of time. The airflow interacts with particles suspended in it, therefore the flow rate defines the speed of the particles in the contacting zone of the lung and hence the entrainment process of the drug formulation. As the air enters into the branching structure of the lung, the flow rate decreases due to the progressive increase of the total cross-section of the airways. The viscosity forces of the particle-air interaction slow particles down, while the particle inertia causes particle impaction on the airway walls. There is a fine balance between the particle size and the flow rate that allows the particle to follow the air stream into the deep lung.

In principle, by controlling the efforts applied to the musculature, humans can produce a variety of inspiratory flows, although the variety is rather limited due to the human physiology. Eventually everyone can be trained to be able to produce a reasonably chosen breathing profile. For example, in leaflets of so-called pressurised

metered dose inhalers (p-MDIs), commonly used in the asthma managing therapies, patients are required to produce a slow long inhalation followed by holding the breath for several seconds before breathing out slowly. Such breathing enhances the penetration of the drug into the deep lung and, therefore, facilitates the effective relief of the acute asthma symptoms. Unfortunately, under asthma attacks patients may lose some muscle control, and as a result of this they fail to produce the required breathing effort and thus fail to receive the required dose of drug, when they most need it. The breathing profile influences the efficacy of the pulmonary drug delivery and is one of the major parameters for engineering purposes of designing a successful pulmonary drug therapy. Figure 1.2 presents a few typical inhalation profiles produced by humans in comparison to the vacuum mode of the breathing machine.

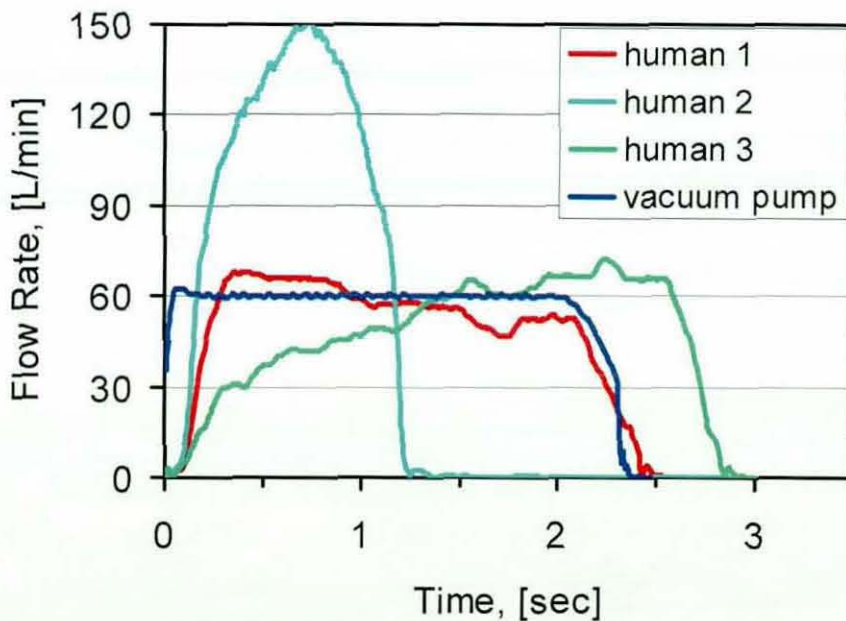


Figure 1.2. Variety of inspiratory profiles.

Alternatively, physicians discuss an airflow in and out of the lungs as a function of the pressure gradient between the alveoli and the atmosphere, with the pressure gradient changing through alterations in the dimensions of the thoracic cavity and subsequently of the lungs (Sherwood L., 2001). The flow rate F through airways depends not only on the pressure gradient ΔP but also on the airway resistance to

the flow R with $F = \frac{\Delta P}{R}$. The primary determinant of resistance to airflow is the radius of the conducting airways. In a healthy respiratory system, the radius of the conducting system is sufficiently large that resistance remains extremely low. It needs only very small pressure gradients of 1 to 2 mm Hg to achieve adequate rates of airflow in and out of the lungs. Resistance becomes an extremely important impediment to airflow when airway lumens become abnormally narrowed as a result of disease. When airway resistance increases, a larger pressure gradient must be established to maintain even a normal airflow rate through increased respiratory muscle exertion. Accordingly, patients with COPD and asthma have to work harder to breathe. Due to the specifics of the lung physiology, the airway resistance during an inspiration is lower than during the expiration. In a normal individual, the airway resistance is always so low that the slight variation occurring between inspiration and expiration is not noticeable, but with an increase of the airway resistance the difference between inspiration and expiration becomes quite noticeable.

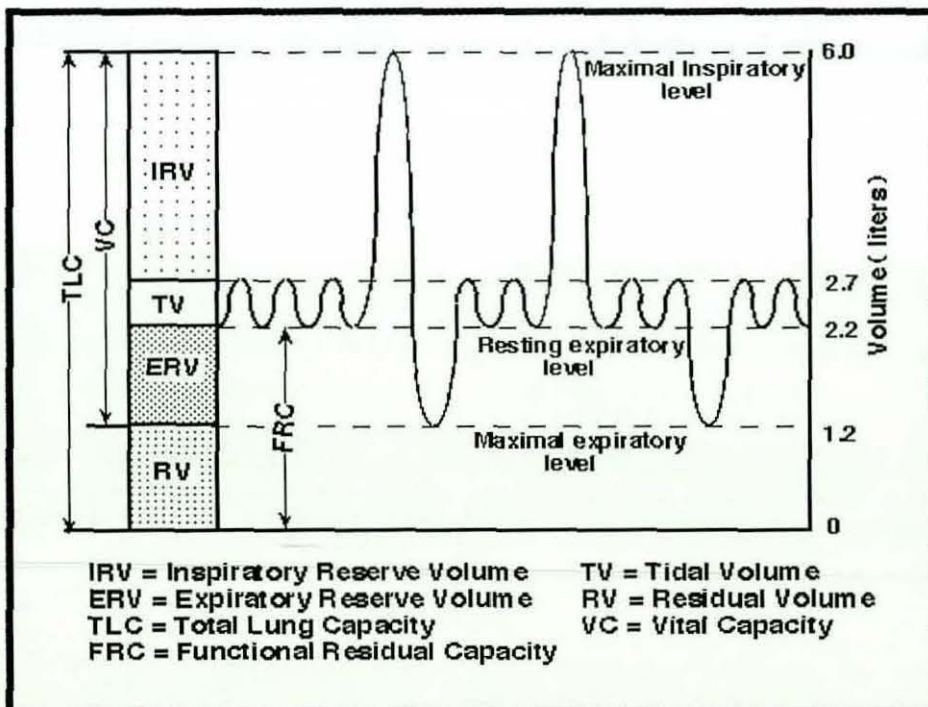


Figure 1.3. Standard (static) lung volumes as measured with a spirometer.

The changes in lung volume that occur with different respiratory efforts can be measured using a spirometer device. Figure 1.3 shows a hypothetical example of a

spirogram in a healthy young adult male. A number of different lung volumes and lung capacities (a lung capacity is the sum of two or more lung volumes) can be determined from the spirogram and are presented in Table 1.2. Measurement of the lungs' various volumes and capacities is of more than academic interest, because such determinations provide a useful tool to the diagnostician in various respiratory disease states. This method is also adopted by physicians and allows an *in-vivo* evaluation of the effectiveness of the pulmonary drug delivery in asthmatic patients. For example, measuring FEV₁ before and after the drug intake gives an indication of the change of the maximal airflow rate that is possible from the lungs. Thus, the effect of the drug onset on the airway resistance can be measured, and therefore, the efficacy of pulmonary delivery can be established.

Table 1.2. Lung Volume Definitions.

Lung Volumes	Definition
Tidal volume (TV)	The volume of air entering or leaving the lung at each breath
Inspiratory reserve volume (IRV)	The volume of air maximally inspired after a normal tidal inspiration
Expiratory reserve volume (ERV)	The volume of air maximally expired after a normal tidal expiration
Residual volume (RV)	The volume of air left in the lung after maximal forced expiration
Functional residual capacity (FRC)	The volume of air remaining in the lung at the end of normal tidal expiration (FRC=ERV+RV)
Inspiratory capacity (IC)	The volume of air maximally inspired after a normal tidal expiration (IC=IRV+TV)
Vital capacity (VC)	The volume of air maximally expired after a maximal forced inspiration (VC=IRV+TV+ERV)
Total lung capacity (TLC)	The volume of air in the lung after a maximal inspiratory effort (TLC=VC+RV)
Forced expiratory volume in one second (FEV ₁)	The volume of air that can be expired during the first second of expiration after a maximal forced inspiration.

1.2.2. Pulmonary drug formulations

Pulmonary drug formulations are intended for lung deposition and are usually prepared in the form of a powder or a liquid solution. With the help of a delivery device the formulation is dispersed as an aerosol that propagates through the respiratory system aiming to deposit the majority of the drug into the respiratory zone of the lungs. The principal mechanisms contributing to lung deposition are inertial impaction, sedimentation and diffusion (Heyder *et al.*, 1986). The aerodynamic diameter (d_a) of an aerosol particle defines the inertial impaction and sedimentation, while the geometric diameter (d_g) controls diffusion. Most authors agree that only particles in the aerodynamic range of 0.5 μm to 5 μm contribute to the deep lung deposition (e.g. Vidgren, 1994). The larger particles are absorbed in the upper parts of the respiratory system mostly due to the inertial impaction on walls. The smaller particles are usually exhaled. The other specific parameter of the pulmonary formulation is the particle flowability. Particles of geometric diameters in the range of 0.5 μm to 5 μm are very cohesive and usually aggregate in clusters. These clusters have reasonable flowability, but if they have failed to de-agglomerate in the airflow they will impact onto the oropharynx and do not contribute to the lung deposition. The liquid formulations must be sprayed. Droplet sizes are defined not only by the spraying mechanism, but also by the ambient conditions such as air temperature, humidity and flow rate, which control the evaporation process during the aerosol propagation and thus the final sizes of the droplets.

The pharmaceutical industry makes enormous efforts to develop drug formulations, which have to provide a good lung deposition of the medication. Here are a few major types of existing pulmonary formulations: 1) drug solutions or drug suspensions, dispersed by a suitable jet-device into a cloud of fine droplets; 2) dry powders of micro-fine drug particles, so-called drug-only formulations; 3) dry-powder mixtures of carrier particles (larger particles with a good flowability) and micro-fine drug particles, which make adhesive bonds with the carrier particles and easily separate from them in the airflow; 4) porous particles with relatively large geometric diameters ($>5\mu\text{m}$) and low mass densities, yielding the aerodynamic diameters that are optimal for the lung deposition.

1.2.3. Delivery devices

Delivery devices are developed to disperse drug formulations in the form of an aerosol. Delivery devices must fulfil numerous requirements concerning operation principles and patients' preferences. The most popular and mainly prescribed by doctors are hand-held devices: either pressurised metered dose inhalers (p-MDIs) or dry powder inhalers (DPIs). Although both types of inhalers have been extensively investigated (the most recent publications: Meakin *et al.*, 1995; Hindle *et al.*, 1995; Kamin *et al.*, 2002) and many efforts have been made to improve their performance, some problems are still associated with their use (Bisgaard *et al.*, 1998; Feddah *et al.*, 2000).

1.2.3.a. Pressurised metered dose inhalers

In the traditional p-MDI (Figure 1.4), fine powder particles are dispersed in hydrofluoroalkane (HFA) propellants, or the drug is dissolved with the aid of a co-solvent, and then sealed under high pressure in an aluminium canister. Surfactants may be added to prevent agglomeration of the particles. Pressing the canister down into the actuation seating allows the valve to release a metered volume of the contents from the metering chamber; the droplets emerge into the air at high speed and, until the propellants have evaporated, are generally quite large ($40\ \mu\text{m}$) (Pedersen, 1995).

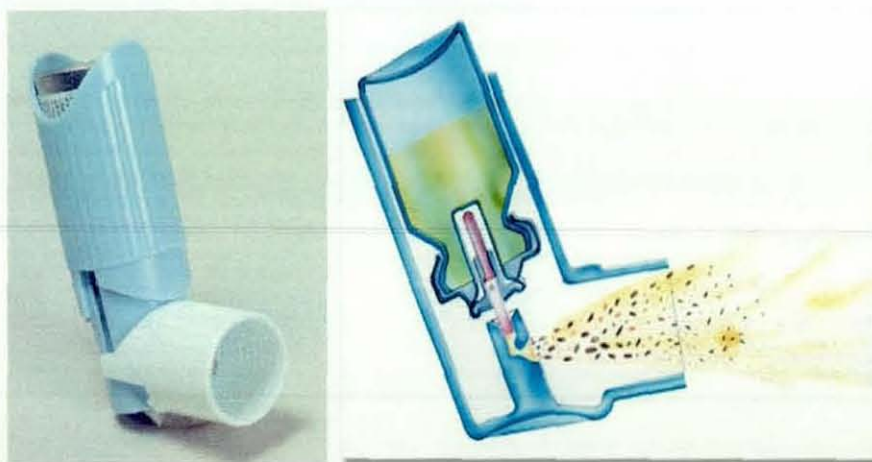


Figure 1.4. A typical pressurised metered dose inhaler (MDI).

When using MDIs, a correct inhalation technique is necessary. The optimal lung deposition is enhanced by a slow deep inhalation followed by holding the breath for several seconds before breathing out slowly (Pauwels *et al.*, 1997). In addition, the MDI inhalation routine requires shaking the device to ensure even distribution of the drug, breathing out before placing the lips around the mouthpiece, and coordinating the device-actuation with the start of the slow inhalation. Studies have shown an alarming degree of incorrect usage, with a typical failure rate of around 60% for slow inhalation and well-timed actuation (Ganderton *et al.*, 1997). Many patients also have difficulty in continuing the inhalation following actuation due to the shock effect of fast-moving 'cold freon', when the propellant spray hits the back of the throat (Crompton, 1982; Ganderton *et al.*, 1997; Hilton, 1990). Poor synchronisation decreases the lung deposition and increases the oropharyngeal deposition, which induces local and systemic side effects.

1.2.3.b. Dry powder inhalers

Dry powder inhalers (DPIs) are used for dispersion of the powder drug formulations. They are inherently breath activated, releasing drug when the patient inhales. The inspiratory airflow of a patient provides the sole energy source to disperse the drug particles and to move the aerosolised particles from the body of the inhaler to the lungs (Prime *et al.*, 1997). In practice, the patient's inspiratory effort will determine the entrainment and dispersion performance and hence the dose delivered by DPIs to the lungs. Individual users may not always actuate the dose consistently and some users may be unable to impart sufficient force to generate an effective dose (Hickey *et al.*, 1994; Newman *et al.*, 1988). The patient inconsistency causes a huge variation in the dose delivered by DPIs, although the formulation and the device also play important parts in achieving accurate, deep-lung deposition.

1.2.3.c. Nebulisers

In intensive care units and in the more serious cases, when the hand-held devices have failed to control disease symptoms, another type of delivery device is used, namely the nebuliser. Nebulisers are pulmonary delivery devices, which produce droplets constantly from a dilute aqueous drug solution. The internal geometry of

conventional nebulisers and their operation are highly variable (Dalby *et al.*, 2003; Niven, 1996). A schematic diagram of an air-jet nebuliser is shown on Figure 1.5. In these systems, pressurised gas is forced through a narrow nozzle, which generates a region of low pressure at the orifice. This negative pressure is used to augment capillarity and draw the drug solution from the bulk into the fast moving air-stream. The bulk drug solution is sheared first into a thin sheet of expanding liquid and ultimately into a range of fast moving droplets with a range of particle sizes. The droplet stream is directed into a solid surface or baffle. Baffles serve to capture larger droplets by inertial impaction allowing only smaller ones, suitable for lung delivery, to be entrained in the air-stream leaving the cup of the nebuliser. The trapped droplets return to the bulk solution. The re-circulation of the drug solution results in the temperature fall of the bulk liquid and droplets due to evaporative cooling. The drug solution concentrates due to the loss of water vapour. A nebuliser typically takes 10-15 minutes to administer a single dose, because most of the bulk drug solution is not converted to an inhalable aerosol in a single pass through the nozzle.

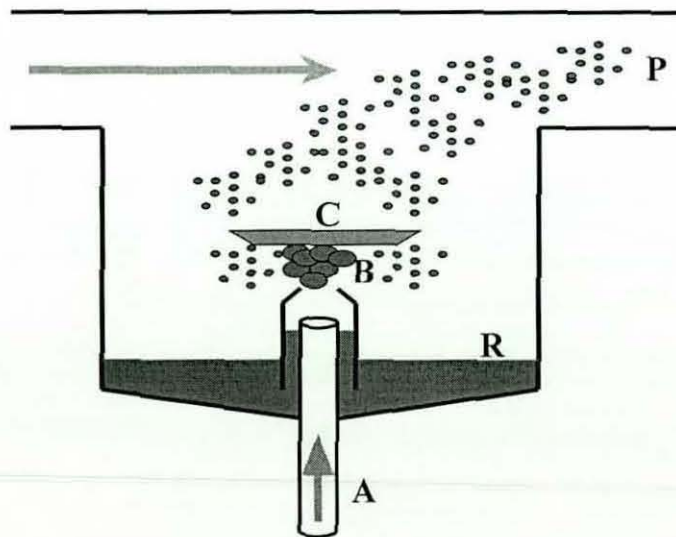


Figure 1.5. Schematic diagram of an air-jet nebuliser: compressed air enters through a narrow tube (A), causing a pressure drop near the venturi (B); the liquid drug formulation is rising from the reservoir (R) and the jet air stream breaks it up into droplets of various sizes; larger droplets fall back into the reservoir deflected by the baffle (C); small droplets leave the nebuliser with the jet stream as a fine mist that is inhaled by the patient (P).

Nebulisers retain two important advantages over other aerosol delivery systems. First, nebulisers require no complex breathing manoeuvres and therefore no training. They deliver aerosols over multiple breaths and tidally breathing patients, breathing spontaneously, or on a ventilator, can be dosed so long as the outlet of the nebuliser remains connected to their inhaled air-stream. Second, because the volume of solution is large and inhaled over multiple breaths, larger doses of drug can be administered compared to the hand-held inhalers. The ability of patients to use nebulisers intuitively, without training, and their ability to deliver some of the drug (if not the optimum amount) continues to preserve their use for ambulatory and intensive care (British Thoracic Society, 2003).

1.3. Efficacy evaluation

1.3.1. Introduction

The ultimate goal of evaluating the efficacy of pulmonary drug delivery is the ability to measure the amount of the drug, which actually reached the targeted part of respiratory system of an individual patient. For asthma-controlling therapies the targeted part of respiratory system is the deep lung. It is not enough to evaluate a drug formulation in respect to particle properties such as particle shape, particle size distribution and homogeneity of the drug distribution over the formulation, which can be measured by common methods of size analysis (Fayed *et al.*, 1984). The evaluation task is more related to the characterisation of the particle size distribution in an aerosol released by a delivery device and entering the patient's respiratory system. Engineers designing a pulmonary delivery device have to evaluate the dose released by the device, the amount of respirable fine particles in the released dose and the variability of these parameters over multiple device actuations. Physicians have to evaluate if an individual patient is getting a prescribed dose of the drug by using a particular inhaler-device with a particular drug formulation.

The success of pulmonary delivery is the culmination of a series of events: a drug is blended into a formulation, this formulation is released by a delivery device in the form of an aerosol with a high proportion of the fine particles, and a patient effectively inhales this aerosol into the deep lung. To evaluate this complex process

there currently exists a number of rigorous testing steps, which can be divided into two major groups: *in vivo* and *in vitro* characterisations, although neither of them resolves the ultimate task.

1.3.2. *In vivo* assessments

In-vivo investigations of pulmonary drug efficacy are normally performed on a group of patients or volunteers to establish a variation caused by the patient and a distribution of drug between the oropharynx and the respiratory zone. The results determine the pulmonary availability of the drug and its variation for users. The main methods for *in vivo* measurement of the pulmonary availability of inhaled material are: Gamma Scintigraphic Imaging, the Pharmacokinetic method and Lung Function Tests (Sherwood L., 2001).

1.3.2.a. Gamma (γ) – Scintigraphy

For γ -scintigraphy the drug formulation is labelled with a radioactive isotope, ^{99m}Tc (Fleming *et al.*, 2000; Fleming *et al.*, 2001; Warren *et al.*, 2002). Upon the drug administration a gamma camera takes images of the upper half of the human body. The dose distribution over the respiratory system is analysed by the contrast in the image related to γ -counts. This method measures only the relative amount of the drug in the different parts of the respiratory system.

Gamma-Scintigraphy of lung deposition provides valuable data on the site-specific drug deposition in the patient's lung. The drawbacks of this technology relate to the radiolabelling of the drug. This means that the drug formulation has been modified by the radiolabelling and may have quite different aerodynamic properties, which in turn will affect the lung deposition. The implementation of Gamma-Scintigraphy also involves complex and sophisticated protocols, including ethical approvals, without mentioning the risk of subjecting individuals to γ radiation.

1.3.2.b. Physiological characterisation

Physiological characterisation evaluates the clinical efficacy of drug administration by measuring specific functions of the human body. In pharmacokinetic tests, the

amount of drug can be directly measured in blood and urine samples. Blood and/or urine samples are collected at the pre-set time intervals after the drug administration. A plot of the drug concentration in plasma/urine, presented as a function of time, allows measurements of the maximum drug concentration, the terminal half-life and the area under curve (AUC). To deduce the absolute amount of drug taken by the lungs requires specific physiological methods, including the gastro-intestinal absorption and the liver metabolism.

In lung function tests, the so-called forced expiratory volume in 1 second (FEV₁) is measured before and after the drug administration (Hughes, 1999). In asthma management this method allows the direct measurement of the physiological effect of the drug on the respiratory function of the patient (e.g. Serra-Batlles *et al.*, 2002).

Physiological tests have a very important role in the patient-centred assessment of medications, although such tests clearly always require ethical approval and hence must have a predicted health benefit. Usually, these tests are unable to answer the questions about which particular part of the delivery device or drug formulation is responsible for any changes in the medical outcome.

1.3.3. *In vitro* assessments

In vitro methodologies have evolved to assess “like *in vivo*” behaviour of the pulmonary delivery system. They remove the unpredictable features of the patient variability and provide the preliminary data on deposition patterns. *In vitro* measurements can evaluate a prototype or a novel delivery system; the development changes of formulations and provide vital information on the combined performance of the device and the formulation prior to volunteer trials. They estimate also batch-to-batch variations and give a good indication on how a system will perform in clinical studies.

1.3.3.a. *Aerodynamic size distribution*

For pulmonary delivery, the key parameter is the particle aerodynamic diameter. Consider the pulmonary dose as a single aerosol cloud released by a delivery device. In this cloud there are populations of particles of different aerodynamic diameters.

The following values are the main parameters, which are normally used to characterise the pulmonary dose delivery. The Mass Median Aerodynamic Diameter (MMAD) and Geometric Standard Deviation (GSD) characterise the cloud as a whole, giving the aerodynamic diameter and its deviation for the particles, which are responsible for 50% of the cloud mass. The amount of drug available for the deep lung deposition is the Fine Particle Dose (FPD) and is measured as the mass of the particles with aerodynamic diameters in the range between approximately 0.5 μm and 5 μm depending on the measurement apparatus. The Metered "Labelled" Dose (MD) is the drug mass in a single dose labelled by the producer: for a pMDI it is the dose measured by the metering valve; for a DPI reservoir device it is the dose measured by a dosing chamber and for a single dose blister it is the drug mass inside the blister. The Emitted Dose (ED) is a drug mass, which has been released from the delivery device during a single actuation. The Fine Particle Fraction (FPF) is defined as the percentage of the delivered dose that can penetrate into the deep lungs:

$$FPF = \frac{FPD}{ED} * 100\%.$$

During *in vitro* studies these parameters are measured and

statistically evaluated for different batches of the same drug formulation, for multiple actuations from the single inhaler device and for performance across multiple devices. If these statistical variations are within the regulatory requirements, the given combination of the drug formulation and the delivery device is allowed for further *in vivo* testing with volunteers and patients.

1.3.3.b. Inertial impaction method

British, European and US Pharmacopoeias (British Pharmacopoeia, 1993; United States Pharmacopeia, 2000) require that the *in vitro* tests have to be performed by means of an inertial impaction device (Olsson *et al.*, 1996). The recommended inertial impaction systems are: the Andersen Cascade Impactor, the Marple Miller Cascade Impactor and the Multi-stage Liquid Impinger. The Next Generation Pharmaceutical Impactor (NGI) has now been rigorously tested (Asking *et al.*, 2003) and may soon be recommended by the Pharmacopoeia.

A cascade impactor can have 3 or up to 12 stages mimicking the various parts of the human respiratory system. The impactor is designed such that, as the aerosol stream passes through each stage, particles having a large enough inertia will impact upon that particular stage plate whilst smaller particles will pass to the next impaction stage. Figure 1.6 shows a simple model of the impaction process. As the direction of flow changes, aerosol particles continue to move in the original direction until the viscosity friction slows them down. Then they “relax” into the new flow direction (Relaxation Time). Placing a collection surface normally to the original flow causes the particles, which have insufficient relaxation time to impact. Small particles relax more quickly, thus do not impact. By controlling the number of jets, their diameters (W) and the impaction stage separation (S) the effective cut-off aerodynamic diameter can be controlled at various flow rates (Rader *et al.*, 1985). For a cascade impactor operating at a given flow rate, each stage directly relates to a cut off aerodynamic diameter. Chemical analysis of each impactor stage allows the mass versus size interpretation of the aerosol contents. And therefore it is possible to calculate all parameters that we have defined for *in vitro* characterisation.

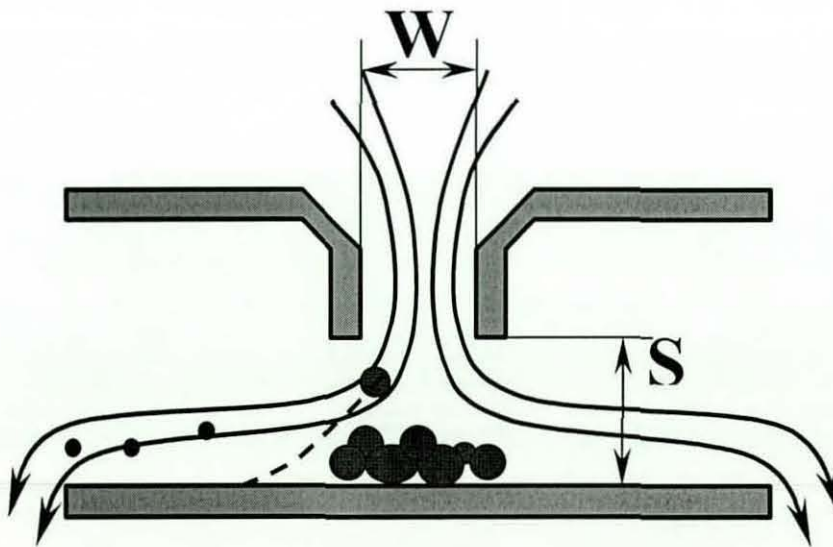


Figure 1.6. Schematic presentation of the inertial impaction process: small particles follow the streamline (solid lines); the trajectory of a large particle (dashed line) intersects the impaction plate; S is the nozzle-to-plate distance and W is the nozzle diameter.

1.3.3.c. Limitations of cascade impactors

Impactor measurements are influenced by many factors such as the precision of the mechanical manufacturing of the impactor's components, the stability of the flow rate (Rader *et al.*, 1985), ballistic bounce and re-entrainment of particles from stages (Hickey, 1990) and the accuracy of an operator. But major concerns are related to the principal drawbacks: 1) the relation between stages and particle sizes is only valid for a given, constant flow rate of the air and therefore the patient respiratory effort cannot be taken into account; 2) due to the sensitivity limits of the chemical analysis, the results are an average over multiple doses; 3) the measurements are extremely time and labour consuming and 4) an automation of the measurement process is not available and has proved difficult to develop.

Despite the efforts of manufacturers to develop a labour saving impactor, the most robust and modern designs involve at least 25 minutes to collect samples from the stages and prepare for the next test. The analysis of the samples takes even more time. Attempts to develop automation for measurements of a cascade impactor appear to be very costly and ineffective. The next generation pharmaceutical impactor (NGI) was designed with the intention that the automation routine will be easier to develop and apply.

The more stages that are present in the impactor, the more the particle size classes in the particle distribution that can be measured. Since the amount of drug delivered in each dose is relatively small, there is a limit to the number of stages that can be used for a single actuation analysis. It is therefore usual for results from cascade impactors with four or more stages to be based upon the average values over a number of actuations (often 5). This results in the *in vitro* data normally overestimating the performance of the pulmonary therapy in comparison to the *in vivo* investigation, where dose evaluations are normally based on a single actuation.

1.3.3.d. Link to humans

Recently, attempts have been made to address the issue of the human respiratory airflow in the inertial impaction investigations (Burnell *et al.*, 1998; Chavan *et al.*, 2000; Chavan *et al.*, 2002). An individual patient can create rather an individual

cloud of drug formulation due to his/her particular inhalation flow profile, and therefore he/she will get an individual dose of the drug. A novel method has been developed to assess the 'like *in-vivo* performance' of DPIs using the Electronic Lung Device (Burnell *et al.*, 1998). The computer-controlled breathing simulator creates designated inhalation airflow, which disperses the drug dose from DPI into the holding chamber. Then, another vacuum pump draws the drug cloud from the holding chamber through a cascade impactor at the fixed flow rate to determine particle sizes. In this way the dose dispersion process is entirely separated from the particle sizing process, therefore an individual patient may be assessed. However, this method still requires labour-consuming measurements of the cascade impactor and the holding chamber may influence the particle distribution.

Richard Dalby's team from the University of Maryland proposed a control system and valves capable of ramping up to the predetermined peak of an airflow through a DPI in conjunction with the *in vitro* testing apparatus MSLI (Chavan *et al.*, 2000; Chavan *et al.*, 2002). These modifications allow the study of the effects of the different parts of the flow-rate profile on the deposition pattern during *in vitro* tests, for example, the effect of the rising edge of the profile and how quickly the flow rate reaches the maximum.

1.3.4. Needs for a fast, non-invasive, patient-related assessment

Developing novel therapies for pulmonary drug delivery, a match between a formulation and a device, should be based on data. The data should be collected on both the drug and device before the match is made. Regulatory tests (*in vitro* and *in vivo*) are not the best tools for device/formulation development or screening (Dalby *et al.*, 2003). *In vitro* measurements are precise and sensitive, but completely irrelevant to the patient variability and are extremely time and labour consuming. *In vivo* studies are accurate in determining the drug deposition into the respiratory system, but are completely inapplicable to the early stages of developing either delivery systems or drug formulations. Therefore, there is a need for a different method of aerosol characterisation. Emerging technologies are looking for a quick (not necessarily metrological) testing procedure that can help to narrow down options rapidly.

A treatment of a patient by a pulmonary therapy strongly depends on the ability of the given patient to use successfully a given inhaler. Currently, patients are only advised to ensure a particular inspiration flow during the drug intake, without any means to evaluate the actual aerosol released by the inhaler at this particular actuation. For some patients the asthma controlling therapy is not working, and doctors are faced with the dilemma of whether to increase the drug dose or to switch to a different inhaler. Eventually, by multiple try-and-see cycles, the right inhaler and the right dose are found. It is undoubtedly beneficial for patients if the pulmonary drug delivery can be evaluated routinely, in real time, actuation-by-actuation. Obviously, the existing *in vivo* methods are unsuitable for this task.

Patients and developers of the pulmonary delivery systems would all benefit from a robust technology that is able to characterise the amount of fine particles in the released drug cloud through *in situ* measurements. Such technology can also help to constantly monitor the patient's performance with respect to therapy compliance and device suitability. The following is a list of desirable features for emerging technologies:

- It is *fast* in comparison with usual cascade impactors. Then, the method can shorten the time taken searching for promising innovations.
- The *fine particle* dose (FPD) and fine particle fraction (FPF) of the released dose are the most desirable values rather than a precise particle size distribution.
- The desired object for the characterisation is the real aerosol cloud actuated by a realistic airflow. Therefore, the method is *in situ* and *in-line* with a patient.
- The measurement affects neither the aerosol nor the airflow. Thus the method is non-invasive.

Section 1.4 discusses the possible method for an *in-line*, non-intrusive characterisation of the pulmonary drug delivery.

1.4. Methods for particle characterisation

1.4.1. Overview

Dispersion processes and the shape of particles makes particle size analysis a more complex matter than it first appears. The first issue is that particles are three-dimensional objects and generally speaking have to be described with three or more numbers. Secondly, there are a huge number of different particles in the sample to be analysed. For example, a typical single dose of Pulmicort® Turbohaler® contains 200µg of budesonide. Then, if all released particles are respirable spheres of 1µm diameter, the total number of particles in the dose cloud will be 250 millions (the budesonide density is 1.54 g/cm³). Moreover, different methods measure a different aspect of the particle size. While imaging technologies such as optical or electron microscopy are looking at some two-dimensional projection and a sieving method characterises the minimal sizes of particles, laser diffraction can give particle volumes. For management purposes, to be able to compare different doses on the basis of their mean particle size and particle size distribution, it is convenient to be able to describe a three-dimensional object by one unique number. This requires an examination of the Equivalent Sphere Theory.

1.4.1.a. Equivalent sphere theory

Only spheres are exactly described by one parameter, their diameters. There are a number of properties of an arbitrary-shaped particle that can be described by one number. For example, the weight is a single unique number as is the volume and surface area. So if we have a technique that measures the weight of the particle, we can then convert this weight into the weight of a sphere and calculate one unique number for the diameter ($2 \cdot r$) of the sphere of the same weight as the arbitrary-

shaped particle: $weight = \frac{4}{3} \pi \cdot r^3 \cdot \rho$, where ρ is the density. Now, by measuring

some property of our particle and assuming that this refers to a sphere, we can derive one unique number (the diameter of this sphere) to describe our particle. This ensures that each three-dimensional particle is described by one unique number which, although less accurate, is more convenient for management purposes. Table

1.3 shows typical methods of expressing size measured by several different techniques.

Table 1.3. Definitions of equivalent sphere diameter.

Volume diameter	The diameter of the sphere having the same volume as the particle
Projected surface diameter	The diameter of the sphere having the same projected area as the particle profile in the position of rest
Surface diameter	The diameter of the sphere having the same surface area as the particle
Stokes' diameter	The diameter of the sphere having the same terminal velocity as the particle
Particle sieve diameter	The width of the minimum square aperture through which the particle will pass
Specific surface diameter	The diameter of the sphere having the same ratio of external surface area to volume as the particle

1.4.1.b. Common methods of size analysis

Many technologies have been developed using different physical principles for measuring particle size. Table 1.4 shows some of the size analysis methods that are commonly used in practice. The techniques range from the mechanical size separation (sieving) to the size evaluation based on particles' interaction with radiation. Some methods measure sizes of individual particles and can hardly be applied for in-line or *in situ* measurements. The others use additional forces like gravitational and centrifugal forces or require particles to enter the measurement area one-by-one; therefore they also cannot be applied for in-line applications. The last column in Table 1.4 shows that only a few techniques can be used for in-line measurements: these are optical and ultrasonic methods.

For meaningful size analysis, each particle should be individually dispersed and be stable with regards to coagulation. Because the way in which the dispersion is carried out can drastically affect the size measurement, a general rule is to measure

particles by a method that is closely related to its end-use properties and in the medium in which it is used. For the reason that ultrasound methods normally require a liquid sample, they have significant disadvantages in comparison with the optical methods for the purpose of characterising pulmonary drug delivery. Taking into account that optical methods are quick, non-invasive and able to operate on dry samples (aerosols), optical principles appear to be the most promising approach to solve the problem of an *in situ* characterisation of the pulmonary delivery in-line with a patient. Section 1.4.2 presents a critical discussion of optical methods that have been successfully used for particle-size measurements for in-line applications.

Table 1.4. Common methods for size analysis.

Method	Condition	Technique	On-line applications
Microscopy	Wet or Dry	Scanning electron microscopy	No
		Optical imaging; Automatic image analysers	Yes
Sieving	Wet or Dry	Wire woven; Micromesh screens	No
Sedimentation	Wet or Dry; Gravity	Micromerograph; Photo- and X-ray sedimentation; β back scattering	No
Sensing zones	Wet	Electrical resistance change	No
	Wet or Dry	Optical scattering; diffraction; obscuration	Yes
X-ray method	Dry	Absorption; low-angle scattering; line broadening	No
	Wet	β ray absorption	
Ultrasonic	Wet	Attenuation momentum transfer	Yes

1.4.2. Optical methods for in-line measurement

The success of optical methods in particle size measurements is based on the amazing richness of the light interaction with particles and of the underlying theory in which these phenomena were implicit. The light-particle interaction depends on

both the properties of the light such as wavelength and polarisation as well as the particle properties such as size, shape and refractive index. Maxwell equations that describe the interaction of light with solid matter are differential equations of the second order with multiple boundary conditions and in many cases bulky numerical calculations are required to solve these equations precisely. High performance computers and huge memory capacity permit the solution of theoretical equations with multiple input parameters. Rapid evolution in light sources, photo-detectors and optical fibres make it also possible to reduce significantly the size of optical systems.

Optical methods are widely used for online control and monitoring of the particle suspensions through industrial processes (beer industry; paint;). Optical methods are also intensively used in the pharmaceutical industry as metrological tools for powder and particle technologies (for example Malvern and TSI particle-sizing instruments). Unfortunately, metrological methods require that only one or a few particles are present in the measurement volume at each measurement period and cannot be applied on a whole, dynamic, multi-particle aerosol released from an inhaler. Similarly, many industrial, online controlling methods are based either on a calibration by samples, when samples are measured by a metrology method and the online sensors are calibrated accordingly, or by extracting a sample from the production line into a bypass where a metrology routine can be applied. Neither of these approaches can work on the aerosol cloud *in-line* with a patient. In this section we consider two optical methods that have been recently tried for measurements on the particle cloud released from an inhaler, and one robust industrial method for online control as generic prototypes for *in-line* characterization of the pulmonary drug delivery.

1.4.2.a. Particle imaging

Shadows, two-dimensional (2D) projections of illuminated particles, possess some limited, but sufficient, information about sizes and shapes of the particles and are often used for particle size measurements. These methods can be seen to consist of two parts, one concerned with imaging and the other with counting. Particle imaging techniques are easily applied for analysis of 'flat', 'stationary' particle samples using optical or scanning electron microscopes. For dynamic online applications, where

the particle suspension fills a three-dimensional (3D) volume the imaging process becomes problematic. The problems relate to the exposure time and the focusing depth of the imaging optics. The exposure time issue can be overcome by combining pulsed (strobe) lasers with high-speed cameras. The short-pulsed lasers enhance camera performance by illuminating a subject with ultra-short pulses of light. Image blur is eliminated, even for particles moving at high velocity. For example, the latest VisiLase system from Oxford Lasers achieves the effective exposure time of 25ns. In this case even the smallest droplets in the spray can be seen clearly – frozen in flight (Oxford Lasers, 2004). Counting methods are well established for many metrological technologies and can facilitate effective counting of particle images according to their size.

The principal drawback relates to the requirements on magnification, field of view and focusing depth. Higher magnification diminishes the field of view and the focusing depth. For the purposes of evaluating on line the fraction of the fine particles (size range from 0.5 μm to 5 μm) in the aerosol (particle size range up to 200 μm) released from an inhaler, a metrological measurement through an imaging technique seems unfeasible. The focusing depth issue can be overcome by forcing the aerosol cloud through a narrow passage creating a nearly 2D layer. In this case the effective imaging and counting procedure can be established. But closely placed walls strongly affect the flow velocity and may introduce a significant air-resistance and therefore cannot be considered as non-intrusive for measurements in-line with a patient.

1.4.2.b. Laser diffraction

After over 30 years of rapid development, laser diffraction has evolved into an extremely efficient method for the analysis of particle size distributions and become the dominant technique for optical particle sizing either in the laboratory (off-line) or directly in the production process (Puckhaber *et al.*, 1999). While ‘off-line application’ characterises different products, ‘in-line application’ integrates representative sampling and supplies the particle size information immediately for continuous monitoring and automated process control. The applicable range according to ISO13320 is 0.1 μm to 3mm.

Figure 1.7 shows the classical Fourier arrangement, where dispersed primary particles interact with the light in the parallel laser beam. The diffraction patterns are collected on a highly sensitive, semicircular, multi-element detector. With this input information, the particle size distribution is calculated using the Fraunhofer approximation or Mie theory. Both methods require the fulfilment of some preconditions. The Mie theory describes accurately the light scattering by a smooth spherical particle and requires the complete knowledge of the complex refractive index. The Fraunhofer approximation assumes that the particle is opaque, and is much larger than the wavelength of the light employed (ISO1332 defines this as being greater than 40λ , i.e. $25\ \mu\text{m}$ when a He-Ne laser is used). Even small deviations from one of these requirements may result in dramatic changes in the calculated size distribution curve, as has been shown in several studies (e.g. Muller *et al.*, 1996).

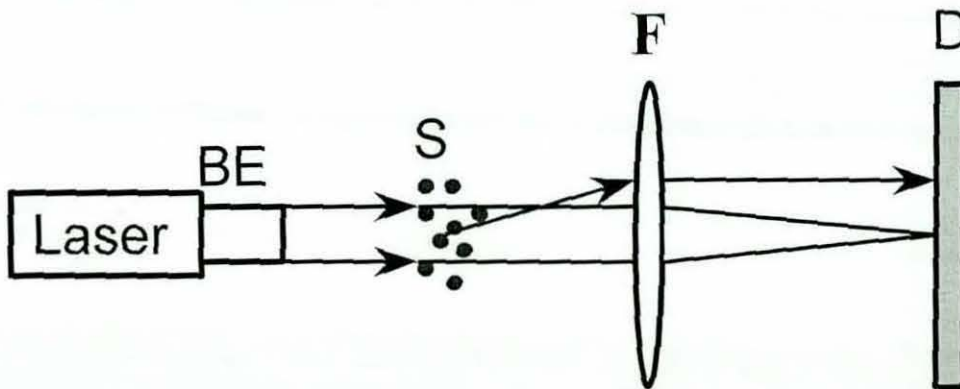


Figure 1.7. Optical set-up for generation of diffraction patterns consists of a laser, a beam expander (BE), Fourier lens and a multi-element photo-detector (D). S is a sample of dispersed particles.

In the last few years, the LD technology has been developed as a very fast and highly reliable alternative to cascade impactor analysis in testing the aerosol cloud released from an inhaler (de Boer *et al.*, 2002; Holmes *et al.*, 2001). Authors critically compared the impactor analysis with the LD technique. They have found out the main theoretical limitations and drawbacks of the LD technique to be the following: 1) measurement of geometrical instead of aerodynamic particle size; 2) volume distribution curves are calculated on the assumption that particles are spherical; 3) the apparent particle density and dynamic shape factors of drug

agglomerates are not known; 4) a choice between Mie and Fraunhofer theory has to be made and 5) evaluations of bimodal mixtures are not reliable. There is no real way to calibrate laser diffraction equipment; it can only be validated, to confirm that it is performing to certain traceable standards.

The use of laser diffraction metrology on-line is technically challenging because the measurement ideally requires a thin sample (to limit multiple scattering) of homogeneously distributed particles illuminated by an expanded laser beam (a few square cm). The whole optical arrangement (source, beam optics, Fourier lens and detector) needs to be in air and such a configuration requires a significant volume (typically 1L) of space. These conditions do not suit the use of laser diffraction metrology in the confines of an inhaler device in-line with a patient.

1.4.3.c. Turbidity measurements

For on-line monitoring of production processes, many industries such as water treatment plants, electricity plants and breweries employ a very simple and effective optical method: turbidity measurement (Sigrist, 1996; Allen, 1997.). Turbidity, cloudiness in fluids, is the reduction of clarity and transparency of a fluid sample due to the presence of suspended and colloidal matter such as clay, silt, soot and microorganisms. Turbidity is neither an absolute nor a metrological method. Turbidity measures neither particle size nor size distribution: for example, the presence of a small amount of the smaller particles can be confused with a much larger amount of the larger particles. Turbidity is an optical method and hence not subject to non-optical parameters like temperature, viscosity, pH or conductivity and is non-invasive to the production process. Despite its non-metrological nature, turbidity allows important management decisions to be made in real-time during industrial production, using an appropriate calibration for a particular application.

For example, in the water treatment industry, when raw water comes from the surface reservoir the turbidity measurement is used to control the amount of flocculant added at the processing stage. Natural phenomena like snowstorms and thunderstorms can render the water temporally unusable. In this case, turbidity control allows real-time decisions to be taken as to whether raw water will be processed or discarded (Sigrist, 1996). The turbidity meters placed between the

settling tank and sand filters monitor the efficiency of the treatment for solid impurity elimination (the flocculation process). Turbidity measurements immediately after the sand filters are used for monitoring the actual filtration efficiency and for optimisation of the sand purging (the backwash) process (Sigrist, 1996).

In practice there are many different methods for turbidity acquisition ranging from the simplest *Secchi depth* to the *optical turbidimeter*. The *Secchi disk* method is often used to measure turbidity in the deep waters of lakes and rivers. The white, 20 cm diameter disk is lowered into the water on a calibrated line and two readings of the depth are taken: 1) when the disk just disappears from sight; and 2) when it becomes visible again during the raising. The average of these two distances is known as the *Secchi depth* and is used as a distinct measurement of turbidity.

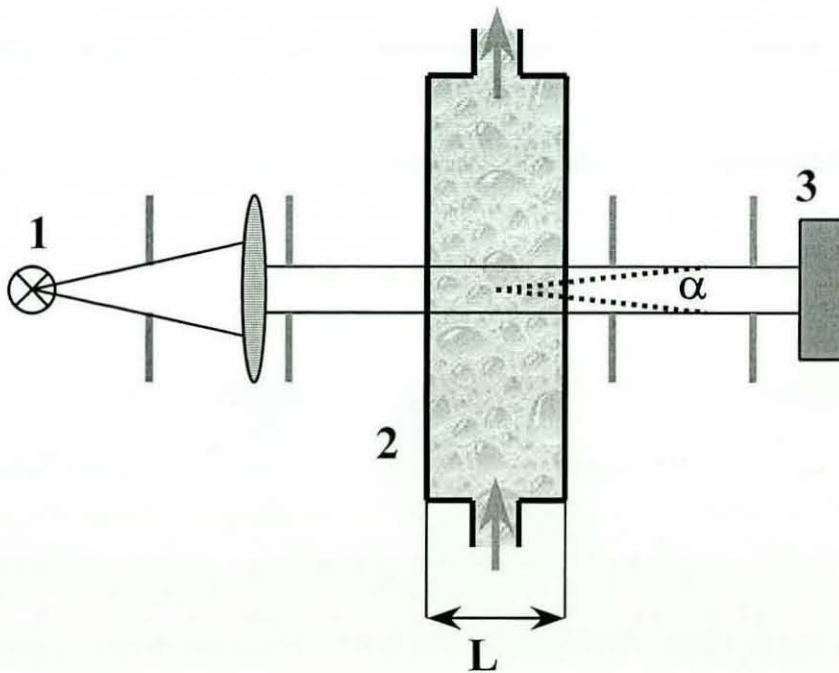


Figure 1.8. Principle of attenuation turbidimeters, comprising a light source (1), a cuvette (2) filled with a suspension, and a photodetector (3) with a small angle aperture (α).

An optical small-angle scheme measuring the attenuation of white light traversing the suspension in a forward direction was recommended for assessment of the degree

of agglomeration in suspensions (Koglin, 1973). Figure 1.8 shows the principle of an attenuation turbidimeter. The parallel light beam (1) traverses the cuvette (2) filled with a suspension. The traversed light intensity is measured by a photo-detector (3) through a small-angle aperture (α). These turbidimeters (so called *attenuation turbidimeters*) are normally used for suspensions when the solid concentration is smaller than 0.1%. If the solid concentration is higher than 1%, measurable transmissions are achieved only for very thin cuvettes. In this case, however, the scattered light intensity at a certain angle can be measured and its changes reflect the changes of agglomeration in the suspension (Koglin, 1977). This type of measurement, originally introduced for relatively dense suspensions, was then modified and used for a wider range of turbidity values. Such devices are commonly referred as *nephelometric turbidimeters* and the turbidity value is defined as a ratio of the scattered and transmitted irradiances.

Measurement units for turbidity have to be calibrated in relation to a standard sample due to the non-metrological nature of the technique. The *Diatomaceous Earth* and the *Formazine Suspension* can be used as such standard samples. The nephelometric turbidity unit (NTU) is defined by the standard ISO 7027 (Water quality; Determination of turbidity) and is often used in practice.

The overwhelming advantages of the turbidity method are its simplicity, non-intrusive nature and ability to measure changes in the degree of the suspension agglomeration directly during the monitoring of the process.

1.5. Conclusions

In summary, the object of the current investigation is a dynamically propagating particle cloud of a pulmonary drug formulation. The particle mass of a single dose is in the range of ten micrograms to two milligrams. The most important parameter is the inhalable part of particles, i.e. Fine Particle Dose (FPD), which is defined as the mass of drug particles in a single pulmonary dose with aerodynamic sizes in the range from 0.5 μm to 5 μm . The main objective is to develop a measurement technology allowing the efficiency of the pulmonary drug delivery to be characterised in-line with a patient. We call this technology VariDose and intend to

measure the delivered dose. The efficiency of the delivery directly relates to the degree of agglomeration in the aerosol released by an inhaler.

The composition of the drug cloud during delivery is a complex function of the formulation, entrainment and dissociation mechanisms as well as the details of the actuation system (human or mechanical). The technology requirement for complete metrological assessment (in space and time) of this cloud during delivery is not currently available. The particle size distribution can vary throughout the cloud and the distribution of density and speeds throughout the cloud is such that a detailed tracking of particle positions and their sizes is not currently feasible. Instead of attempting such a metrological analysis, we use the macroscopic principles of optical absorption and scattering to generate signatures of the delivered cloud. A simple optical sensing technology similar to the turbidity measurement has been developed. It has the potential for actuation-by-actuation assessment of pulmonary drug delivery in-line with a patient. Data obtained in the specially designed experiments are discussed to establish if this technology can provide useful information about the released drug-cloud: its dose value and the fine particle fraction.

Chapter 2

The Model

This model describes the aerosol cloud released by an inhaler and propagating through a cylindrical tube for the purposes of measuring the optical density of the cloud. The intensity of the light beam proceeding through an aerosol decreases due to the light scattered by particles. These losses due to scattering depend on aerosol properties and are defined by the optical density of the aerosol. It is common knowledge that the air filled with rain droplets is transparent, while the fog may significantly obscure the view. In physics this fact means that the volume filled with rain droplets has a lower optical density than if it is filled with a fog. To support this concept numerical calculations have been made using the Mie theory for light scattering by spheres.

2.1. Model description

The model qualitatively and quantitatively describes the interaction of a collimated light beam with a cloud of airborne particles released by an inhaler and moving in a direction perpendicular to the light propagation.

2.1.1. Aims of the model

The purpose of this model is to evaluate the design concept of the proposed technology (VariDose) for the pulmonary delivery assessment in-line with a patient. Using a well-established theory of the interaction of light with small particles, the model investigates the following aspects:

- The optical obscuration of the collimated beam by a particle cloud;
- The dependence on the light wavelength;
- The sensitivity to the fine particles.

The model also predicts the obscuration values for a given set of data measured by a conventional inertial impaction device. For these purposes the model divides the particle population of the cloud into sub-species of different sizes and considers relative contributions from each particle type.

2.1.2. Applicability

The model can be applied to any turbid medium. The main limit of applicability relates to the optical density of the medium. The limit arises from the assumptions made to calculate the reduction of the light intensity of the collimated beam through the scattering by particles. To establish relationships between the light reduction and the microstructure of the aerosol, we calculate the extinction coefficient using the Mie theory and suggest a simple spatial distribution of particles.

The general Mie theory includes two main assumptions: 1) the light interaction is a single independent scattering and 2) the particles are spheres. In our model the single scattering requirement is further softened allowing a degree of multi-scattering.

Particles in the measurement volume are considered independent; i.e. they are sufficiently far from each other that the electromagnetic fields within them do not

interact with each other. This assumption allows the addition of intensities from individual particles. Estimates have shown that a separation distance of $3r$ (three times the particle radius) is a sufficient condition for *independence* (van der Hulst, 1981). In the case of a mono-dispersion of spheres, to fulfil the independence criterion the volume concentration should not exceed 3% ($C_v = \frac{4}{3}\pi r^3 / (5r)^3$).

Single scattering means that the light scattered by an individual particle is regarded as being unaffected by other particles. In reality, each individual particle is illuminated by the direct light from a source and by the light, which has been scattered by other particles. For the single scattering, the multi-scattering component is assumed to be negligible in comparison to the light intensity directly incident upon the particle. Therefore, the single scattering would prevail if the particle concentration stays sufficiently low that the probability of the secondary scattering is low. In our model, when the extinction of a small collimated beam is considered, the requirements of single scattering can be relaxed allowing a degree of multi-scattering. Indeed, in this case we need to compare the intensity of the light, which has been scattered by particles and does not reach the receiving detector, with the light intensity that reaches the detector through the subsequent scattering events. The probability for light re-entering the collimated beam is the probability of secondary scattering multiplied by the probability for scattering into the defined direction, and therefore, is significantly smaller than the probability of the second scattering. For particle concentrations, when the second scattering is noticeable, the intensity of the re-entered light can still stay negligible. An estimation of the particle concentration limit for the model's applicability involves many parameters: particles' sizes, the spatial distribution, the length of the optical path and the properties of the receiver. Therefore it cannot be expressed in general form for such a dynamic and complex cloud as an aerosol cloud released by an inhaler. Instead, the concentration limit is studied on a few model clouds considering particles in the range of the pulmonary delivery: the fine particles and the coarse particles with the size range from $0.5\mu\text{m}$ to $5\mu\text{m}$ and from $6\mu\text{m}$ to $100\mu\text{m}$, respectively.

The distribution of particle species in the cloud is generally unknown and can be highly inhomogeneous and continuously varying in time. A generic complexity of the cloud dynamics is simplified to the scope of the measurement method and is

modelled as a “snapshot signature” of the temporal variation of the optical density at a given spatial location. For this conceptual study and for the transparency of the model conclusions the particle distribution is considered as being one-dimensional and following a homogeneous, Gaussian distribution.

The spherical approximation for the particle shape is considered as reasonable for arbitrary-shaped particles (micronised dry powder formulations) and liquid droplets (p-MDI formulations) and is applied in the terms of the equivalent sphere theory (section 1.4.1.a).

2.2. Particle distribution in a moving cloud

An aerosol cloud released by an inhaler consists of a huge population of particles. These particles possess different shapes and sizes, might possess electrostatic charge and often form agglomerates due to the adhesion and Coulomb attraction. Many physical processes take place when particles and agglomerates enter the airflow. Most of these processes strongly depend on the particle size and initial conditions such as velocity, temperature and time.

Particles tend to reach the velocity of the flow through the viscosity and drag action of the airflow. Generally, the smaller particles react to variations of the flow rate quicker than the larger particles (Rudinger, 1980). On the other hand, large particles, such as agglomerates, carrier and excipient particles, usually possess a better flowability and leave the powder bed easier, while the fine drug particles may stay in the powder bed longer due to their stronger adhesion.

In sprays released by p-MDIs, the larger droplets possess the larger inertia and more slowly relax down to the flow velocity, suggesting that the larger droplets may be in the front part of the cloud. However, the solvent evaporation from the droplets has a higher rate for the larger surface area and at higher droplet velocity, and therefore may result in a rather unpredictable distribution of particles through the aerosol cloud.

As a result in the most general case, the particle distribution in the released cloud can be inhomogeneous and continuously varying during the cloud propagation.

2.2.1. Spatial distribution

An aerosol cloud of a single-dose actuation moves with the airflow and occupies a limited volume of air. Most of the cloud parameters such as the cloud volume, the cloud velocity and the particle distribution are temporal variables. Figure 2.1 shows schematically an aerosol cloud with two types of particles: two sub-clouds of mono-dispersed particles. The volume concentration of particles is zero at the cloud boundaries and rises inside the cloud.

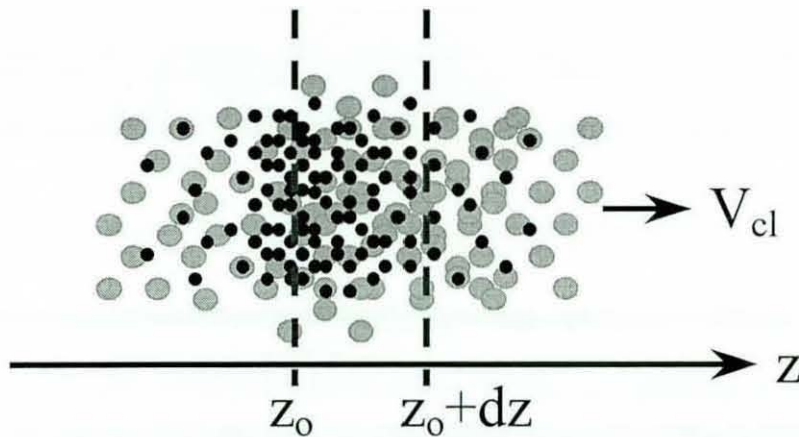


Figure 2.1. Schematic presentation of an aerosol cloud.

For modelling purposes, the particle distribution is significantly simplified to evaluate the main concepts of the technology. It is assumed that the particles are spread according to a Gaussian distribution for each sub-cloud. Then, in the one-dimensional approach, the volume concentration of airborne particles can be described by the following equation:

$$C_v(z) = \sum_{i=1}^{N_i} C_{vi} \exp \left[-\frac{(z_0 - z + \phi_i)^2}{2\varepsilon_i^2} \right], \quad [2.1]$$

where C_{vi} are maximal values and ε_i are characteristic spreads of the particle distribution in the z -direction for each particle type, N_i is the number of different types of particles, z is the coordinate, z_0 is the coordinate of the middle of the cloud and ϕ_i describes the relative positions of the different sub-clouds to this middle parameter.

There are straightforward relationships between the volume concentration C_{vi} , the particle number concentration N , the particle volume v_{pi} of a single i -type particle and the particle number concentration n_i for each particle type:

$$N(z) = \sum_{i=1}^{N_i} n_i(z) = \sum_{i=1}^{N_i} \frac{C_{vi}}{v_{pi}}, \quad [2.2]$$

For convenience the further general discussion is carried out in terms of the volume concentration and equation [2.2] acts as a transition between the two methods of presentation. Note, that for a multi-species cloud the combined distribution of airborne particles can be non-Gaussian due to the spatial shifts between the contributing distributions.

2.2.2. Interpretation of the temporal and spatial variation

In the proposed technology a single sensor is placed perpendicular to the direction of propagation. The sensor gives information about particles within a small volume, which is defined by the sensor's properties and the device geometry, and commonly called the measurement volume. The sensor records, for example, a variation of the optical density while the aerosol passes through the measurement volume. Each measurement data characterises particles within this measurement volume at the sensor position z_d and is recorded as a temporal variable. Although such data present a temporal variation of optical measurements, in reality they include also the spatial variation of the aerosol. Indeed, for a temporal sequence of measurements the individual reading corresponds to the different parts of the aerosol, which enter the measurement volume one-by-one. As a result, the sensor measurements depend strongly on the position of the sensor down the stream of the aerosol propagation.

Therefore, in practice, to compare the cloud characterisation from different experiments the position of the optical sensor must be taken into consideration. It is also important to find an optimal position for the sensor in each specific case, i.e. for a given combination of the drug formulation, the delivery device and the inhalation effort. An interpretation of the recorded data would include some elements of assumption and deduction and requires a thorough discussion for an individual experimental set-up. Generally, in this thesis, the temporal data of a single sensor is

treated as “a snapshot” of the cloud in time, which accumulated both processes: the evolution of an aerosol cloud and the cloud propagation.

For the modelling purposes of a dynamic cloud, we assume that a multi-species cloud is described by the Equation 2.1 and the cloud moves as a whole at a constant velocity V_{cl} , neglecting possible variations of the particle distribution due to the cloud evolution, e.g. de-agglomeration and agglomeration of some particles. As the front edge of the cloud approaches the sensor position z_d the time scale is triggered and the temporal variation of the volume concentration can be described as follows:

$$C_v(z_d, t) = \sum_{i=1}^{N_i} C_{vi} \exp \left[-\frac{(z_d - V_{cl}t + \phi_i)^2}{2\varepsilon_i^2} \right] \quad [2.3]$$

2.3. Theory of light extinction

The general mathematical description of the propagation and absorption of light in a turbid medium is based on the photon transport theory (Chandrasekhar, 1960; Ishimaru, 1978; van de Hulst, 1980). Transport equations can rarely be solved analytically using microscopic properties of the medium; more often the solution is obtained by introducing macroscopic characterisation for the medium.

The main purposes of our model are to find out the role of the fine particles in the optical density of an aerosol and to evaluate if the transmittance of the collimated light beam characterises the dose of the fine particles. Therefore the microscopic properties are important for our model. The physical model is simplified to the level where the microstructure of the cloud can be evaluated. A fundamental solution can be achieved in the linear limit using the Lambert-Beer law and applying the Mie theory to calculate the extinction coefficient.

2.3.1. Lambert-Beer law

A linear transport equation is a differential equation of the first order and describes linear losses of the light intensity through the scattering:

$$\frac{dI}{dz} = -\gamma I \quad [2.4]$$

where I is the radiation intensity, z is the space coordinate in the direction of propagation and γ is the so-called extinction coefficient. The solution of this equation is usually referred to as the Lambert-Beer law, which describes the exponential decay of the radiation intensity due to absorption and scattering in the homogeneous medium:

$$I = I_o \exp(-\gamma L) \quad [2.5]$$

where I_o is the intensity of the incident light and L is the length of the path in the medium. The essential assumptions of the Lambert-Beer law are the homogeneity of the medium, i.e. the extinction coefficient does not depend on the space coordinate, and that the extinction coefficient is independent of the light intensity. The intensity independence requires that the concentration of the scattering/absorbing centres in the medium is not too high, $C < 0.01M$, (Skoog *et al.*, 1997).

The Lambert-Beer law has been successfully used in practice, for example in analytical chemistry (Skoog *et al.*, 1997). Indeed, measuring the transmission of light for different thicknesses (L) of a homogeneous medium enables the experimental value of the extinction coefficient to be deduced. Then it is possible to determine the concentration of absorbing centres in the solution via measuring the light transmittance ($T = I/I_o$) and using a working curve of transmittance versus concentration derived from standards.

Unfortunately, for aerosol applications, creating standards is a rather challenging task due to the uncontrollable nature of the agglomeration/de-agglomeration processes. For this reason we assume that particles are spheres and calculate the extinction coefficient using Mie theory.

2.3.2. Mie theory method

The scattering of light by particles cannot be treated in a general way, other than by the formal solution of Maxwell's equations with the appropriate boundary conditions. The problem of light scattering by homogeneous spheres in single scattering approximation was rigorously investigated in the second half of 19th century. The general solution was published by Gustav Mie (Mie, 1908) and is

usually referred to as the Mie theory. The scattering of light by homogeneous spherical particles composed of isotropic materials can be computed readily using the conventional Mie theory or its modification. Here we introduced basic formulas and values used in the model, following notations and mathematical equations developed by van de Hulst (van de Hulst, 1981).

2.3.2.a. Mie coefficients

The Mie solution gives the fields of the electromagnetic wave at any point inside and outside the particle. In principle it is possible to calculate the light intensity at any point of the space. In order to simplify the notation, consider the outside medium to be a vacuum ($m_2 = 1$) and the material of the sphere to have a refractive index m , following van de Hulst's notations (van de Hulst, 1981). General solutions are expressed in the Mie coefficients a_n and b_n , which are calculated through the Riccati-Bessel functions ψ_n , χ_n , ζ_n and the derivatives of these functions (denoted by primes):

$$a_n = \frac{\psi'_n(y)\psi_n(x) - m\psi_n(y)\psi'_n(x)}{\psi'_n(y)\zeta_n(x) - m\psi_n(y)\zeta'_n(x)} \tag{2.6}$$

$$b_n = \frac{m\psi'_n(y)\psi_n(x) - \psi_n(y)\psi'_n(x)}{m\psi'_n(y)\zeta_n(x) - \psi_n(y)\zeta'_n(x)}$$

The parameter n is an integer from 1 to infinity. The arguments x and y depend on the radius of the sphere r and the wavelength of the light λ :

$$x = \frac{2\pi r}{\lambda} \tag{2.7}$$

$$y = \frac{m2\pi r}{\lambda}$$

The parameter x , which equals the ratio of the circumference of the sphere to the wavelength, is the most important parameter here and sometimes is cited as the size parameter.

2.3.2.b. Extinction coefficient

For a light beam propagating through vacuum ($m_2 = 1$), which contains N mono-dispersed spheres per unit volume, according to Mie theory, the extinction coefficient γ is computed from the following formula:

$$\gamma = N\pi r^2 Q_{ext}(r, \lambda) \quad [2.8]$$

independently of the polarisation state of the incident light. The value of the extinction efficiency Q_{ext} depends on the radius of spheres, the refractive index (m) of the sphere material and the wavelength of light ($x = 2\pi r/\lambda$) and is expressed in the Mie coefficients as follows:

$$Q_{ext} = \frac{2}{x^2} \sum_{n=1}^{\infty} (2n+1) \Re[a_n(x, m) + b_n(x, m)] \quad [2.9]$$

The symbol \Re denotes the mathematical operation of taking the real part of the complex number.

According to many authors (van de Hulst, 1981; Bohren *et al*, 1983) the scattered field series are uniformly convergent and, therefore, the infinite sum can be terminated after a finite number of terms, $n = n_c$. The resulting truncation error can be made arbitrary small by taking sufficient terms. An extensive study of this issue, conducted by Wiscombe (Wiscombe, 1980), suggests a finite number which depends on the size argument x :

$$n_c = x + 4.05\sqrt[3]{x} + 2 \quad [2.10]$$

It has been shown (Barnett, 2000) that the Wiscombe criterion indicates the convergence point accurately for a range of the particle sizes ($10^{-2} < x < 10^3$) and a selection of refractive indexes ($1.1 < m < 5$). This range of parameters are covered the entire range of particles, which are used in the pulmonary drug delivery and are the subject of this thesis. Therefore, we can apply the Wiscombe criterion in our calculations.

For a medium, which contains multiple particles of different radii, and if there are $N(r)dr$ particles of radii between r and $r + dr$ per unit volume, the extinction coefficient includes contributions from all particles and is expressed by the following integral equation:

$$\gamma = \int_0^{\infty} Q_{ext}(r, \lambda) N(r) \pi r^2 dr \quad [2.11]$$

In our study we consider only a discrete number of different particles, therefore this integral equation is simplified to the sum:

$$\gamma = \sum_{i=1}^{N_i} Q_{ext}(r_i, \lambda) N_i \pi r_i^2 \quad [2.12]$$

Mie theory considers individual particles and therefore it is convenient to operate in particle numbers. On the other hand, for the dose cloud it is convenient to consider the volume concentration of the airborne material C_v and fractions of each particle type (equation [2.7]). The conversion relation between the particle number per unit volume N and the volume concentration C_v includes the volume of a single particle and has the following form, supposing particles are spheres of the diameter $d = 2r$:

$$N = \frac{6C_v}{\pi d^3} \quad [2.13]$$

$$N = \frac{6}{\pi} \sum_{i=1}^{N_i} \frac{C_{vi}}{d_i^3} \quad [2.14]$$

for mono and poly dispersed media, respectively.

Applying the Lambert-Beer law for the light propagation (equation [2.5]) and Mie theory for the extinction coefficient (equations [2.9], [2.12] and [2.14]), we can calculate the light transmittance through a medium using its optical properties and microstructure (equation [2.3]). For an aerosol cloud containing N_i types of spheres

(diameters d_i) and passing at a constant velocity V_{cl} the optical sensor, which is located at the position z_d , the light transmittance takes the following form:

$$T(z_d, t, d_{1...N_i}, \lambda) = \exp \left\{ - \frac{3L}{2} \sum_{i=1}^{N_i} Q_{ext}(d_i, \lambda) \frac{C_{vi} \exp \left[- \frac{(z_d - V_{cl}t + \phi_i)^2}{2\varepsilon_i^2} \right]}{d_i} \right\} \quad [2.15]$$

2.4. Light extinction by a cloud of particles

This section 2.4 presents calculation results for some basic situations, which illustrate the specific role of the fine particles for the technology concept. Three types of cloud are investigated:

- Stationary mono-dispersed clouds show the dependence of light extinction on particle sizes and light wavelengths.
- The example of a two-species cloud interprets the relative contributions of different components to the light obscuration and its temporal profile.
- The example of a nine-species cloud is considered for the purposes to compare the optical data with conventional inertial impaction data (NGI) and to discuss issues related to the volume concentration of airborne material and particle sizes.

We consider light with the wavelength range from 400nm to 900nm, assuming that this range is less affected by the material absorption (electron excitations and molecular vibrations). In all further calculations the refractive index of particles is a real value and equal to 1.25 (being typical of drug particles).

2.4.1. Stationary mono-dispersed clouds

Consider the collimated beam of a monochromatic light source illuminating an aerosol cloud that consists of mono-dispersed spheres. The particles are homogeneously distributed in the cloud and possess a volume concentration of 10ppm (parts per million). The cloud thickness in the transmission direction is 1cm. The light transmittance through this cloud is calculated by equations [2.8] and [2.13] for

a single type of particles ($N_i = 1$). The extinction coefficient and the Mie coefficients are calculated using the MatLab code developed by D.M. Barnett (Barnett, 2000). Figure 2.2 shows the light transmittance as a function of the particle diameter at three light-wavelengths.

This dependence shows that for a fixed volume concentration of the airborne drug material, the optical attenuation is highest for particles of a certain diameter, the value of which slightly varies around $1\mu\text{m}$ with the light wavelength. For the pulmonary delivery the most important particles (the fine particles, section 1.3.3.a) are approximately in the size range from $0.5\mu\text{m}$ to $5\mu\text{m}$. It seems that the light wavelength of 650nm is a good choice for optical sensing of the pulmonary delivery due to a high sensitivity to the fine particles and a negligible absorption in the case of typical drug formulations. For a multi-species cloud the spectral optimum of the maximal “sensitivity” may depend on formulation and aerosol properties and has to be established experimentally for a given set of a drug formulation and a delivery device.

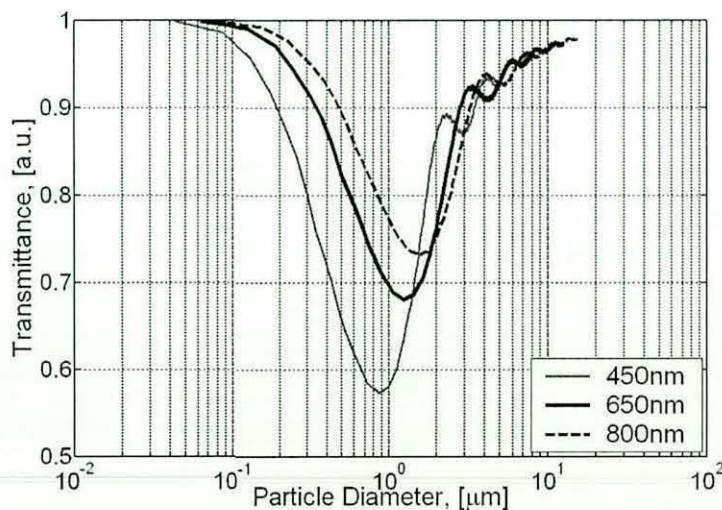


Figure 2.2. Transmittance as a function of the particle diameter for three different wavelengths of light

Note that these results are based on many assumptions (which have been made to simplify the calculation) and, therefore, have only qualitative viability. One of the areas where significant discrepancies can appear is the drug formulations based on

relatively large and porous particles of small aerodynamic sizes. In this case a much more complex model for light extinction by particles must be employed.

2.4.2. A dynamic cloud containing two species

A key feature of the technology implementation that we propose is that it is sensitive to the dynamics of the cloud, not only in terms of its density but also in terms of its homogeneity. In making the hypothesis that the distribution of particles in the drug cloud is not homogeneous, it is also implied that the degree of inhomogeneity will characterise the actuation, formulation, device and user. One way in which the cloud might be inhomogeneous is in terms of the spatial distribution of particle size and this might be a consequence of the dissociation and entrainment mechanism of cloud formation. To illustrate the effect of combining particles in a cloud, consider a simple case in which the cloud is composed of two types of spheres: $d_1 = 1\mu m$ and $d_2 = 6\mu m$. For the purposes of illustration, assume that both particle clouds follow a Gaussian type of distribution in space and are displaced from each other. If the combined cloud moves as a whole with a velocity V_{cl} , then the temporal variation of the volume concentration for each species is described by the equation [2.3] and takes the following forms:

$$C_{v1}(z_d, t, d_1) = C_v \exp\left[-\frac{(z_d - V_{cl}t)^2}{\varepsilon_1^2}\right] \quad [2.16]$$

$$C_{v2}(z_d, t, d_2) = C_v \exp\left[-\frac{(z_d - V_{cl}t + \phi)^2}{\varepsilon_2^2}\right] \quad [2.17]$$

where $C_v = 10ppm$ is the maximal volume concentration, ε_i is the standard deviation for each distribution and z_d is the spatial coordinate of the sensor position chosen along the cloud propagation axis, the time origin ($t = 0$) is when the front edge of the cloud approaches the sensor position z_d . A phase difference ϕ reflects the spatial displacement between the two clouds. The particle distributions are graphically presented in Figure 2.3 by the dotted and dashed lines, for particles of $1\mu m$ and $6\mu m$ diameters respectively.

For this combined cloud we calculate the optical obscuration as a function of time $Obs(t) = 100\%[1 - I(t)/I_o]$ at the light wavelength of 650nm. The transmittance is calculated using equations [2.19] supposing that for each moment of time there are two particle components controlled by equations [2.20] and [2.21]. The solid line at the figure 2.3 presents the obscuration profile of the combined cloud. At the same volume concentrations, at the maximums of individual distributions, the obscuration is 25% and 4% for particles of the $1\mu\text{m}$ and $6\mu\text{m}$ diameter, respectively.

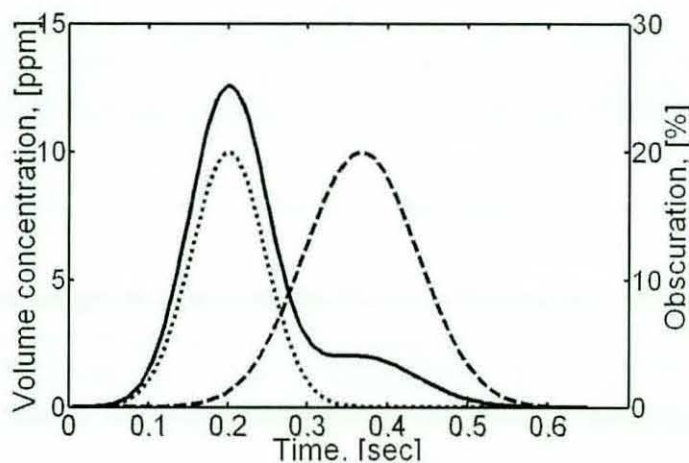


Figure 2.3. The model calculation provides the obscuration of a dynamic cloud (the solid line), propagating with velocity of 3 m/sec and containing two particle types. The dashed and dotted lines present the dynamic volume concentrations for the $6\mu\text{m}$ spheres and the $1\mu\text{m}$ spheres, respectively.

Clearly the obscuration measurement does not resolve the complex issue between the particle volume concentration and the particle size distribution, however, it may be able to detect the presence of the fine particles. Indeed, this example shows that the cloud with maximal concentration of 10ppm induces a light obscuration of approximately 4%, if particles are spheres of $6\mu\text{m}$ diameter, while for the $1\mu\text{m}$ spheres the obscuration rises to over 25%.

There are two main conclusions from this simple example. Firstly, for the same mass of the drug formulation the higher obscuration takes place if more particles deagglomerate to sizes of around $1\mu\text{m}$. Therefore, the optical obscuration can be a measure of the fine particle dose of an individual actuation, but only if the total

doses have the same load of the same drug formulation. Secondly, although particles larger than $6\mu\text{m}$, contribute significantly less to the obscuration, their effect is not negligible. Therefore, a non-Gaussian profile of the obscuration can be explained either by a non-Gaussian spatial distribution of the fine particles or by a spatial separation of the cloud species, which may individually follow a Gaussian distribution.

This experiment shows that the interpretation of optical data requires a cautious and thorough analysis in each specific application. In the next section we consider one example of such an interpretation in relation to NGI measurements.

2.4.3. Multi-species clouds and NGI measurements

For further investigation of the role of the particle-size distribution on the optical obscuration we consider a nine-species aerosol, which establishes a direct relationship with the data obtained by the Next Generation Pharmaceutical Impactor.

The performance of a pulmonary drug delivery system is normally evaluated by means of a multi-stage cascade impaction system (see section 1.3.3). The Next Generation Pharmaceutical Impactor (NGI) is the most advanced device for testing the pulmonary delivery systems (Asking *et al.*, 2003). The NGI system consists of nine impaction stages. Each stage collects particles of the specified aerodynamic sizes and is characterised by the median of the diameter distribution (D_{50}). The median parameters for the NGI system are ranged from $0.13\mu\text{m}$ to $10\mu\text{m}$: $10\mu\text{m}$, $7.8\mu\text{m}$, $4.6\mu\text{m}$, $2.7\mu\text{m}$, $1.6\mu\text{m}$, $0.9\mu\text{m}$, $0.5\mu\text{m}$, $0.3\mu\text{m}$ and $0.13\mu\text{m}$. The result of the NGI measurement is the distribution of the drug mass over particle aerodynamic-sizes accordingly to the drug mass collected on each stage.

There is no attempt to solve precisely the reverse problem in this complex case due to the ambiguity of the optical responses (see section 2.4.2). Instead, the model describes the relative contribution of different species to the optical obscuration by an aerosol cloud with the particular specified properties and discusses the issues of the aerosol density (the volume concentration of the airborne material) and the fine particle dose.

2.4.3.a. Model equations and further assumptions

The NGI data present the mean values of a whole aerosol cloud; and very often the averaging process takes place not only for a single cloud, but also over several consecutive actuations (often 5) due to the existing limits for the drug detection. Therefore, the NGI data provide no temporal variations of the aerosol cloud. On the contrary, the proposed optical technology is intended to characterise a single actuation and an inhomogeneity in a single cloud. For illustrative purposes, we introduce, as an example, a Gaussian distribution for all sub-clouds and for the cloud as a whole. Equation [2.1] is modified for the nine-species cloud, where $\varepsilon_i = \varepsilon_o$ and $\phi_i = 0$ are the same for all sub-clouds:

$$C_v(z) = \sum_{i=1}^9 C_{vi} = C_{vo} \exp\left[-\frac{(z_o - z)^2}{2\varepsilon_o^2}\right], \quad [2.18]$$

$$C_{vi}(z, d_i) = f_i C_{vo} \exp\left[-\frac{(z_o - z)^2}{2\varepsilon_o^2}\right], \quad [2.19]$$

where C_{vo} is a parameter for the volume concentration and f_i are parameters for the volume fraction of different species. The volume fractions are defined via the mass ratios $f_i = m_i / \sum_{i=1}^9 m_i$ and assumed constant throughout the entire cloud.

Using equations [2.12], [2.9], [2.18] and [2.19] the extinction coefficient and efficiency can be expressed in the following:

$$\gamma(\lambda, f_{1..9}, d_{1..9}) = \frac{3\lambda^2 C_v}{\pi^2} \sum_{i=1}^9 \frac{f_i q_i(\lambda, d_i)}{d_i^3} \quad [2.20]$$

$$q_i(\lambda, d_i) = \sum_{n=1}^{n_c} (2n+1) \Re[a_n(x_i(\lambda, d_i)) + b_n(x_i(\lambda, d_i))] \quad [2.21]$$

where C_v is the total volume concentration of the drug formulation and d_i are the median particle diameters for the NGI stages. Note that the extinction coefficient is

strongly dependent on the particle sizes, the particle fractions and the light wavelength.

The purpose of the model is to investigate the effect of the volume concentration and the fine particle fraction on the optical extinction. Therefore, the volume concentration is treated as a parameter with a wide range of values. In reality the volume concentration can be estimated from the experimental data:

$$\langle C_v \rangle = \frac{\sum_{i=1}^9 m_i}{\rho \int_{t_1}^{t_2} F(t) dt} \quad [2.22]$$

where m_i are the drug masses at the NGI stages, ρ is the material density of the drug, $F(t)$ is the flow rate and t_1 and t_2 are the times of the cloud observation. Aspects of the flow measurement and specifics of the flow interaction with the drug formulation are irrelevant to the proof of the technology concept and exceed the scope of this thesis.

The further calculations (sections 2.3.3.b and 2.3.3.c) are performed using the data of one real measurement by NGI. The drug formulation, for this data, is a mixture of salbutamol sulphate (40%), micronised through a milling process, and Respitose (60%) with a particle range from 45 μ m to 90 μ m. Five consecutive actuations were analysed as one averaged set of NGI data. Table 2.1 shows the NGI data, the mean values of the drug mass collected on each stage. The metered dose of the actuation is 263 μ g, the mean emitted dose is 232.04 μ g and the fine particle dose is 226.19 μ g. The fine particle dose (FPD) equals the sum of the stages from 2 to 6, inclusive, for the further definitions please refer to section 1.3.3.a. Note that lactose particles contribute neither to the chemical analysis of NGI measurements nor to the optical measurements. The extinction coefficient for such large particles as Respitose powder is much smaller than for the micronised drug particles. Therefore, the Respitose particles introduce only a negligible obscuration (this has been confirmed by the experimental data, presented in Chapter 4).

Table 2.1. NGI data on particle size distribution.

	Throat	Stage 1	Stage 2	Stage 3	Stage 4	Stage 5	Stage 6	Stage 7	Filter
D_{50} , [μm]	>10	7.8	4.6	2.7	1.6	0.9	0.5	0.3	0.13
Real cloud, [μg]	0.72	0.72	5.36	39.74	94.56	62.98	10.02	1.64	16.30
Hypothetical cloud, [μg]	135.0	135.0	5.0	5.0	5.0	5.0	5.0	5.0	5.0

2.4.3.b. Concentration issue

The issue of the concentration range, at which the VariDose technology can be successfully applied for the purposes of assessing the pulmonary delivery, is discussed using two examples of the drug cloud, presented in Table 2.1: the real and hypothetical clouds.

Using equations [2.20] and [2.21] we calculate the optical obscuration $Obs = 100\%[1 - I/I_o] = 100\%[1 - \exp(-\gamma L)]$ assuming different values of the volume concentration (C_v) and keeping the species ratios at a constant. In the other words, we calculate the obscuration as the airborne mass of particles increases keeping the particle fractions f_i ($i = 1, 2, \dots, 9$) constant. The L parameter equals 25mm and describes the geometry of the optical sensor (please refer to Chapter 3).

Figure 2.4 shows the monotonic increase of the optical obscuration up to a complete obscuration. In reality the complete obscuration does not happen because the model assumptions are broken at sufficiently high optical density. Indeed, at high particle concentrations the collimated beam transforms into a diffuse illumination of the turbid medium due to a significant multi-scattering. In that case the light propagation is normally described through a diffusion theory (Ishimaru, 1978; Cheong *et al.*, 1990), and the transmitted intensity would be determined via the diffusion coefficient rather than scattering. One can see that the concentration range also depends on the light wavelength. The figure 2.4 shows that for this given particle-

size distribution the blue light ($\lambda = 450\text{nm}$) would be more appropriate for assessment of the lower doses, while the near infrared light ($\lambda = 800\text{nm}$) would be better for the slightly higher doses.

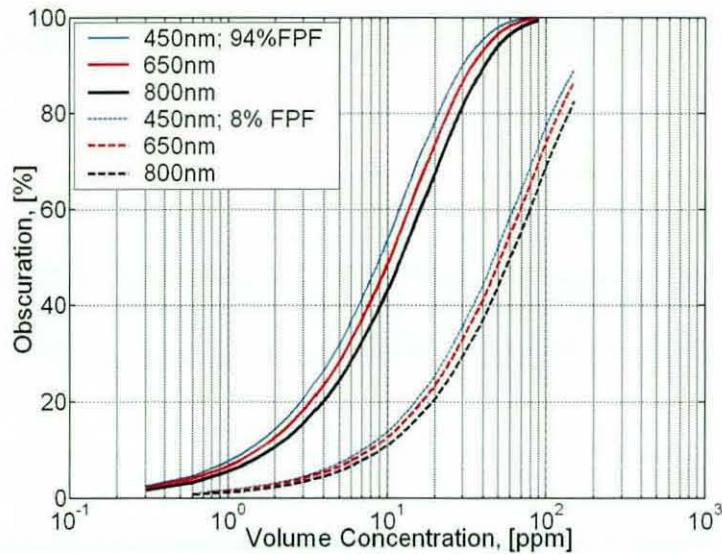


Figure 2.4. Optical obscuration as a function of the volume concentration.

The given example of the real cloud is characterised with an extremely high fine particle fraction of 94%. For such drug formulations (the solid lines on Figure 2.4) the volume concentration of 20ppm probably would be too high for the model assumptions. For a different drug formulation or a different delivery device, when the fine particle fraction can be significantly lower, the concentration limit could be higher. For comparison, the dashed lines present the optical obscuration for a cloud containing 8% of the fine particles and the same delivered dose (the hypothetical cloud in Table 2.1). Indeed, for the same obscuration level (for example 40%) the volume concentration increases by 5 times: from 8ppm to 40ppm for the light wavelength of 650nm.

This numerical investigation shows that the volume concentration of 20ppm may be considered as the applicability limit for the VariDose technology, which is aimed to produce clouds with a substantial amount of fine particles. Although, if the drug formulation fails to de-agglomerate, the obscuration would be low and dose

assessment could be performed on a cloud with the volume concentration of the airborne particles up to 100ppm (0.01%). For applications where a different range of particle sizes has to be assessed, this model can be used to evaluate the concentration limit of the method's applicability.

The other conclusion is that at a given volume concentration the obscuration value measures the dispersion of the drug formulation: the higher the obscuration is, the higher is the fine particle fraction. For example, at the volume concentration of 10ppm and the light wavelength of 650nm the obscuration of 48% would correspond to the FPF of 94%, while the obscuration of 12% would indicate a poor de-agglomeration with the FPF of 8%. Therefore, for the given metered dose of the drug formulation the optical obscuration can characterise the fine particle fraction in the released aerosol, which is the most important and highly unpredictable parameter in the pulmonary delivery.

2.4.3.c. A dynamic cloud and fine particles

In this section we investigate the optical obscuration of a moving cloud and the 'signature' of the fine particles on the obscuration profile. We continue to consider nine types of particles relevant to NGI data (refer to Table 2.1). These particles are divided into three groups, which present three types of the particle behaviour in the pulmonary delivery:

1. The finest particles with aerodynamic diameters of $0.3\mu\text{m}$ and $0.13\mu\text{m}$ are collected on stage 7 and the final filter of the NGI system. They are normally thought of as being exhaled from the lung and therefore not contributing to the lung deposition.
2. The fine particles with an aerodynamic diameter between $0.5\mu\text{m}$ and $5\mu\text{m}$ are collected on four stages (from stage 2 to stage 6). They are usually regarded as being penetrated into the deep lung and considered as the lung deposition dose (the fine particle dose FPD).
3. The coarse particles with aerodynamic diameters of $7.8\mu\text{m}$ and $10\mu\text{m}$ are collected on stage 1 and the throat, and are normally related to the oropharynx deposition.

To separate the obscuration contribution from these three groups of particles, we introduce a canonical model experiment:

- The total volume concentration, the sum of all particles C_v^{total} , rises and falls sharply, and stays constant at 5ppm throughout the entire cloud forming a step-function (the solid line on Figure 2.5.a).
- The fine particles have a one-dimensional Gaussian distribution with the maximum of 5ppm and this extends throughout the entire cloud, $C_v^{FP}(z)$ (the dashed line on Figure 2.5.a). Partial fractions of different particles are kept constant over the distribution $f_i = m_i / \sum_{i=3}^7 m_i$ for the indexes from 3 to 7 (using as an example the data from Table 2.1).
- The finest particles are in the forward part of the cloud. The volume concentration of these particles, C_v^{SP} (the dotted line on Figure 2.5.a), is adjusted so that the sum with the fine particles produces the constant total value of 5ppm, $C_v^{SP}(z) = C_v^{total} - C_v^{FP}(z)$. Partial fractions of two components are $f_i = m_i / \sum_{i=8}^9 m_i$ for indexes 8 and 9 (using the data from Table 2.1).
- The coarse particles are in the rear part of the cloud. The volume concentration, C_v^{CP} (the dashed-dotted line on Figure 2.5.a), is complementing the fine particle distribution with the total particle concentration constant, $C_v^{CP}(z) = C_v^{total} - C_v^{FP}(z)$. Masses from stage 1 and the throat (Table 2.1) define the partial fractions of these two components, $f_i = m_i / \sum_{i=1}^2 m_i$, as an example.
- The entire cloud is moving at a constant velocity of 3m/sec.

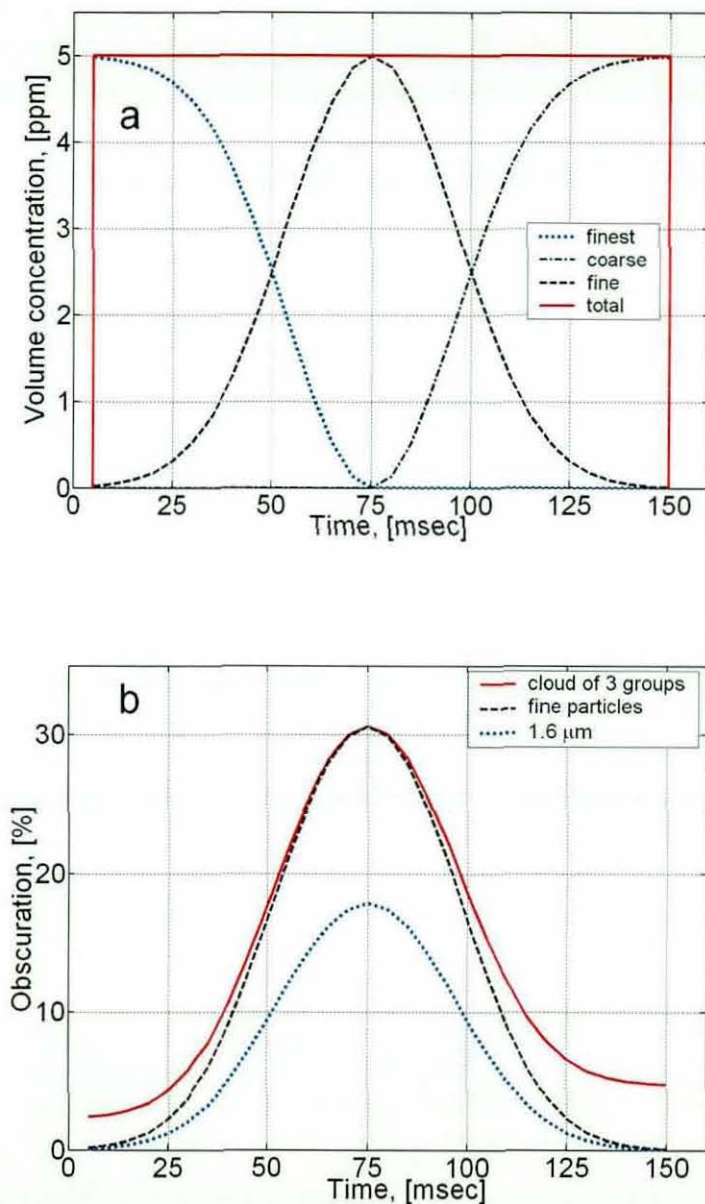


Figure 2.5. Light obscuration calculated for a canonical model experiment. The aerosol contains three groups of particles (finest, fine and coarse) and moves at a constant velocity through the observation plane: (a) presents distributions of the volume concentration for the particle groups; (b) compares the obscuration profiles of the total cloud, the sub-cloud of fine particles and the sub-cloud of mono-dispersed spheres of $1.6\mu\text{m}$ diameter.

Figure 2.5.a presents the profile of the volume concentration (the solid line) and locations of three sub-clouds: the finest particles (the dotted line), the fine particles (the dashed line) and the largest particles (the dashed-dotted line). The space

coordinate is converted to the time using the cloud velocity of 3m/sec to allow a direct comparison with the temporal profile of the obscuration (Figure 2.5.b).

Figure 2.5.b shows the obscuration profile for this cloud (the solid line), which is calculated exploiting the independent scattering by all particles and using equations [2.20] and [2.21] at the light wavelength of 650nm. For comparison, the light obscuration has been also calculated for the further two clouds. One of them contains only the fine particles and has the same particle distribution as in the sub-cloud of the fine particles in the multi-species cloud (the dashed line on Figure 2.5.b). This curve presents the contribution of the fine particles into the cloud obscuration. Another cloud contains only mono-dispersed spheres of 1.6 μm diameter and the particle distribution is identical to the sub-cloud of this type of particles in the multi-species cloud (the dotted line on Figure 2.5.b). This curve shows the contribution of these most efficient scatterers to the light obscuration of the entire cloud.

As one can see on Figure 2.5.b, at the volume concentration of 5ppm different particles obscure different amounts of the light intensity: for the finest particles it is 2.3%, for the coarse particles it is 4.7% and for the fine particle it is a massive 31%. When half of the airborne matter is fine particles and the other half is coarse particles, i.e. a fine particle fraction (FPF) of 50%, the cloud obscuration is 19%, the majority of which is caused by the fine particles (17%, the dashed line). For the cloud of finest and fine particles with FPF of 50% the results are similar with 18% and 17%, respectively.

Therefore, for actuations with a good particle dispersion, when the FPF exceeds 50% (please refer to the middle of the cloud on Figure 2.5), we can expect that the fine particles mainly cause the light obscuration; and the obscuration value can be regarded as a measure of the fine particle dose (FPD).

For actuations with a poor particle dispersion, when the FPF is less than 6% (please refer to the tail of the cloud), the light obscuration is mainly caused by the coarse particles; and the obscuration value characterises the emitted dose (ED) rather than the FPD.

For the majority of other cases, when the FPF is moderate, around 20%, the interpretation of obscuration data is not straightforward and requires a detailed analysis. The main steps of such analysis can be as following:

1. Estimate the volume of airborne matter by dividing the mass of the drug formulation on its material density.
2. Estimate the cloud volume by integrating the flow rate of the inhalation over the duration of the obscuration profile.
3. Then, estimate possible value of the volume concentration of the airborne matter by dividing the estimated volume of airborne matter on the estimated cloud volume (also refer to Equation [2.22]).
4. Calculate the light obscuration for different types of particles at this volume concentration using our model and compare the model values with the measured obscuration.
5. Due to the large difference in the obscuration efficiency for fine and other particles, the presence/absence of the fine particles can be established for each particular case, while a general relationship between the obscuration value and the FPD for any drug cloud is restricted by the optical ambiguity.

2.5. Summary

The developed model calculates the light obscuration of the collimated beam assuming an independent scattering by airborne particles. The cloud content is presented as an ensemble of different groups of particles, relative to particle sizes. Using the Beer-Lambert law for light extinction and the Mie theory for light scattering, the model calculated the light obscuration using a spherical approximation for the particle shape. The model shows that a relatively simple optical sensing may provide valuable information about the particle deagglomeration in the emitted aerosol, without attempting to solve a precise metrological problem. It has been shown that the fine particles, which are able to reach the deep lung and are the main objective in the pulmonary drug delivery,

possess the highest scattering efficiency in comparison to the other particle sizes at the wavelength range from 450nm to 800nm.

The model proved the main concept of the VariDose technology showing a selective sensitivity of the transmitted light to the fine particle fraction in the turbid medium. It also shows that temporal variation of the transmitted intensity of a collimated light beam may provide unique information on the cloud inhomogeneity, measured directly on an emitted dose and in-line with a patient. The presence of the fine particles is characterised by a higher optical obscuration, supposing the amount of the drug formulation is metered and is sufficiently low. The higher the fine particle fraction is, the higher is the obscuration. Therefore, it may be possible to calibrate the sensor to measure the fine particle dose for a particular drug formulation. Such a calibration curve may enable a fast and robust assessment of the pulmonary delivery systems without using metrological methods, which are normally invasive, time-consuming and not suitable for use in-line with a patient.

Using a prototype device and specially designed experiments the model conclusions are examined empirically and results are presented in Chapter 4.

Chapter 3

Method for in-line Assessment

This chapter describes a prototype device, data acquisition and analytical routine for efficacy characterisation of the pulmonary delivery in-line with a patient. This technology is called VariDose. Its aim is to measure the fine particle dose during an actual pulmonary delivery and to evaluate the dose variation due to ambient conditions. At this early stage of the technology development, the major objective was to prove the concept rather than to optimise the measurement parameters. A specific technical arrangement and analysis method have been developed and tested.

3.1. Prototype device.

The model developed in Chapter 2 shows that the light attenuation across the aerosol cloud strongly depends on the aerosol particles. It has been shown that not only optical properties such as refractive index and light wavelength control the light attenuation, but also the particle sizes and the particle distribution over the aerosol cloud. There is a strong indication that the measure of light attenuation can provide a signature of the particle content in the cloud. The simplest arrangement to measure the light attenuation requires a collimated beam of light and a light detector in the line-of-sight position. This pair of the light source and detector will be referred to as a 'sensor module' or a 'sensor'.

One of the possible positions of the sensor is perpendicularly to the direction of the cloud propagation. Consider an aerosol, discharged from an inhaler. The aerosol cloud is propagating from an inhaler to the respiratory system of a patient through a designated air-path. In this case the light attenuation is determined by particles within the illuminated volume of the moving aerosol. The value of light attenuation changes as the particle content of the illuminated volume changes due to the aerosol propagation. The temporal profile of attenuation contains a signature of the cloud dynamics. This information is rather limited and unable to resolve the complexity of particle distribution in space and time, however, it may still characterise the de-agglomeration of the drug formulation (see section 2.1).

The in-line requirement puts dimensional restrictions on an optical attenuation device: 1) the air-resistance of the device has to be much smaller than the inhaler's air-resistance; and 2) the device volume has to be much lower than the inspiration volume of a patient (usually 2L or 3L). A standard mouthpiece, a cylindrical tube of 25mm diameter and 65mm long, commonly used in clinical trials of inhalers, is a good mechanical base for the proposed technology. The air velocity through this tube is near 3m/sec at the flow rate of 60L/min. When an aerosol propagates through such a tube, the optical density increases from zero (no cloud) to the maximum value and returns to a small value, which results from a particle deposit on the tube (the wall residue). The average volumetric density of particles in a cloud is expected to be less than 1%.

3.1.1 Essential equipment

Figure 3.1 shows the essential components of the VariDose technology. A patient, or a breathing simulating machine, or a vacuum pump can provide airflow. The airflow actuates an inhaler device creating the particle cloud. The cloud propagates through a glass tube and the sensor module makes measurements at a given distance from the inhaler's mouthpiece. All connections in the flow path are airtight and the tube is screened from the ambient light.

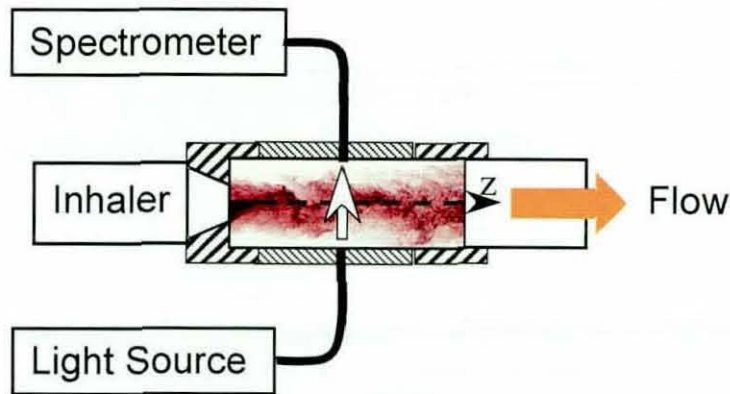


Figure 3.1. Schematic diagram for optical characterisation of the pulmonary drug delivery.

The collimated light beam is formed by a SELFOC ® fibre collimator and Ocean Optics tungsten halogen light source (bulb colour temperature 3,100°K). The SELFOC ® fibre collimator is comprised of a 0.25 pitch GRIN lens and a 200µm fibre with numerical aperture of 0.50 and beam divergence angle of 6.5°. The same fibre collimator is used for collecting the light passing through the cloud. An Ocean Optics fibre optic variable attenuator FVA-UV controls the illuminating intensity.

3.1.2. Measurement volume

For an optical characterisation there is always a question about the measured sample. The incident light may interact with an entire cloud or only with a limited part of the cloud. The light leaving the aerosol cloud could be collected as a whole or at strategic places. The geometry of the illuminating beam and collecting optics defines the volume of the cloud that actually takes part in a given measurement. This volume

is often referred as the measurement volume or the measurement sample. The choice of the right sample is essential for the success of any optical technology.

For this pilot investigation the collimated light illuminates a cylindrical volume of 1.9 millimetres diameter (d) and 25mm length (the diameter of the glass tube L). Figure 3.2 illustrates how the measurement volume depends also on the cloud velocity V_{cl} and the integration period τ of the detector; and Equation [3.1] expresses this dependence in mathematical form:

$$V_{sample} = \left(V_{cl}\tau d + \frac{\pi d^2}{4} \right) L \quad [3.1]$$

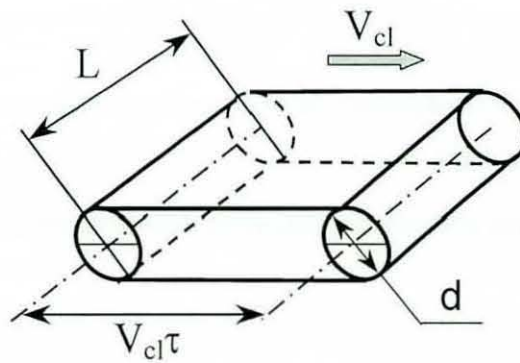


Figure 3.2. Schematic presentation of the measurement sample. A collimated beam of light illuminates a cylindrical volume at any single moment. During the measurement time, τ , the measurement sample increases accordingly to this scheme.

This measurement volume could be considered as a representative sample of the cloud and at the same time it allows the dynamics of the aerosol development to be followed. The optimisation of the volume size requires future research and a further, narrower specification for the system.

3.1.3. Sensor position

The position of the sensor down the stream of propagation produces a profound influence on the aerosol sample that has been actually measured. For example, if the sensor were adjacent to the mouthpiece of the inhaler, the measurement would characterise particles in the immediate vicinity of the inhaler. In the case of p-MDI these would be fast-moving droplets of relatively large sizes. The sensor placed, for example, 20cm down the stream would measure droplets of the smaller sizes due to evaporation and these droplets are moving slower due to relaxation to the velocity of the flow.

The sensor records an accumulative effect of temporal and spatial variations in the cloud (see Chapter 2). The right position for the sensor depends on the aims and purposes of the measurement. For example, multiple sensors placed along the cloud path may provide information on the cloud development. For pulmonary delivery the aim is to characterise the cloud that is entering the respiratory system. In this case, the cloud in the middle of the mouth represents a viable sample of the particles, which would be available for deep lung deposition. In the prototype device for VariDose technology a distance of 55mm from the inhaler mouthpiece has been used. This arrangement allows analysis of the drug cloud, which would be developed approximately in the middle of the patient's mouth and introduces only a small (~30ml) extra volume for a patient to inhale.

Particles moving along the glass tube are experiencing gravity and interaction with the tube walls. As a result, the walls are constantly contaminated with particle sediment. The wall sediment affects the intensities of the illuminating and collected light. The residue of fine particles can be taken into account by the data analysis and may even contribute to the aerosol's characterisation. On the contrary, large particles can considerably distort the measurement if one particle accidentally falls onto the optical window. To reduce the contamination of optical windows by large particles the attenuation measurement is performed in the horizontal plane.

Figure 3.3 shows a set of the laboratory prototype device including: the sensor head, a light source, a breath-simulating machine and a spectrometer. As an example, on this picture VariDose is connected with a Turbohaler®, a reservoir dry powder

inhaler. Out side the U.K. this inhaler is commonly known as Turbuhaler. The auxiliary gas exchange cylinder prevents contamination of the breathing simulator with drug particles.

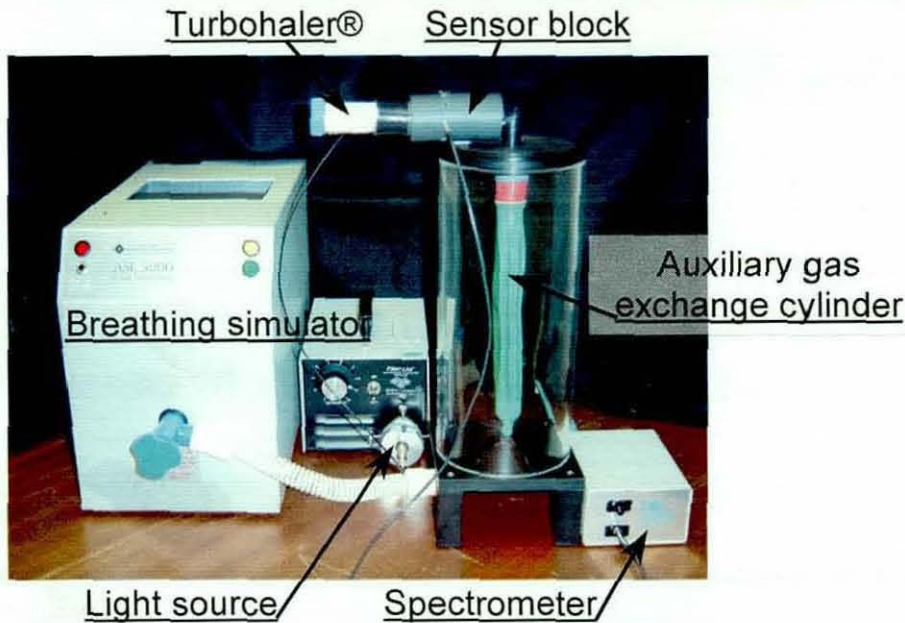


Figure 3.3. Prototype device for VariDose technology.

3.2. Data Acquisition.

According to the model of VariDose technology, the data to be acquired are values of light intensity as a function of time. A light detector provides a signal that is proportional to the number of photons accumulated by the detector during the measurement period. The measurement period is a time period and is often referred to as the integration time for the detection system. The detector's readings are streamed to computer memory with the time stamps, using an appropriate integration time. A computer stores the data for further analysis. The light intensity, detector's sensitivity and the integration time are the main variable parameters, which control the accuracy and efficiency of the measurement. At this stage of the technology development, the major objective was to prove the concept rather than to optimise the measurement parameters. Therefore, a readily available acquisition system with approximately suitable parameters has been used. The acquisition system consists of

an Ocean Optics spectrometer S2000 and A/D converter ADC2000-PCI. The use of a spectrometer also permits an experimental evaluation of the spectral sensitivity.

3.2.1. Acquisition frequency.

The measurement object normally dictates the technical requirements for the acquisition system. The object for VariDose technology is an aerosol of particles. The aerosol is released by a delivery device and therefore possesses such characteristics as volume, the start and the end of the cloud release, particle properties and the propagation velocity. The cloud volume and geometric dimensions of the passage define the cloud length, which can be expressed in units of time or length. A single optical sensor records the light intensity as a function of time; therefore each actuation is characterised by a temporal profile of light intensity. The question is how many measurement points are needed to be sufficient for an adequate characterisation of the cloud?

A typical requirement for airflow in the pulmonary drug delivery is 60L/min. An average person can inhale an air volume of 2.5L. This means that the inhalation duration is in the range of a few seconds. For successful delivery, the drug cloud has to occupy only the front part of the inhaled volume. Only then can the drug particles reach the end of the conducting zone of the lung in one second, allowing particles to penetrate to the deep lung during the remaining period of inhalation. In the 25mm diameter tube the flow rate of 60L/min corresponds to an air velocity of 3m/sec. The duration of the cloud (the temporal length of the cloud) may be well under one second. Ocean Optics supplies readily available systems with the acquisition rate of 200Hz. This frequency seems a suitable start for development of the proposed technology. The minimal integration time is 5 milliseconds allowing 20 data-points for a profile of 100 milliseconds.

3.2.2. Attenuation value.

Each set of experimental data is a two-dimensional array of light intensity in the time-spectral field. The scattered losses of the collimated light are measured as an obscuration: a percentage of the light-intensity, which has been lost due to the scattering $Obs(\lambda, t) = 100 \cdot [1 - I(\lambda, t)/I_o(\lambda)]$, where $I(\lambda)$ and $I_o(\lambda)$ are intensities

of transmitted and illuminating light, respectively. The illuminating intensity may slightly fluctuate due to variations of the ambient conditions and would be reduced by the particle deposition on the walls of the air-passage. Therefore, the transmitted intensity through the sensor tube without the cloud is regarded as the incident intensity $I_o(\lambda) = \langle I(\lambda, t_o, \Delta t) \rangle$, where t_o , Δt is the time and the averaging period, respectively. To address the issue of measuring the transmitted light just before the cloud entering the measurement volume, a special triggering procedure is employed.

3.2.2.a. A spectral variation of the light obscuration.

We have discussed in Chapter 2 that the particle-light interaction depends on particle properties, both material and geometrical, and also on the light wavelength. We may expect that a spectral variation of the optical obscuration will be caused by properties of the drug formulation. In this thesis, spectral variations of the obscuration have been studied on a few standard drug formulations in the spectral range of 350nm to 850nm. This range is chosen to avoid the light absorption by electrons and phonons. In future research this material absorption can be used for gaining additional information about the drug in the cloud. For example, the drug might be marked with a strong optical absorption/emission line, and then the obscuration at this particular wavelength would be proportional to the drug amount.

The obscuration at the given light wavelength λ_i is obtained from the recorded two-dimensional array of light intensity in the time-spectral field using the following formula:

$$Obs(\lambda_i, \Delta\lambda, t, \Delta t) = 100 \cdot \left(1 - \frac{\langle I(\lambda_i, \Delta\lambda, t) \rangle}{\langle I(\lambda_i, \Delta\lambda, t_o, \Delta t) \rangle} \right), \quad [3.2]$$

where $\Delta\lambda$ is the spectral range for a few adjacent pixels of the spectrometer and the brackets $\langle \dots \rangle$ denote averaging.

3.2.3. Triggering issues.

The acquisition triggering is arranged in such a way that there are a few detector readings before the particle cloud reaches the observation plane. The mean value of these readings is taken as the illuminating intensity for the entire measurement of a cloud actuation. In this way, each measurement has the actual intensity of the light illumination.

In most cases measurements can be triggered when the flow rate of the inhalation has reached a particular level. In cases, when airflow is created by a vacuum pump or when a p-MDI inhaler is not breath-actuated, the synchronisation of the actuation and the acquisition is difficult and a manual triggering is preferable. The manual triggering requires more computer memory per cloud-actuation and some skills from an operator.

3.2.3.a. Software control.

A virtual instrument developed using the LabView software controls the data acquisition. A standard code supplied by the spectrometer manufacturer was used in subroutines for the software control of the acquisition process.

3.3. Data Analysis.

The model of the VariDose technology shows the relationship between the aerosol content and the light obscuration at a given wavelength. The current technical solution for the technology provides a spectrum of the transmitted light intensity for every 5 milliseconds. This two-dimensional array of data allows the extraction of an obscuration profile as a function of time for a given spectral range. Figure 3.4 presents a few examples of obscuration profiles for a drug cloud released by an inhaler at the narrow spectral range of 648nm to 666nm. In general, profiles can be quite different due to the complexity of the cloud formation.

How do we compare and assess them? Ideally we are looking for a single value deduced from the obscuration curve. A desirable feature of this value is a monotonic dependence on the success of the drug delivery.

The shape of the profile is similar to the shape of emission/absorption lines in spectroscopy. Analogous to spectroscopy, the profile can be characterised by the position of the maximum (the peak position), the maximal value (the peak value) and the full width of the half maximum (FWHM). An analytical procedure has been developed to smooth the experimental data and to define basic characteristics for the measured profiles.

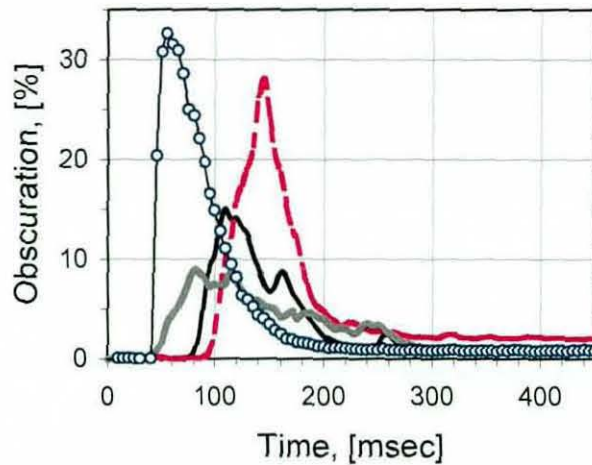


Figure 3.4. Examples of the light-obscuration profile for an aerosol cloud released by an inhaler. These profiles present different actuations of Bricanyl® Turbihalers® at the flow rate of 60L/min.

The possible physical meanings of these parameters are introduced and discussed in this section. Here we also consider and decide on the optimal spectral range for the assessment of the fine particle dose in the case of a dry-powder inhaler.

3.3.1. Mathematical fit to an obscuration profile.

The analysis procedure starts with fitting a smooth mathematical curve to the experimental data. The best fit has been achieved by a sum of two functions with seven fitting parameters. Figure 3.5 shows an example of the fitting result.

A lognormal function describes the smooth variation of the obscuration due to the presence of suspended particles in the air (curve 1):

$$y_1(t) = A \frac{\exp\left(-\frac{\{\ln[(t-a)/\xi]\}^2}{2\varepsilon^2}\right)}{(t-a)\varepsilon\sqrt{2\pi}} \quad [3.3]$$

where y is the obscuration data, t is the time variable and A , a , ξ and ε are the fitting parameters. The fitting parameters reflect the position and the shape of the curve 1 and are described in Table 3.1.

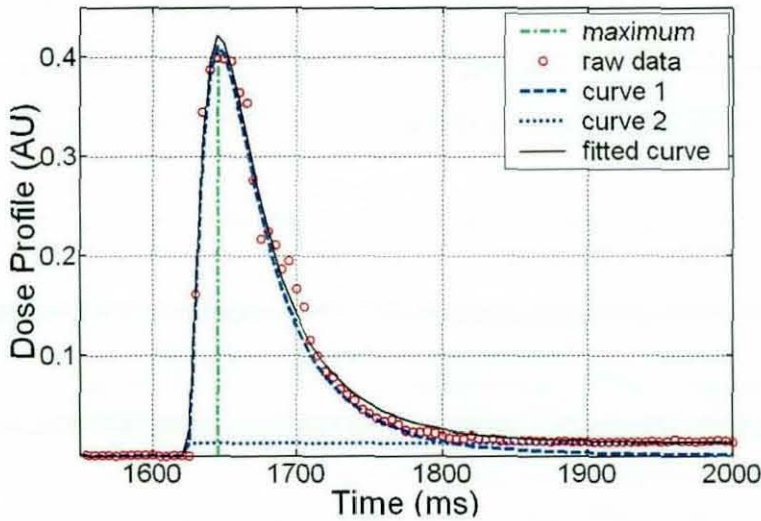


Figure 3.5. An example of mathematical fitting to experimental data.

A smooth transition between two levels (curve 2) is describes by the following formula:

$$y_2(t) = R\{1 - \exp[-\alpha(t-b)]\} \quad [3.4]$$

This function has three fitting parameters, R , α and b , and presents the light losses due to the particle residue on the walls. The zero attenuation level corresponds to clean walls and non-zero levels result from the particle residue. Physical meanings for the fitting parameters of this function are listed in Table 3.1.

Table 3.1. Description of fitting parameters.

Fitting parameter	Description
A	Relates to the peak value and characterises the maximal obscuration by an aerosol cloud.
a	Reflects the peak position and mainly characterises the triggering process.
ξ	Relates to the time and might characterise the cloud velocity.
ε	Reflects the shape of the curve and characterises the FWHM.
R	Characterises the obscuration level by the particle residue on the walls.
α	Reflects the slope of the transition between two levels and might characterise the wall deposition rate.
b	Reflects the position of the slope and characterises only the triggering process.

Calculating the root mean square (rms) between the fitting function $y = y_1 + y_2$ and the experimental data, a computer program performs the iteration process to find the best fit. Final fitting parameters and the value of rms are used for characterisation of the aerosol cloud. The fitting parameters a, b reflect only the synchronisation between the cloud actuation and the start of data acquisition, and therefore do not contribute to the aerosol characterisation.

3.3.2. Aerosol characterisation.

The shape of an obscuration profile suggests possible parameters, which can be deduced and used for the aerosol characterisation. The most obvious parameter is the degree of deviation from the fitted curve. The root mean square estimates these deviations and may characterise the cloud homogeneity. The other interesting parameter is the maximum of obscuration, which according to the model (Chapter 2)

may be an indicator for the fine particle dose. There is a small obscuration that remains at the end of the profile when the entire cloud has passed the sensor module. This remaining obscuration results from particles deposited on the walls and may characterise drug losses during propagation. Time-related parameters might measure the length and the asymmetry of the cloud.

3.3.2.a. Cloud homogeneity.

Inhomogeneous distribution of particles over the cloud causes fluctuations of the recorded obscuration. The large chunk of agglomerated particles strongly obscures the light beam, while a lack of fine particles results in a high transparency and a low obscuration. Fluxes of air turbulence create areas of higher and lower densities of the fine particles. This inhomogeneity results also in the obscuration fluctuations. The homogeneity (H) of the aerosol cloud has been estimated by calculating the following value for the fitting results (y) and the measured data (Dat):

$$H = 100\% \left(1 - \frac{\sqrt{\langle (y - Dat)^2 \rangle}}{\langle Dat \rangle} \right) \quad [3.5]$$

$$\langle Dat \rangle = \frac{1}{N} \sum_{i=1}^N Dat_i \quad [3.6]$$

The mean value for the data set ($\langle Dat \rangle$) is calculated for the data points where the obscuration exceeds half of the maximal obscuration. In this way, if the data coincide with the fitted function the homogeneity equals 100%. This means the particles of all sizes are smoothly distributed over the cloud and there are no large chunks of agglomerates. Deviations from the fitted function result from lower homogeneity.

3.3.2.b. Fine particle dose.

The most important parameter for pulmonary drug delivery is the amount of fine particles, which actually reach the deep lung during a particular actuation. As we have discussed, the issue of the fine particle dose is a very complex matter with

respect to the aerosol formation (refer to section 1.3.). There are many components which affect the entrainment and development of an aerosol: 1) the delivery device itself; 2), the drug formulation; 3) ambient conditions such as temperature and humidity; 4) the patient's respiratory effort and the profile of the flow rate.

The light obscuration is also a result of complex interactions. Light interacts with a particle ensemble. If the number of particles in the ensemble, their geometrical and optical properties, are known the light obscuration is strictly defined and can be readily calculated. Unfortunately, there exists an ambiguity between the total particle mass (volume concentration) and particle sizes. For example, a small amount of particles of 1 μ m diameter produces much higher obscuration than the same mass of the larger particles. And the same level of obscuration can be produced by a small mass of fine particles and by a much larger mass of coarse particles (see Chapter 2).

Despite this complexity, the peak value of the fitted curve 1 can be representative of the de-agglomeration level of the drug formulation if all mechanical and optical conditions are the same. This means that for a given inhaler, with a fixed dose of a particular drug formulation and at a fixed flow profile, the peak value of the light obscuration can characterise the degree of particle agglomeration.

The peak value of curve 1 is a major feature of the obscuration profile. It may characterise the fine particle dose in the aerosol cloud, which is the major parameter for the success of the pulmonary delivery. The main aim of this thesis is to seek the empirical support for this relation between the peak value of obscuration and the fine particle dose. Note that the peak value of curve 1 takes into account only the particles in the air, while the wall's residue contributes to curve 2.

3.3.2.c. Wall residue.

Particles deposited on the tube walls reduce the light intensities of the incident and transmitted beam. The remaining obscuration, recorded by the sensor after the cloud has passed, is a characteristic measure of this particle sediment on the walls. The ratio of the mean obscuration, caused by the sediment and the suspended particles, presents a units-independent value and can be expressed as a percentage:

$$\Lambda = 100\% \frac{\sum_{i=1}^N y_2(t_i + \Delta)}{\sum_{i=1}^N y_1(t_i) + \sum_{i=1}^N y_2(t_i + \Delta)} \quad [3.7]$$

Averaging is performed over the same number of data for both fitted curves. For the curve 1 the data are for the time-moments when the obscuration is higher than half of the maximum. For the curve 2 the data are for the same time-period at the end of the recorded profile. The time delay, Δ , reflects the fact that the data for the sediment evaluation are taken later than the data for the cloud evaluation, i.e. when the entire cloud of suspended particles left the sampling area. The value of this time delay depends on the cloud length and can be set as a multiple of the full width of the half maximum (FWHM). This ratio provides a characteristic number for comparing dose-actuations within the same experimental set-up.

The meaning of this parameter for the pulmonary delivery reflects the drug losses due to wall deposition at a given moment of the cloud propagation, which is defined by the sensor position. It should be noted that, although the number is expressed as a percentage, it possesses no metrological meaning: it does not mean that this percentage of particles has been deposited on the walls. The wall-residue parameter can be used only as a characteristic number for purposes of comparing different actuations in regards to drug losses due to the wall impaction.

3.3.2.d. Time related parameters.

There are a number of time-related parameters, which can be deduced from the obscuration profile. A few of them deal with the length of the profile. The full width at the half maximum (FWHM) is a common parameter for the characterisation of bell shaped curves. The FWHM time ($\Delta t_{FWHM} = t_1^{FWHM} - t_2^{FWHM}$) allows the calculation of the volume (M) of the cloud that contains the highest number of fine particles:

$$M = \int_{t_1^{FWHM}}^{t_2^{FWHM}} F(t) dt \quad [3.8]$$

where $F(t)$ is the flow rate of inhalation.

The time width of the profile can also be measured at the lower level of obscuration than the half maximum. In this case the fitted curve 1 provides the full length ($\Delta t_\chi = t_{\chi 2} - t_{\chi 1}$) of the cloud for a given level (χ) of the obscuration:

$$\begin{aligned}
 t_{\chi 1} &= \xi \exp(-\varepsilon^2(\psi + 1)) + a, \\
 t_{\chi 2} &= \xi \exp(\varepsilon^2(\psi - 1)) + a, \\
 \psi &= \sqrt{1 - (2/\varepsilon^2) \ln(\chi \xi \varepsilon \sqrt{2\pi}/A)},
 \end{aligned}
 \tag{3.9}$$

where A , a , ξ and ε are final parameters of the best fit.

The curve 1 can be highly asymmetrical. Mathematically it is easy to introduce an asymmetry parameter, using the coordinate of the maximum and the level interceptions:

$$\begin{aligned}
 t_{\max} &= \xi \exp(-\varepsilon^2) + a, \\
 \text{Asymmetry} &= \frac{t_{\max} - t_{\chi 1}}{t_{\chi 2} - t_{\max}}
 \end{aligned}
 \tag{3.10}$$

In some cases the asymmetry parameter may suggest the location of the fine particles in the cloud: in the front, in the centre or in the tail of the released aerosol. One should be very cautious in making this type of conclusion due to the ambiguity of the light obscuration.

Of special interest is the area under the fitted curve 1, which can be found by calculating the integral between two given points:

$$\Sigma = \int_{t_1}^{t_2} y_1(t) dt = \frac{A}{2} \operatorname{erf} \left[\frac{\ln((t-a)/\xi)}{\varepsilon\sqrt{2}} \right]_{t_1}^{t_2}
 \tag{3.11}$$

The physical meaning of the area is speculative and requires further investigations. Table 3.2 summarises the characterisation parameters and their physical meaning, based on generally accepted knowledge.

Table 3.2. Parameters for aerosol characterisation.

Parameter	Description and physical meaning
Peak value	The measure of the highest density of fine particles in a cloud. Defined as the maximum of the mathematically fitted function (eqn. [3.3]). The measurement unit is the percent of obscuration; it is possible to calibrate as the mass of fine particles for a particular inhaler-drug formulation combination.
Homogeneity	The measure of the cloud inhomogeneity such as large chunks and uneven cloud density. Defined as deviation from the exact fit using the root mean square eqn. [3.5]. The measurement unit is percent: 100% means complete homogeneity and the lower percentage means a higher inhomogeneity.
Residue	The measure of the tube contamination by formulation particles after the passage of the cloud. Defined as the ratio of the average obscuration by the cloud and the remaining obscuration (eqn.[3.7]). The measurement unit is percent. The higher the value, the larger the deposit on the walls and the higher the losses of the dose.
Length	The measure of the cloud volume. Defined as the time of the cloud propagation through the observation plane. The measurement unit is the millisecond. The volume is calculated by integrating the flow rate profile (eqn.[3.8]).
Asymmetry	The measure of the position of fine particles (FP) in the cloud. Defined as the ratio of the front half and the tail half of the cloud length (eqn. [3.10]). Value 1 means that the FP are in the middle; <1 in the front and >1 in the tailing part.

3.4. Spectral sensitivity.

We have developed the analysing routine that derives the quantified values from the shape of the obscuration profile and produces the indicator for the effectiveness of the pulmonary drug delivery. In the current experimental set-up the analysis can be performed at any light wavelength from the spectral range of the illuminating beam. An empirical investigation of which spectral range provides the better analysis was undertaken using the experimental data from Chapter 4. Two dry powder inhalers have been investigated, the AstraZeneca Turbohaler® and a novel prototype device. The Turbohaler® is characterised by a relatively high fine particle fraction (of around 70%) and a high variation of emitted doses (the coefficient of variation is around 25%). The novel inhaler is characterised by an extremely high fine particle fraction (over 80%) and a low coefficient of variation.

These two cases covered a significant range of the pulmonary delivery applications and may establish the range of light wavelengths, which is the most suitable for the assessment of the pulmonary-delivery effectiveness through the VariDose technology.

3.4.1. Spectrum of the illuminating beam.

The spectrum of the light intensity, recorded by a detector, is usually a combined characteristic of the light source, the detector's spectral sensitivity and the optical properties of the optical path. In the current set-up the spectral output of the light source is between 350nm and 950nm with the power increasing from the lower wavelength to the higher one. For the detector the best efficiency (>30%) is in the range from 350nm to 850nm and peaks at 650nm. Figure 3.6 presents spectra of the light, transmitted through the VariDose system and recorded by the spectrometer, for a clean system (without a cloud) and for the system during and after an aerosol cloud.

One can see that the entire spectral range of the current set-up is sensitive to the presence of the aerosol cloud. It is possible that different spectral ranges may have different sensitivities to the fine particles. The next section investigates the temporal profiles of the light obscuration against the light wavelength.

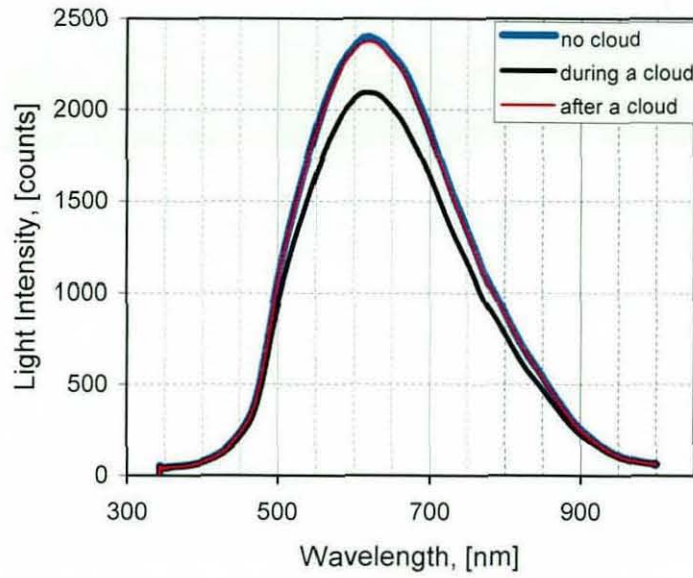


Figure 3.6. Spectrum of the illuminating light.

3.4.2. Spectral behaviour of obscuration profiles.

In the case of the Turbohaler® the released dose varies significantly in relation to both the metered dose (MD) and the fine particle fraction (FPF). To find out if the amount of fine particles affects the spectrum of the transmitted light we considered two actuations. One actuation is characterised with the highest FPF (76%) and another actuation exhibits the lowest FPF (26%) for the data set presented in section 4.2. Temporal obscuration profiles are calculated for a number of light wavelengths by averaging the intensities of a few spectrometer pixels in the wavelength range.

Figure 3.7 presents 3D-plots of the obscuration profiles against the light wavelength. The obscuration profiles follow a similar pattern for the entire spectral range and both actuations. At the lower wavelengths (from 400nm to 500nm) and at the highest (850nm) the signal-to-noise ratio is not so good as for the middle values (from 550nm to 800nm). There is less obscuration and more fluctuations for the dose of the smaller FPF than for the dose of the larger FPF. One can also see, that each individual fluctuation exhibits itself in all profiles. The fluctuation of the obscuration

relates to a temporal fraction of the cloud and characterises the particle population in this cloud fraction regardless of the light wavelength.

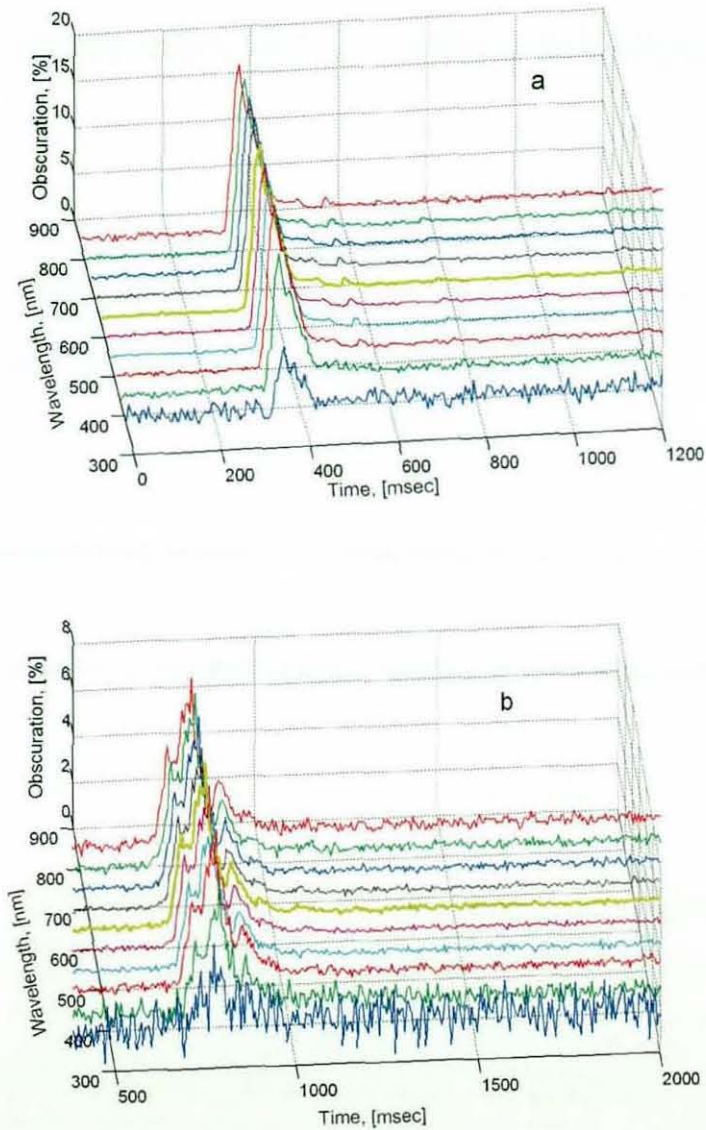


Figure 3.7. Temporal profiles of the light obscuration at different wavelengths for an aerosol cloud, released by the Turbohaler®: a) the actuation, which is characterised with the high FPF=76%; b) the actuation, which is characterised with the low FPF=26%.

Therefore, for the Turbohaler® applications any light wavelength within the range of 500nm to 800nm may be used for the drug delivery assessment.

For another inhaler, a novel prototype, two actuations are characterised with the fine particle fraction of 90% and 94%, respectively. Figure 3.8 shows 3D-plots of the light obscuration for these two clouds. The obscuration profiles are much smoother than in the Turbuhaler® case, although the spectral behaviour is very similar.

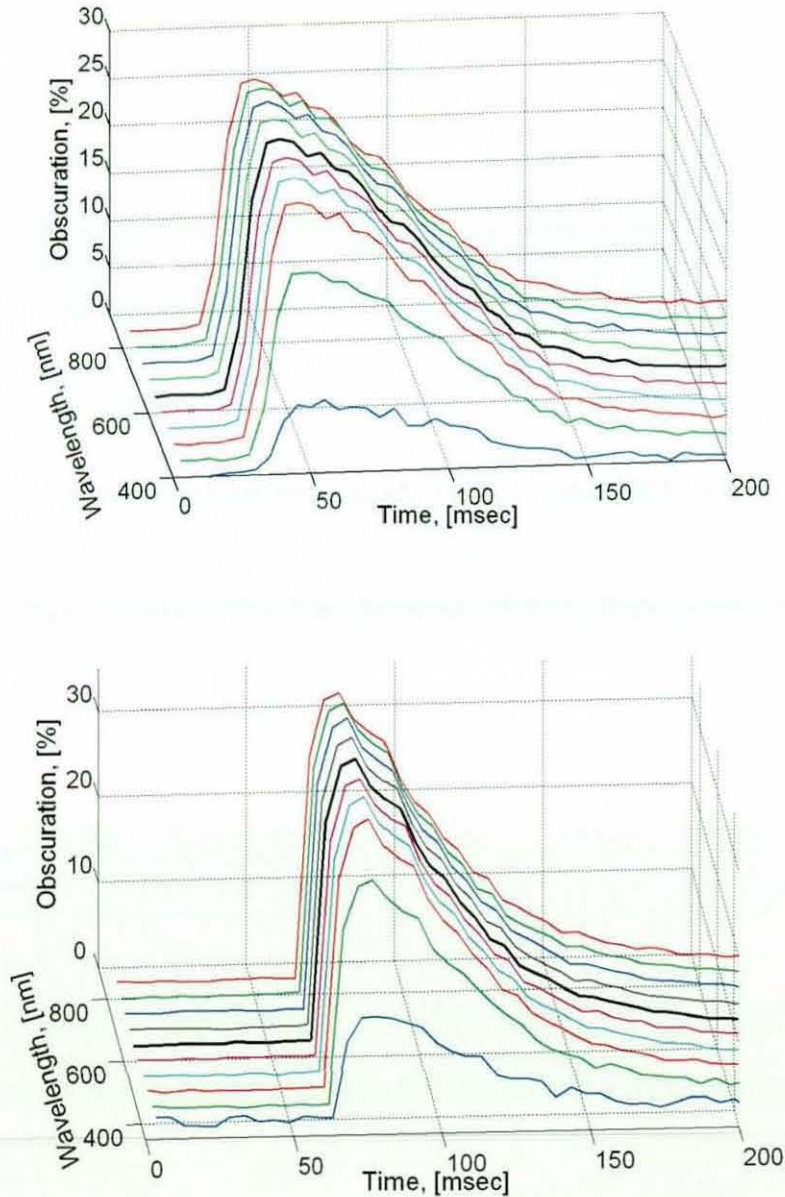


Figure 3.8. Temporal profiles of the light obscuration at different wavelengths for an aerosol cloud, released by a novel prototype inhaler.

For all four actuations, it seems that the light obscuration is smaller at the 'blue' end of the spectrum (up to 500nm) than at the higher wavelengths (from 550nm to 800nm). According to our model (please see Chapter 2), the peak obscuration may

be indicative of the fine particle dose of the actuation. Therefore, the large range of the parameter would benefit the accuracy of the dose measurement. Figure 3.9 presents the peak obscuration as a function of the light wavelength for the four considered actuations.

From the theoretical model (Chapter 2), we expect that the fine particles (the size range from $0.5\ \mu\text{m}$ to $5\ \mu\text{m}$) scattered the blue light (450nm) more than the other visible light (650nm to 800nm) (please see Figure 2.2). This contradiction between the experimental data and the model could be explained by the insufficient sensitivity of the experimental system to the blue light. Indeed, Figure 3.6 shows a very low intensity for the wavelength range from 350nm to 475nm . At such low level of the light intensity, any changes of the transmitted intensity cannot be detected due to the insufficient sensitivity of the detector. The most likely reason for the low intensity of the blue light is the damping effect of the fibre patch on the rays of this spectral range. Therefore, to simultaneously investigate the obscuration effect for the blue, red and infrared light, the arrangement for the optical sensor should not include a fibre patch.

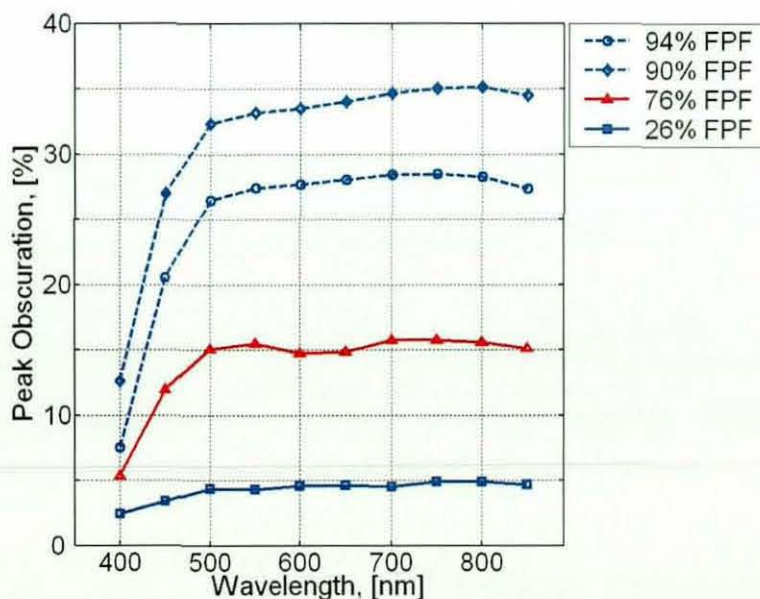


Figure 3.9. Spectral behaviour of the characteristic parameter, the peak obscuration, for four different dose actuations. The fine particle fraction is 26%, 76%, 90% and 94%, respectively.

We can see that any wavelength within the range 500nm to 800nm would have a similar range of the peak obscuration for a wide range of fine particle doses. For the sake of certainty (and practicality) the data analysis was performed only for the narrow range near 650nm. This wavelength corresponds to the highest sensitivity of the spectrometer and is likely to be less affected by both the thermal vibrations and electron excitations of the drug formulation. The large range of the parameter would also benefit the accuracy of the dose measurement.

3.5. Summary.

We have proposed and described in detail the in-line technology for the assessment of the pulmonary drug delivery. This technology is named VariDose for its sensitivity to variations of the released dose on an actuation-by-actuation basis. The VariDose (VD) technology comprises the optical sensor, the data acquisition card and the software for data analysis. The stationary sensor records the spectrum of the transmitted light intensity as a temporal function. The spectral range near 650nm has been proven to be sensitive and to provide a sufficient range for the assessment of the fine particle dose. The analysis program calculates the temporal profile of the light obscuration and fits these data with a mathematical function. The fitting procedure requires six independent parameters.

Several parameters are introduced and discussed for the aerosol characterisation using the best mathematical fit for the obscuration data. Table 3.2 presents the characterisation parameters and their physical meaning. The proposed physical meaning of the deduced parameters is based on generally accepted knowledge and needs to be validated with regard to the cloud properties measured by conventional methods (CM). The main objectives are to establish empirical relationships between the peak obscuration (VD) and the fine particle dose (CM).

For this purposes a number of the specially designed experiments were performed, which are presented and discussed in Chapter 4.

Chapter 4

Experimental Evaluation

A general concept for assessment of the pulmonary delivery in-line with a patient has been developed in Chapter 3. The model calculations (Chapter 2) show that VariDose data have the highest sensitivity to the fine particles and, therefore, it may be possible to measure the fine particle dose directly during the drug delivery. VariDose technology measures values that are proportional to the optical density of the particle ensemble. Therefore, VariDose measures neither particle sizes nor particle-size distribution, but rather the degree to which the agglomerates of the drug formulation are dissociated during an inhalation. In principle, for a given drug formulation the VariDose data can be calibrated against the fine particle dose. This chapter presents a number of experiments, which support the technology concept. The aim of the first experiment is to show the technology's sensitivity to the fine particles. The second and third experiments present the calibration studies for several drug formulations performed with a Twin Stage Impinger (TSI) and a Next Generation Pharmaceutical Impactor (NGI). And the final experiment applies the VariDose method to the development of a novel delivery device and drug formulation.

4.1. Turbohaler® dose variation

A Turbohaler® is a dry powder inhaler with a multi-dose reservoir and a dose metering unit. This inhaler has been chosen for this experiment for two particular reasons. Firstly, it exhibits a significant variation of the delivered dose, even for a standard breathing manoeuvre. And secondly, it has significant clinical usage and has been thoroughly investigated by many independent authors. In this experiment, for the technology evaluation we compare the VariDose data with the published result for single dose delivery efficiency of the Turbohaler® in Meakin *et al.*, (1995). Meakin's study was performed using a twin stage impinger (TSI). The aim of this comparison is to show that, even with no calibration, the VariDose method has the capability to assess the statistical variation of doses, released by an inhaler.

4.1.1. Experimental set

The Bricanyl® Turbohaler® device contains 100 actuations of pure terbutaline sulphate, housed in a small reservoir at the base of the inhaler. The metered dose is prepared by twisting the turning grip and by inhaling the drug particles through the spiral path mouthpiece of the Turbohaler. Each actuation is nominated to contain 500 µg of the medication.

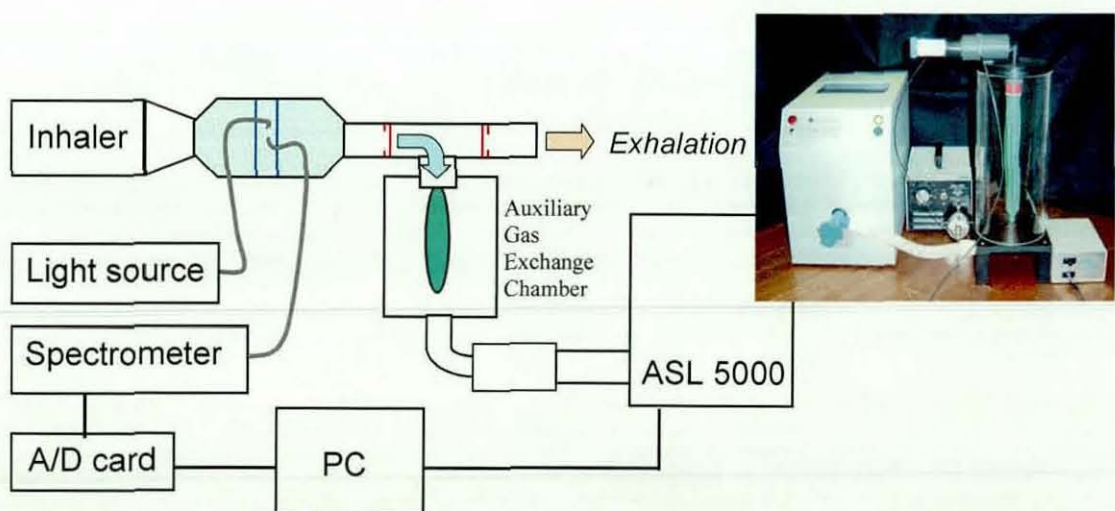


Figure 4.1. Set up for the study of a dose variation of an inhaler by VariDose.

Figure 4.1 shows a schematic diagram and a photographic image of the experimental set-up. The Turbohaler is connected to the sensor unit of VariDose and a breathing simulator is actuating the dose release. The breathing simulator, Active Servo Lung (ASL 5000), is manufactured by IngMar Medical and can simulate the breath profiles based on the physiological model of the lung or reproduce the breath profile recorded from an actual patient; it can operate in a vacuum pump mode. To avoid the entry of the exhalation flow into the inhaler, a set of one-directional valves was used. The Auxiliary Gas Exchange Cylinder (AGEC) traps the particle cloud and prevents dust contamination of ASL.

The peak value of the obscuration is measured for each actuation at the light wavelength of 650nm. According to the model (Chapter 2) this value characterises the maximum optical density of the cloud and can be considered to be proportional to the fine particle dose for each individual actuation. After every ten actuations the glass tube of the sensor head was changed for a clean one. Statistical analysis of the data was performed in terms of the mean value and variance. These allow the spread and the frequency of the Turbohaler® dose variation to be shown.

4.1.2. Inhalation profile.

Several *in vitro* as well as *in vivo* studies have emphasised the importance of generating a particular inspiratory flow profile for dry powder inhalers (Clark *et al.*, 1996; de Boer *et al.*, 1997; Burnell *et al.*, 1996; Everard *et al.*, 1996). The most important parameters are:

- The peak inspiratory flow rate (PIF);
- The acceleration of the flow, the so-called flow increase rate (FIR_{20-80%});
- The time needed to reach PIF (time to PIF);
- The time during which a certain flow through the inhaler can be maintained, the so-called dwell time; and
- The total inspiratory volume.

The breath-simulating machine, used in our study, is multi-functional and can create a wide variety of inhalation profiles controlling many of the parameters mentioned above. For this comparative study the simulated inhalation manoeuvre is set in the way that most closely corresponds to the flow required for the standard TSI protocol

(British Pharmacopoeia, 1993). The breathing simulator works in the vacuum pump mode producing a steady inhalation flow of 60L/min with very sharp flow increase rate, the time to PIF is approximately 25msec. The total inhaled volume is set to 2.2 litres. In this way it is possible to assume that the dose entrainment is similar to the TSI study and to make comparison between data. The inhalation cycle, which actuates the drug release, was followed by two further cycles at the higher inspiratory flow rate of 90L/min. These additional inhalation cycles partially remove the wall residue, deposited during the inhaler actuated cycle.

4.1.3. Results.

For this study 60 available doses from two Turbohaler® devices from the same batch were used. The first 20 doses (shots 1 to 20) are fired from the first device and the other 40 doses (shots 21 to 60) are fired from the second device. All doses are the last doses of the device's range, i.e. actuations 81 to 100 and 61 to 100, respectively. All 60 doses were separately analysed by VariDose and the peak obscuration is regarded as the dose value for the individual actuation. In this experiment we analyse the statistical variation of the VariDose data to answer the following questions:

- a) Is there any bias in sequential sets of VariDose measurements? Does the tube wall residue affect the measurements?
- b) Are VariDose data in agreement with a known statistical behaviour of the pulmonary delivery system?

4.1.3.a. Issues of the wall residue.

The particle deposit on the walls of the sensor glass tube may cause a bias in the VariDose measurement. One might think that using a clean tube for each dose actuation would benefit the precision of measurements. In reality the process of particle deposition on the wall is complex and depends on many factors, often unknown and unpredictable, such as electrical charges of particles and absorption centres on the wall surface. In some cases "primed" walls, with small residues of a fine powder, cause less particle deposition than the clean walls. Indeed, fine particles interact with absorption centres neutralising their absorption ability. Therefore for

the next dose actuation there are no trapping centres on the walls and less particle deposition.

Figure 4.2 shows a variation of the dose value for 60 consecutive actuations of the Bricanyl® Turbohaler®. The abscissa gridlines indicate the moments of changing the glass tube, after every ten actuations. There is no noticeable repeated pattern in these sub-sequences. There is also no tendency of the dose variation over the entire sequence (no increasing/decreasing bias).

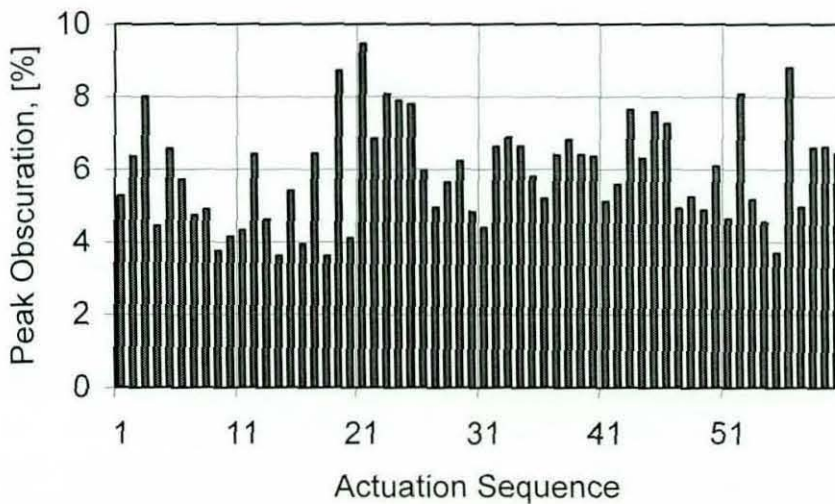


Figure 4.2. VariDose data of the dose variation for a Turbohaler®.

To support these visual observations we performed a statistical test, Analysis Of Variance (ANOVA) (Miller, 1997). This test can detect significant differences between several treatments. The requirements for this test are:

1. The same number of replicates for each treatment (in our case there are 10 actuations per each subsequence);
2. All treatments (in our case six sub-sequences) have similar variance.

To check if our treatments have similar variance, we use a statistical test for the homogeneity of variance. We calculate the variance for each treatment

$$\sigma^2 = \frac{\sum (x - \langle x \rangle)^2}{(n-1)},$$

where $\langle x \rangle$ is the treatment's mean and $n=10$ is the

number of replicates per treatment. The test statistic for homogeneity of variance is

the ratio of the highest value of the variance to its lowest value; and for our data (see Table 4.1) it equals 4.26. The hypothesis of homogeneity of variance is true, when the test statistic does not exceed the tabulated value of F_{\max} , which depends on the number of treatments and the degrees of freedom ($n-1$). In our case F_{\max} equals 7.80. Therefore, the null hypothesis of the homogeneity of variance is true and we are safe to proceed with the ANOVA test.

There are six groups of measurements ($u = 6$, treatments A,...,F). Each group contains 10 measurements ($v = 10$). Analysis of Variance involves the partitioning of the total variance into (1) variance associated with the different groups and (2) random variance, evidenced by the variability within the groups. The sample variance is defined as the sum of squares of deviations (SS) divided by the degree of freedom ($df = n - 1$, where n is the population number of the sample). According to the ANOVA algorithm we calculate the following values, where the j -index relates to the actuation number within the group and the i -index presents different groups:

$$A = \sum_{i=1}^u \sum_{j=1}^v x_{ij}^2;$$

$$B = \sum_{i=1}^u \left[\frac{\left(\sum_{j=1}^v x_{ij} \right)^2}{v} \right];$$

[4.1]

$$T = \sum_{i=1}^u \sum_{j=1}^v x_{ij};$$

$$D = \frac{T^2}{uv}$$

Then, the sum of the squares of deviations between the groups is $B - D$ and the degree of freedom is $df = u - 1$. For the variance within groups $SS = A - B$ and $df = u(v - 1)$. Finally, for the total population $SS = A - D$ and $df = uv - 1$. Table 4.1 presents the summary of the ANOVA test for the VariDose data.

Table 4.1. Summary of the analysis of variance (ANOVA test).

Summary				
Groups	Count	Sum	Average	Variance
Treatment A	10	53.95	5.395	1.677
Treatment B	10	51.23	5.123	2.700
Treatment C	10	67.70	6.770	2.289
Treatment D	10	61.51	6.151	0.634
Treatment E	10	60.66	6.066	1.199
Treatment F	10	59.56	5.956	2.692
ANOVA				
<i>Source of Variance</i>	SS	df	MS	F
Between Groups	17.094	5	3.419	1.833
Within Groups	100.71	54	1.865	
Total	117.81	59	1.997	

Note for Table 4.1: **SS** is the sum of squares, **df** is the degree of freedom, **MS** is the mean of the sum of squares, and **F** is the statistic number.

Using the mean squares in the final column of this table, we calculate a variance ratio test to obtain an **F** value:

$$F = \text{Between treatment mean square} / \text{Within groups mean square} \quad [4.2]$$

The calculated value *F* is compared with the *F* values from the test table for the different levels of significance (*p* value). If the calculated *F* value exceeds the tabulated value at $p=0.05$ there is significant difference between treatments. If so, it is necessary to see if the treatment differences are more highly significant by looking at the *F* values for $p=0.01$ and then 0.001. In our case the tabulated *F* value is equal to 2.4 for $p=0.05$, while the calculated *F* is only 1.833. Therefore, there are no significant differences between different groups of the VariDose measurements.

This test shows that for this drug formulation the wall residue during the sequence of ten actuations produces no noticeable effect on VariDose measurements. The overall set of data can be considered as the sample population for the identification of the distribution parameters such as mean, variance and standard deviation.

In the next section we compare the distribution of the Turbohaler doses measured by VariDose and the published data on the Turbohaler dose variation measured by a conventional twin stage impinger (TSI) (Meakin *et al.*, 1995).

4.1.3.b. Dose variation.

In Meakin's study eleven devices of the same batch (lot E in the reference, Meakin *et al.*, 1995) were investigated to establish the degree of replication and evaluate the comparative performance of the Turbohaler®. Shots from 1 to 10 of each device were fired to waste and the following shots from 11 to 20 were evaluated. Ten doses of each device were measured by a twin-stage impinger to provide the emitted dose and the fine particle dose for the individual actuation (a total of 110 actuations). The coefficient of variation is reported as 17.3% for emitted doses (ED) and 25% for the fine particle doses (FPD), respectively.

In the VariDose study the mean value of the peak obscuration is 5.91% with the standard deviation of 1.413%. The coefficient of variation is 23.9%, which is very similar to the coefficient of variation of FPDs in the Meakin's study. We would like to test if these two datasets belong to the same distribution. The Kolmogorov-Smirnov test, KS-test (Kanji, 1999), can determine if two samples differ significantly without making an assumption about the distribution, and therefore, can establish differences in the distribution for these two datasets.

For the KS-test the dataset is graphically presented through the cumulative fraction function, which can also be referred to as the empirical distribution function. To calculate the cumulative fraction function, the data is sorted in ascending order. Then, for each data-point, the fraction of the data smaller than this data-point is calculated. The cumulative fraction function is plotted against data-values. Both sample data are presented on the same graph, and the maximum vertical deviation between the two curves is the statistical value D of the KS-test. If the observed value

exceeds the critical value (from the test's table), the null hypothesis that the two population distributions are identical is rejected.

To perform the KS-test for the VariDose data and the TSI measurements, the dose values have to be expressed in the same measurement units. For this purpose we presented the dose value as a percentage of the mean value, $\frac{Dose}{mean(Dose)}100\%$.

Figure 4.3 shows the cumulative fraction function of the dose value for single doses emitted from the Turbohaler®.

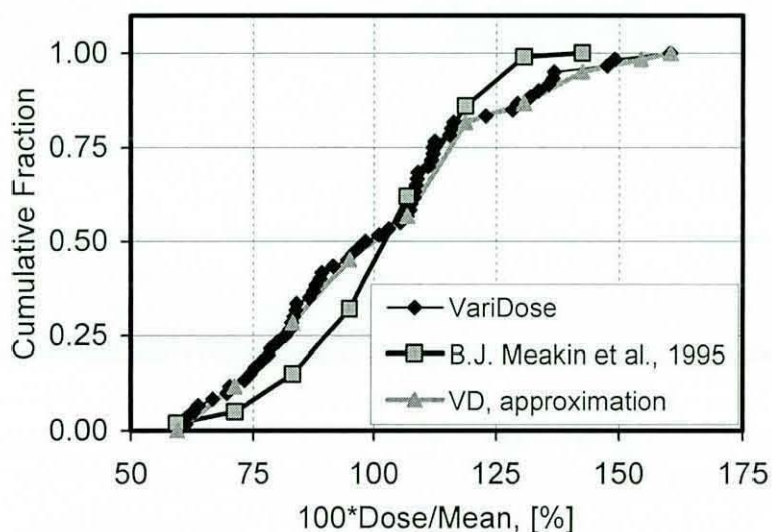


Figure 4.3. Cumulative fraction function for single doses emitted from the Turbohaler®.

The maximal difference between two curves is 0.133. This value does not exceed the critical value even for the level of significance $\alpha = 0.20$ ($D_{critical} = 0.138, 0.157$ and 0.210 for $\alpha = 0.20, 0.1$ and 0.01 , respectively). This means that there are no significant differences between these two distributions and we can conclude with a high degree of certainty that data of these two datasets are similarly distributed.

This experiment shows that VariDose technology has realistically assessed the statistical distribution of the fine particle doses released by the Turbohaler®. During this experiment we have accidentally found one of the benefits of the VariDose technology, namely its ability to provide a quick assessment of the inhaler

performance in relation to the fine particle dose. The next section describes this episode.

4.1.3.c. *Quick check on an inhaler routine.*

The main benefit of the VariDose for anyone involved in the testing and developing of a pulmonary delivery system is as a quick and simple tool to estimate the emitted fine particle dose. An example of a quick check on one aspect of the inhaler performance is considered here.

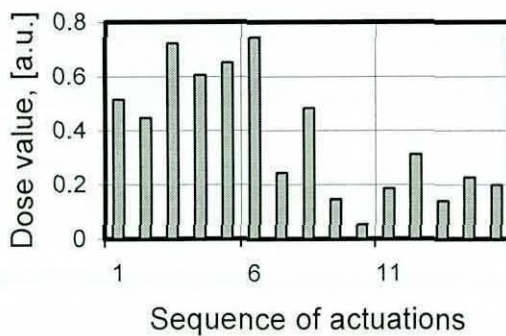


Figure 4.4. Incorrect use of Turbohaler®.

The fifteen consecutive doses were prepared, actuated and evaluated. Figure 4.4 shows that emitted doses of single actuation are significantly decreased after a few incorrect preparations of the metered dose.

The entire test took only 10 minutes. At the end of the test one can be absolutely certain that the chosen routine is incorrect, although the dose values are expressed only in arbitrary units.

4.1.4. Conclusions.

This straightforward and simple study shows that VariDose technology, in the case of the Turbohaler®, correctly reflects the statistical variation of the emitted doses. This supports the idea that the optical obscuration can provide a measure of the released dose without measuring the size distribution and weight of aerosol particles. The main requirement for success is that only one parameter should be allowed to vary. In this experiment the inspiratory flow profile, the drug formulation and the

The leaflet for the Turbohaler® instructs the user to twist the grip keeping the inhaler in a *vertical* position when preparing the dose. This instruction is very easy to overlook. To find out what happens if this requirement is not fulfilled, the Turbohaler® inhaler is connected to the sensor head of the VariDose in the *horizontal* position. The

delivery device were constant. Therefore the change of optical obscuration can be attributed to the change of aerosol content.

4.2. Calibration of VariDose against TSI.

The aim of the second study is to investigate the possibility of establishing the calibrating relationship between the VariDose data and the data conventionally used for the evaluation of a pulmonary delivery system. The simplest conventional way is measurements by a twin-stage impinger (TSI). The TSI evaluates the fine particle dose and the coarse particle dose in terms of weight units. Therefore a simultaneous analysis of the delivered dose by VariDose technology and a twin-stage impinger (TSI) may calibrate the optical data of the VariDose into weight units. This study is also performed on the Turbohaler®. This inhaler delivers relatively high doses of fine particles and exhibits a large dose variation, and therefore, one can expect a significant range of fine particle doses.

4.2.1. Experimental set-up.

A schematic diagram of the experimental set-up is presented in Figure 4.5. The sensor head of the VariDose (VD) is placed between the mouthpiece of the inhaler and the entrance of the TSI. As in the previous experiment, the sensor head of the VariDose has a volume of 30ml and optical measurements take place at a 50mm distance from the mouthpiece of the inhaler. The Bricanyl® Turbohaler®, containing 100 actuations of pure terbutaline sulphate is used as the test inhaler. Each actuation is nominated to contain 500 µg of terbutaline sulphate.

The total dose, the fine particle dose and the fine particle fraction were determined using Apparatus A (British Pharmacopoeia, 1993), a glass twin-stage impinger (TSI), calibrated at a flow rate of 60 ± 5 L/min. The VariDose measurement was performed on the cloud, entering the inlet of the TSI during Turbohaler firing. For each single Turbohaler actuation the drug was collected and evaluated for three stages: the 'throat', stage 1 and stage 2. The TSI was assembled with 7ml of solvent in stage 1 and 30 ml in stage 2. Drug samples, collected on each stage of the TSI, were washed out with purified water. Each sample was filled up to 100 ml. The

concentration of terbutaline sulphate was analysed by fluorescence spectroscopy, using an excitation wavelength of 273 nm and the emission wavelength of 311 nm.

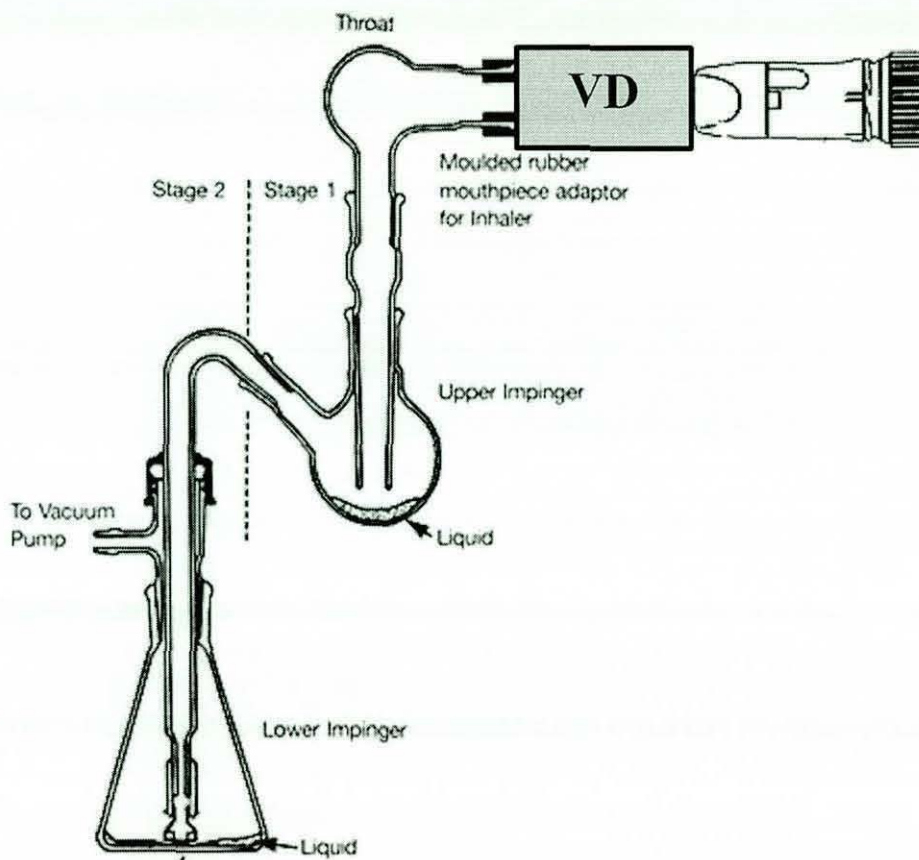


Figure 4.5. A schematic diagram of the experimental set-up for simultaneous measurements by VariDose and TSI.

Particles with mass median aerodynamic diameter (MMAD) 0.5-6.4 μm are trapped in stage 2 and are considered as the fine particle dose (FPD), which is able to reach the lung. The total delivered dose is defined as the total amount of drug delivered to the TSI under the experimental conditions, i.e. the sum of three stages. The fine particle fraction (FPF) is the mass of drug deposited in stage 2 expressed as a percentage of the total dose.

4.2.2. Results.

A sequence of 21 actuations was performed, representing a typical variation in the total released dose and the fine particle dose for the Turbohaler®. Figure 4.6 shows the amount of terbutaline sulphate recovered in the twin stage impinger as the fine

particle dose and the delivered dose on actuation from the Turbohaler device at 60L/min. The mean FPD was 172 μ g and the mean delivered dose 260 μ g with the coefficients of variation 45% and 27%, respectively. The mean FPF was 63% with the coefficient of variation being 27%.

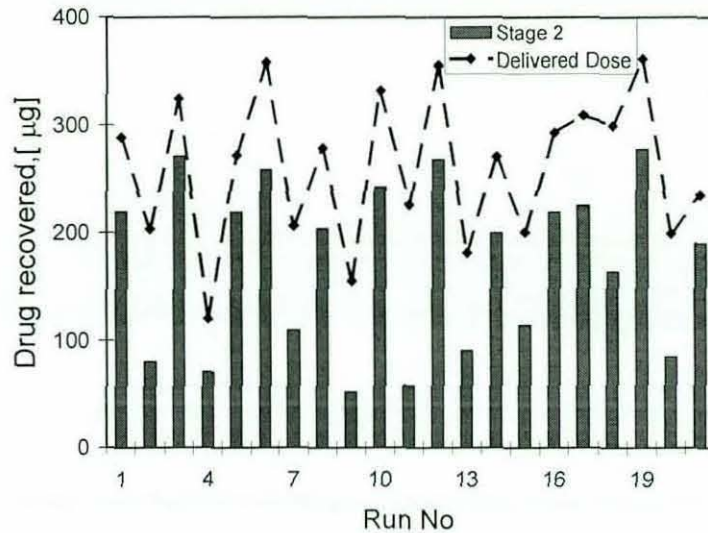


Figure 4.6. Deposition of Terbutaline Sulphate as Fine Particle Dose (Stage 2) and Delivered Dose in the Twin-stage Impinger at 60l/min (n=21).

4.2.2.a. Fine particle dose.

The VariDose system can measure a number of parameters, which assess the physical properties of the particle cloud (please refer to section 3.3). Figure 4.7 presents obscuration profiles for two actuations, which are characterised by the TSI with the highest and the lowest fine particle doses. One can see that both profiles may be characterised with very similar cloud volumes. For this experiment, when the flow is provided by a calibrated vacuum pump, the cloud volume is linearly proportional to the propagation duration (the temporal length of the cloud). As we have discussed (Chapter 2), the obscuration depends on the volume concentration of the airborne material and the particle size distribution. The mean volume concentration is linearly proportional to the delivered dose due to the cloud having approximately the same volume for all actuations, but the spatial distribution of particles is unknown.

There is an ambiguity in optical obscuration: a high obscuration value can be explained by a high concentration of airborne matter as well as by a high fraction of the fine particles and at a much smaller concentration (section 2.3.2). The TSI data show that DD, FPD and FPF vary significantly for individual actuations. Here we consider a few estimations to choose a parameter of the obscuration profile, which would most reliably characterise the fine particle dose in the released cloud when all three components (DD, FPD and FPF) have a wide range of variation.

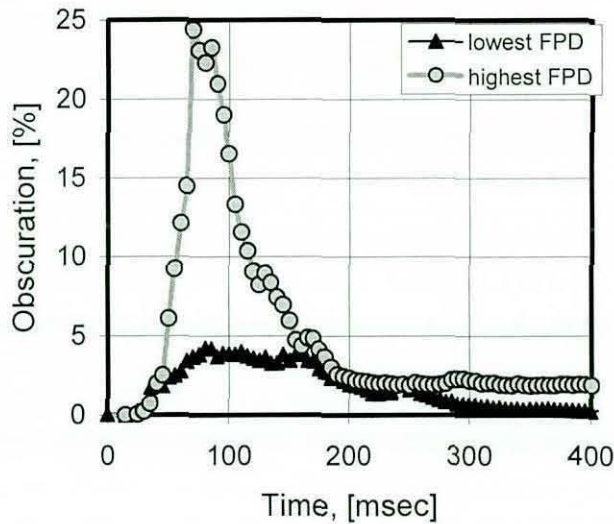


Figure 4.7. Examples of the VariDose obscuration profile for drug actuations with the lowest and the highest FPD as measured by TSI.

From Figure 4.7 we may estimate the minimal cloud volume that corresponds to the peak obscuration. There are 4 measurement periods on the top of the profile. This gives the peak duration of 20msec; and at the flow rate of 60L/min this results in the volume of 20mL. The highest DD, measured by TSI, is 361 μ g. Assume that this total mass of the drug formulation is concentrated inside the estimated volume of 20mL and the material density is 1.54g/cm³, then the volume concentration (C_v) of the airborne material would be 10ppm (parts per million). If all this matter would be spheres of 1 μ m the light obscuration would reach 27% according to the model (please refer to Figure 2.3). While if the same amount of the matter would be spheres of 6 μ m the light obscuration would be only 4%. Therefore, the obscuration, caused by coarse particles (>6 μ m), is expected not to exceed 4%. In reality, particles may

be spread over the entire cloud volume (150mL, meaning the seven-times lower C_v) and particle sizes may be larger than $6\ \mu\text{m}$ (meaning the smaller extinction coefficients), therefore the maximal obscuration due to coarse particles might be significantly lower than 4%.

The measured peak obscuration ranges from 4% to 25% for different actuations. These are well inside the estimated values and just above the estimated maximum for the coarse particles. It is reasonable to suggest that the peak obscuration relates to the cloud part with the highest fraction of fine particles and may correlate with the fine particle dose of an actuation. The other possible parameter in this experiment, which may correlate with FPD, would be the area under the profile curve between two points, for example, at the half maximum of the obscuration (the so-called full width of the half maximum, FWHM). For convenience, we call this parameter “the dose value”, reflecting the integral of obscuration.

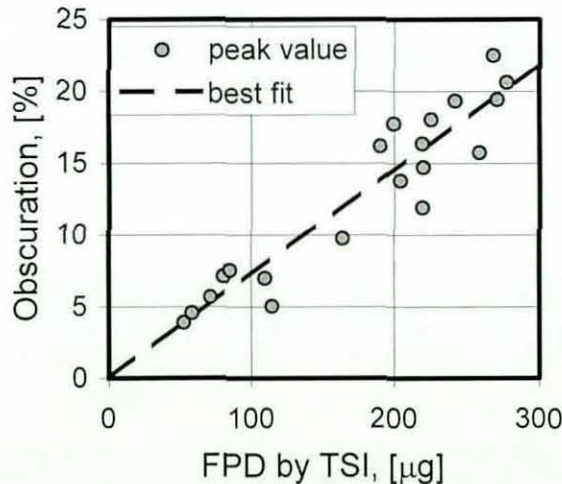


Figure 4.8. A calibration of the VariDose parameter, the peak value, against the fine particle dose, measured by TSI.

Experimental data show a statistically significant correlation between the fine particle dose, measured by TSI, and the peak value of obscuration as defined by the VariDose technology. The correlation coefficient is 0.94 and $p < 0.0001$. In contrast the correlation coefficient of FPD against the dose value parameter is only 0.48 and $p = 0.03$. Figure 4.8 presents a calibration plot for the fine particle dose in the released

aerosol, measured by the two methods. The best-fit line goes through the origin and can serve to calibrate VariDose measurements in term of mass units.

The noticeable spread of data (up to $\pm 25\%$ from the fitted straight line) may be attributed to the fact that the VariDose sensor is placed up-stream to the TSI. It is well known, that for dry powder formulations the backside of the L-shaped throat may serve as an additional de-agglomeration stage through the bouncing mechanism (Dzubay *et al.*, 1976). Covering the throat-stage surface with a ‘sticky stuff’ can reduce this effect (Turner *et al.*, 1987; Dunbar *et al.*, 2005), but this is not a regulatory requirement and very often is not used because it increases labour and time burdens on measurements and reduces performance-important values of FPD. This experiment was conducted in collaboration with the Department of Pharmacy and Pharmacology of the University of Bath. Unfortunately, they were reluctant to use the ‘sticky stuff’ in the throat piece of TSI to improve the accuracy of the calibration. Currently, we can only conclude that the spread of the observed data does not entirely reflect the accuracy of the VariDose technology, but rather may illustrate some disadvantages of the TSI measurement.

The coefficient of variation for both methods is found to be similar: 45% for the TSI measurements and 48% for VariDose. The observed large variation is consistent with typical dose variations delivered by the Turbohaler® device (Hindle *et al.*, 1995; Kamin *et al.*, 2002; Meakin *et al.*, 1995) rather than the variation of VariDose or TSI measurements.

4.2.2.b. Cloud homogeneity.

The homogeneity of the aerosol cloud, released by an inhaler, is not currently assessed by any technology commonly used in the pharmaceutical industry. It is difficult to predict if this parameter is important for the efficiency of pulmonary drug delivery, but from the general physical point of view a more homogeneous cloud might benefit the lung deposition. In this thesis the data on cloud homogeneity are presented with the only purpose of gathering empirical data for future research.

For this experiment we have used a readily available medication, which is widely prescribed by doctors, with the trade name Bricanyl® Turbohaler®. This system of

the drug formulation and the delivery device has been rigorously tested, including clinical studies, and has passed the strict regulatory requirements. It is likely that this lengthy process of development and optimisation of the system explains the high homogeneity of the released cloud. Figure 4.9 presents the homogeneity parameter of each actuation against the fine particle dose of this actuation. For comparison the homogeneity is plotted against two values of the fine particle dose (FPD): one measured by the TSI (diamond-markers) and the other assessed by VariDose using the calibration for the 'peak-value' parameter (asterisk-markers). One can see that the actuations of a higher FPD are characterised with a slightly better homogeneity than the actuations of a lower FPD.

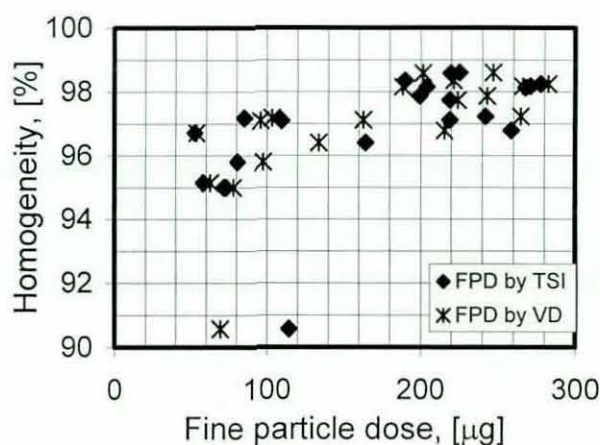


Figure 4.9. Experimental data on the homogeneity of aerosol clouds released from a Turbohaler®.

The homogeneity parameter may be useful during the development process of a pulmonary system. These include the development of delivery devices, drug formulations and a process of matching a drug formulation with a delivery device. For example, the VariDose assessment of the aerosol homogeneity can detect technical solutions, which result in the low homogeneity. In this way, a developer may quickly narrow options before going to *in vitro* measurements that are labour and time consuming.

4.2.3. Conclusions.

Aerosol doses, released by a Turbohaler®, have been simultaneously assessed using two technologies: a twin stage impinger and the VariDose optical method. Experimental data show a good correlation for measured values of the fine particle doses. The correlation coefficient is 0.94 with the p-value of less than 0.0001. This experiment proved that the VariDose technology could be calibrated for mass units of the fine particle dose for a particular case. This means that for this chosen drug formulation and the chosen delivery device the peak value of the obscuration profile characterises the fine particle dose in the released aerosol and could be expressed in the mass units.

Having this calibration, it is now possible to assess without using an impactor many practical aspects:

- Statistical variation of FPD for the entire content of the Turbohaler® device. The time saving could be enormous. The measurement rate for VariDose is a minute instead of hours for an inertial impactor.
- Statistical variation between different inhaler devices and different batches can be measured in hours, not months.
- The performance of the drug formulation can be quickly assessed during prolonged storage.
- The suitability of the Turbohaler® for a particular patient can be established. The breath-simulating machine actuates the dose release by applying the flow profile recorded for this patient and VariDose measures the FPD.
- An individual patient can be monitored in respect of the actual dosage using the VariDose sensor attached to the Turbohaler®.

The homogeneity parameter may be useful during the development process of a pulmonary system. These include the development of delivery devices, drug formulations and a process of matching a drug formulation with a delivery device. For example, the VariDose assessment of the aerosol homogeneity can detect technical solutions, which result in the low homogeneity. In this way, a developer may quickly narrow options before going to *in vitro* measurements that are labour and time consuming.

4.3. Comparing in-line optical and NGI measurements.

The next step in the evaluation of this emerging technology is to use a different type of the drug formulation and another delivery device. It is also important to see how different species of the fine particles affect the light obscuration. This experiment is design to test the applicability of the VariDose technology to a carrier-based formulation and a delivery device with high FPF. The purpose of the study is to compare the optical data of Varidose and the impaction data of a multi-stage impactor considering a number of size-classes in the range of the fine particles.

4.3.1. Experimental set-up.

The experimental set-up includes a Next Generation Pharmaceutical Impactor (NGI), Varidose and a Vectura prototype active inhaler device. The dose actuation is facilitated by a vacuum pump at the flow rate of 60 L/min. Figure 4.10 shows a diagram of the experimental set-up. All connections between the devices are airtight. The sensor-head of Varidose has an internal volume of approximately 30mL (that is much smaller than the NGI's volume) and contributes a negligible air-resistance.

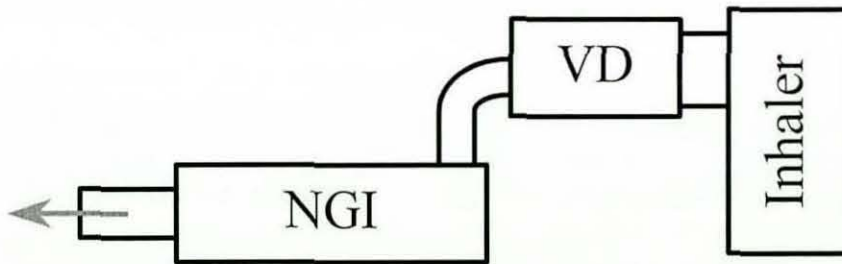


Figure 4.10. A schematic diagram of the experimental set up shows the airtight connection of the pharmaceutical impactor NGI, the optical sensor-head of Varidose (VD) and the delivery device. The arrow represents the flow direction, created by a vacuum pump.

The NGI system consists of nine impaction stages. Each stage collects particles of the specified aerodynamic sizes and is characterised by the median of the diameter distribution (D_{50}). The median parameters for the NGI system range from $0.13\mu\text{m}$ to $10\mu\text{m}$: $10\mu\text{m}$ (the Throat), $7.8\mu\text{m}$, $4.6\mu\text{m}$, $2.7\mu\text{m}$, $1.6\mu\text{m}$, $0.9\mu\text{m}$, $0.5\mu\text{m}$, $0.3\mu\text{m}$ and $0.13\mu\text{m}$ (the final Filter). The result of the NGI measurement is the distribution of

the drug mass over particle aerodynamic-sizes according to the drug mass collected on each stage. The drug mass is measured by the photo-luminescence assay. The number of collection stages and the sensitivity limit of the assay prohibit a single shot NGI measurement, therefore a cumulative sequence of five actuations is analysed as a single assay-run. On the contrary, Varidose measures each single actuation.

The prototype active inhaler device is a breath-actuated system and creates aerosols from a single-dose blister of a powder formulation. Doses delivered from this unit are usually characterised with a high Fine Particle Fraction (FPF). For this study we used a so-called carrier-based drug formulation, which includes the micronised salbutamol sulphate (40%), the drug, and Respirose (60%), the carrier particles. Respirose is a lactose powder with the particle range of 45 μ m to 90 μ m. A significant advantage of using this formulation is the fact that Respirose particles of these sizes have negligible contribution to optical effects measured by Varidose. Therefore, neither NGI nor Varidose assesses Respirose particles.

Measurements were performed using blisters with a formulation load of approximately 0.8mg and 1.0mg. Due to the hand filling of the blisters there are slight variations in the metered dose (MD). Metered doses of the drug range from 320 μ g to 336 μ g and from 400 μ g to 424 μ g for the two types of blister, respectively. The two different loads are intended to allow Varidose calibration over a range of powder doses.

The sensor position is kept the same for all experiments in this thesis, 5cm from the mouthpiece of the inhaler. The temporal resolution is 5msec. This arrangement ensures that the optical measurement is made on the cloud, which would be developed in the middle of the patient's mouth, and results in sufficient data-points for analytical purposes.

4.3.2. Results.

Overall, 30 actuations of the delivery device have been simultaneously analysed by Varidose and the Next Generation Pharmaceutical Impactor (NGI). The NGI produced six sets of data averaged over five consecutive actuations, while Varidose

characterised each individual actuation. Experimental results show a significant de-agglomeration of drug particles at the airflow of 60L/min. The NGI results are compared against the optical parameters, supposing that the particle de-agglomeration takes place mainly before entering the NGI, and that the NGI structure makes an insignificant contribution to the de-agglomeration process.

4.3.2.a. NGI data.

The NGI data-set presents drug masses collected on the impactor stages per single actuation and are considered as the drug distribution over the aerodynamic particle sizes for the “average” cloud entrained. Table 4.2 summarises the NGI data for the six sets. The table also includes the median diameter D_{50} , which corresponds to each stage at the flow rate of 60L/min.

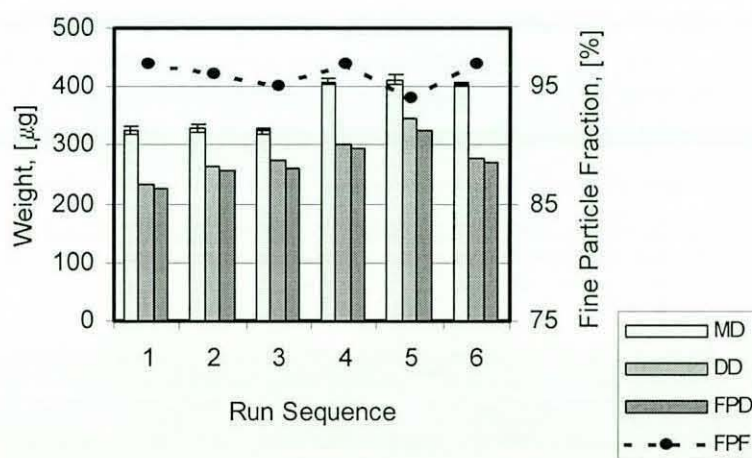


Figure 4.11. Released doses measured by NGI: MD is the mean value of the metered dose and error bars show the STDV of the loads for the run; DD is the delivered dose; FPD is the fine particle dose and FPF is the fine particle fraction.

Using the size distribution of the particles the NGI software calculates pharmaceutically important parameters: the Delivered Dose (DD), the Fine Particle Dose (FPD) and the Fine Particle Fraction (FPF). The definitions of these parameters are discussed in the section 1.3.3a of this thesis. Figure 4.11 shows a summary of the dose distribution through the given data sets. All released doses are characterised with high values of the FPF, which range approximately from 94% to 97% and corresponds to the fine particle masses, FPD, ranging from 226 μg to 324 μg .

Table 4.2. Summary of NGI data.

	Throat	Stage 1	Stage 2	Stage 3	Stage 4	Stage 5	Stage 6	Stage 7	Filter
D ₅₀ [μm]	>10	7.8	4.6	2.7	1.6	0.9	0.5	0.3	0.13
Set 1 [μg]	0.72	1.64	8.16	51.82	120.58	77.84	17.44	5.36	18.16
Set 2 [μg]	0.72	10.94	12.8	62.04	129.86	79.70	17.44	5.36	26.54
Set 3 [μg]	1.64	0.72	5.36	49.96	112.22	72.26	15.58	3.50	17.24
Set 4 [μg]	0.72	0.72	5.36	39.74	94.56	62.98	10.02	1.64	16.30
Set 5 [μg]	0.72	1.64	9.08	47.18	100.14	68.54	14.66	4.44	19.10
Set 6 [μg]	0.72	4.44	10.02	43.46	102.00	75.98	13.72	3.50	20.02

For the blisters of 0.8mg the coefficient of variation of the delivered doses is 8.6%, while the variation coefficient for the formulation loads is under 2.3%. Similar discrepancies are observed for 1.0mg blisters: 6.3% for the delivered doses and 2.0% for the formulation loads (MD). Therefore, although NGI gives no data on the single dose variation (they are averaged over 5 doses), the variation coefficient of the released doses for the blisters of the same load will be considered as the variation coefficient of a single dose. This approximation is the lowest estimation of the variation and is used to compare the NGI data with the VariDose data.

4.3.2.b. VariDose data.

VariDose characterises each individual actuation by recording the temporal profile of the light transmission through the propagating cloud. Figure 4.12 shows a few profiles recorded for this experiment. Curve 1 presents the cloud with a higher FPD and curve 2 corresponds to the actuation of a smaller FPD. For comparison there is also a typical profile for the actuation containing only the Respirose component, without the drug load. To draw the obscuration on the logarithmic scale a small bias of 0.08% was added to all data points avoiding negative values due to the measurement noise.

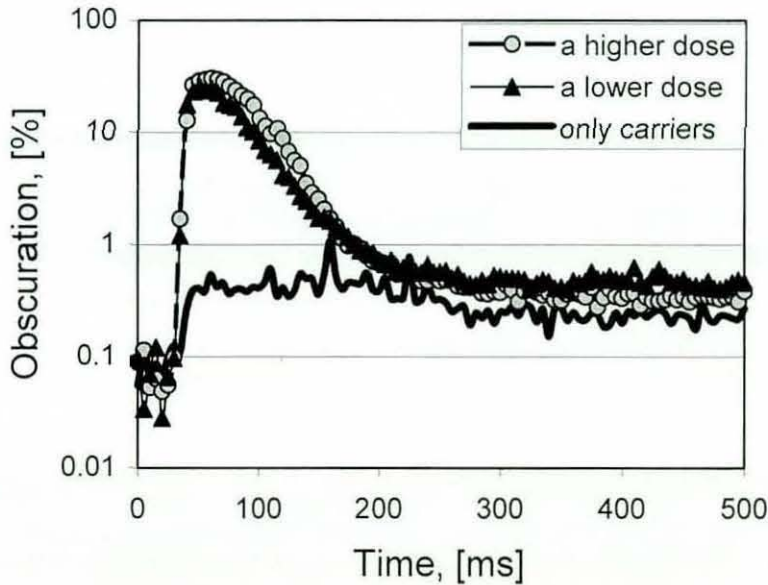


Figure 4.12. Samples of the obscuration profiles.

From these graphs one can see that the carrier particles only slightly contribute to the obscuration. Therefore the majority of the obscuration should be attributed to the drug particles.

The drug particles released by an inhaler consists of a large particle population. These particles possess different shapes and sizes and create an aerosol cloud of a certain limited volume. The particle distribution over the aerosol cloud is generally unknown and can be highly inhomogeneous. The temporal profile of the cloud

obscuration gives a “snap shot” of the variation of the cloud’s optical density in space without resolving the entire complexity of the time-space cloud development. To evaluate the cloud homogeneity we introduced a characteristic parameter named “homogeneity” (please refer to the model section 3.3.2.a). The cloud homogeneity measures the deviation of the experimental points from the fitted curve and ranges from 98% to 99% for these 30 actuations. This high homogeneity allows the suggestion that particles are smoothly distributed in the cloud and that the model assumptions are fulfilled. Next we compare the model calculation and the observed values of the obscuration.

4.3.2.c. Comparing the model with the observed obscuration.

The NGI data provide the size distribution of particles in the aerosol. This distribution has a number of limitations such as: 1) the aerosol cloud is unreal, but average for a given assay-run; 2) there is no information about the spatial distribution of particles; and 3) there is an uncertainty that de-agglomeration processes have completed before the cloud enters the throat stage of the NGI. Despite these limitations, the NGI gives a good estimate of the particle contents in the cloud. The ratio of the drug mass of an individual stage to the total drug mass of all stages gives the fraction of each type of particles. While the precise spatial distribution of particles is unknown, for estimation purposes we assume the homogeneous distributions of particles over a limited cloud volume. Then, partial volume concentrations of each particle type and equations [2.6], [2.19], and [2.20] allow the calculation of the optical obscuration for an individual cloud. The only undefined parameter left is the cloud volume.

The cloud volume can be estimated by the duration of the cloud and the flow rate. The flow rate is constant and equal to 60L/min. The duration is extracted from the temporal profile of obscuration. For visualisation of the following discussion, figure 4.13 shows one of the obscuration profiles and the chosen time periods. Consider three time periods:

1. The lowest time is the measurement period of 5ms. It is quite absurd to suggest that all particles are assembled in such a volume when there are at least 20 measurement points in the profile. This small time is used to estimate

the highest possible obscuration. In this case we assumed that the particles from stage 4, which have the highest extinction coefficient, occupy only this small volume and all other particles are distributed over the entire cloud.

2. The other characteristic time is the time period between two points at the half maximum of the obscuration. These values are referred to in this thesis as t_{FWHM} and V_{FWHM} for the time and volume, respectively. This time corresponds to the main body of the cloud.
3. One of the largest clouds corresponds to the time period measured between two points of the interception of the fitted curve and the level line of obscuration. The obscuration of 1% gives the largest cloud without interfering with the level of the residue obscuration.

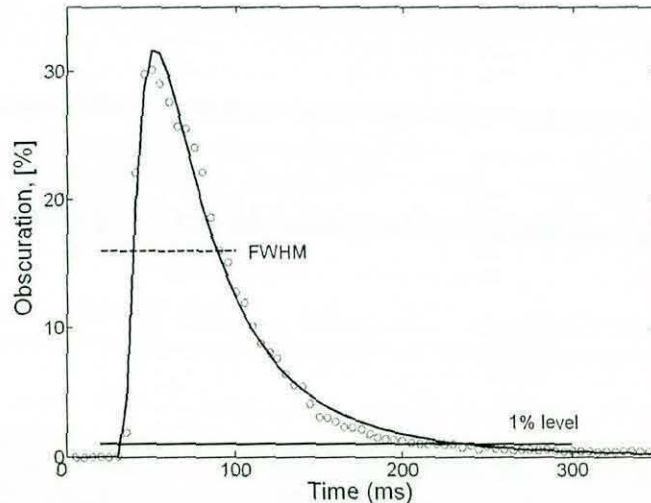


Figure 4.13. A graphical presentation of definitions for the cloud duration and the cloud volume.

Figure 4.14 presents the results of the model calculations using the above assumptions. As we expected, the absurd suggestion that all particles are assembled in a small volume, corresponded to a single measurement of 5ms, results in nearly absolute obscuration (>90%). This result is invalid, because the obscuration values exceed 50% and therefore the model assumption of single scattering is broken. For such a dense media the light transmittance must be considered through the diffusion theory (Chandrasekhar, 1960; Ishimaru, 1978). The case of the 5ms cloud has been considered here only to conclude that particles have to be distributed in a larger

volume than 5mL. From the other point of view, a suggestion that all types of particles are homogeneously distributed through the entire cloud, measured at the 1% obscuration level, results in a rather lower obscuration than that observed in the experiment.

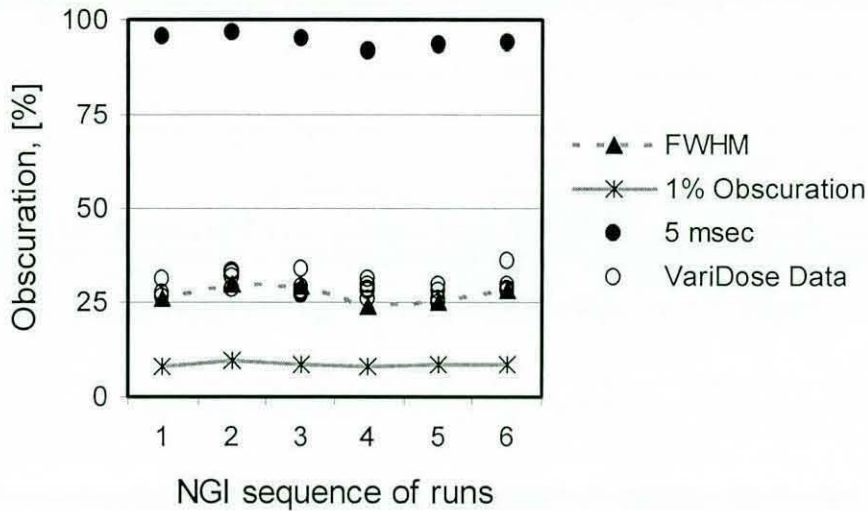


Figure 4.14. A comparison of the model calculations and VariDose measurements for the peak obscuration of an aerosol cloud.

The best agreement between the model and experimental data is observed for an assumption that all particles are homogeneously distributed over the cloud volume, which corresponds to the full time width of the profile at the half maximum of the obscuration (FWHM).

4.3.2.d. Value of the FPD.

In the comparative study of TSI and VariDose we used the Turbohaler® device and a drug formulation that contained only micronised drug particles. For that case the variation coefficient of the fine particle dose was high, 48%, the mean value of the fine particle fraction was 63% with the variation coefficient of 27%, and the peak value of obscuration (the maximum of the fitted curve) had a statistically significant correlation, 0.94, with the FPD (section 4.2.2). On the contrary, for this study the variation coefficient of the delivered dose is well under 10% (8.6% and 6.3% for different loads of blisters), and the FPF ranges only from 94% to 97% (section 4.3.2.a). There is one more significant difference between these two studies. In the

first study the correlation was established for the single actuations, while in the second study the correlation can be established only between the mean values for the NGI assay-runs.

According to the method of the VariDose data analysis (section 3.3.2b) two parameters can characterise the FPD in the cloud: the “peak value” and the “dose value”. The dose value is the integral of the fitted curve between two points, and therefore, it depends on the choice of these points. Here we consider two dose values DV_{FWHM} and $DV_{1\%}$, where the first is the sum of the data that are larger than the half maximum, and the second is the integral of the fitted curve between the points of the interception of this curve and the line of 1% obscuration.

To compare the sets of data for fine particle doses, the correlation between the mean values for the individual runs is established. The correlation coefficients for the NGI data of FPD and the peak values is only 0.57 with $p=0.23$. In the case of DV_{FWHM} and FPD data, the correlation coefficient is 0.82 and $p=0.05$. Statistically significant correlation has been observed for the mean values of $DV_{1\%}$ and the NGI data for FPD with the correlation coefficient of 0.87 and the p -value of 0.02. This significant correlation can be used to calibrate the VariDose parameter of the fine particle dose $DV_{1\%}$ for the conventional mass units. It also indicates that the fine particles are distributed over the entire cloud and make the major contribution to the light obscuration. Therefore, to account for all fine particles in the released dose, the integral of the entire profile should be taken. This situation would probably be true for all combinations of a delivery device and the drug formulation when actuations are characterised with a very high Fine Particle Fraction.

Figure 4.15 shows a possible calibration of Varidose measurements for the given experimental set-up. The best fit for the experimental data (the solid line), calculated using the least squares method, is not crossing the origin. Note that mean values of Varidose data are also characterised with variance, which reflects the variation of the dose for a single actuation in each run of 5shots. The variation coefficient ranges from $\pm 4\%$ to $\pm 10\%$ for individual runs. Unfortunately, the NGI provides only average values for each run. A single shot variation for the NGI data is adopted from the variation across the blisters of the same load. According to the calibration, the dose variation is within the dose range measured by NGI (dotted lines). This fact

confirms that VariDose measurements may reliably characterise the fine particle dose for a single actuation, although the calibration precision would benefit from more experimental data.

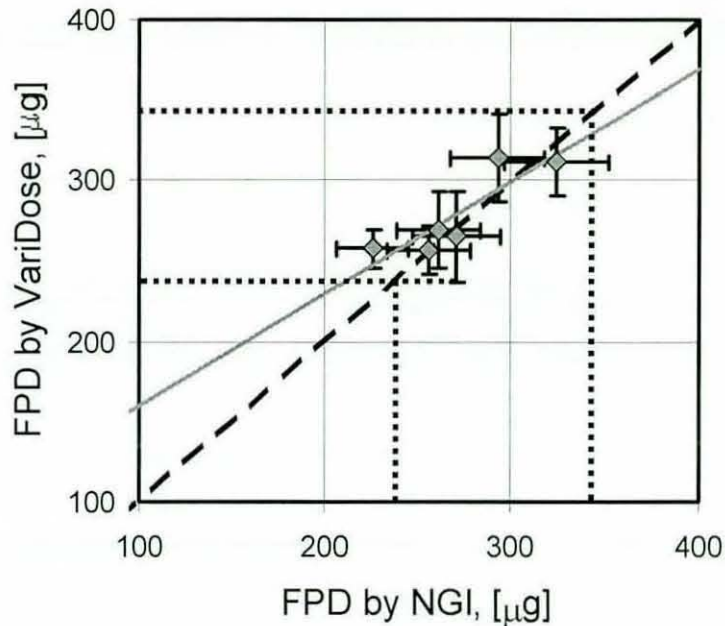


Figure 4.15. Data correlation of fine particle doses measured by NGI and VariDose.

4.3.3. Conclusions.

This experiment shows that the VariDose technology has been successfully applied to one more combination of the delivery device and the drug formulation. In this case delivered doses are characterised with a low variation coefficient and a high fine particle fraction. The one VariDose parameter that is related to the fine particle dose by the model shows a good correlation (the correlation coefficient 0.87 and $p=0.02$) with the fine particle dose measured by a next generation pharmaceutical impactor (NGI). It also demonstrates good agreement between the model predictions and the observed values of light obscuration.

4.4. Summary

The laboratory prototype VariDose system has enabled the investigation of the validity of several key assumptions and theoretical results used to obtain a model for the light obscuration by airborne particles in the pulmonary drug delivery. The temporal length of the obscuration profile gives a good estimation for the cloud volume. The obscuration maximum indicates a possible maximum of the particle concentration in the fine particle distribution. Several pulmonary delivery systems have been studied and practical assessments of the fine particle dose have been achieved.

Simultaneous measurements of the drug delivery by the VariDose technology and conventional *in vitro* methods allow the evaluation of the performance of this quick, robust and *in situ* method. The practical experiments show that VariDose has been successfully applied for a statistical assessment of the Turbohaler® performance. Useful results have been achieved even without a calibration of the VariDose optical units into the mass units. The VariDose system can be “trained” to measure the mass of the delivered fine particles through the calibration against an inertial impaction system. The training process has been tested on two benchmark systems: a well studied Turbohaler® with a “drug only” formulation, and an advanced prototype device with a carrier-based formulation. These studies indicate a wide potential for the VariDose usage in the pharmaceutical industry and in the clinical management of pulmonary drug delivery.

The Varidose technology is a useful tool for a quick assessment of the quality of pulmonary delivery in-line with a user, although it cannot entirely substitute for an inertial impaction system. The wide area of unique and complementary applications for Varidose is related to the specifics of its operation:

- VariDose is much quicker (1 minute instead of hours) than any inertial impaction system due to its capability of in-line direct measurement during a real actuation.
- VariDose assesses the fine particle dose of a single actuation and can be calibrated to the mass unit for a given drug formulation.

- VariDose can operate in-line with a patient, as well as with a virtual patient (a breath simulating machine) or an impactor.

VariDose can characterise many physical properties of the aerosol cloud, which currently are not considered in relation to pulmonary delivery, such as the cloud homogeneity, the volume of the cloud, and the spatial location of fine particles in the cloud. Some possible future experiments are discussed in Chapter 5.

Chapter 5

Conclusions and Discussion

The primary aim of this thesis has been to investigate the possibility of assessing the pulmonary drug delivery in-line with a patient. For this purpose an optical method based on the interaction of light with particles has been designed and tested in benchmark applications. A theoretical model has been developed and justified for the operational principles of the method. It has been shown that this technology is successful in measuring the fine particle dose of an aerosol released by an inhaler. It is further suggested that this method not only facilitates the dose assessment in-line with a patient, but also improves the characterisation of aerosols to levels that have hitherto been impossible.

5.1. Conclusions

Pulmonary drug delivery is a fast-growing branch in the healing and symptom-managing therapies. The main attraction of inhaling drugs is a rapid onset of action and more efficient and targeted treatment of lung disorders, i.e. smaller doses are required in comparison to the oral delivery causing fewer systemic side effects. The pulmonary delivery is a non-invasive alternative to injection and, therefore, is a very attractive route for delivering innovative, protein-based drugs. The pulmonary route offers the highest bioavailability of any non-invasive route and facilitates more rapid drug absorption in the bloodstream compared with subcutaneous injection. Inhalation drug systems are a particularly attractive treatment option for diseases such as diabetes and multiple sclerosis and for pain, seizures, cardiovascular events, anaphylaxis and other conditions requiring frequent injections for a rapid symptom relief.

For the realisation of the benefits of pulmonary drug delivery there are three main requirements:

1. The drug has to be formulated to efficiently reach the alveoli of the deep lung, where it can be rapidly absorbed into the bloodstream.
2. The delivery device has to facilitate the entrainment and dispersion of the drug formulation into an aerosol with particle sizes in the range of 0.5 μm to 5 μm .
3. The patient has to be compliant with procedure and produce a sufficient inhalation effort.

Due to this complexity of the pulmonary drug delivery the actual delivered dose is unknown. Complex *in-vitro* and *in-vivo* tests and clinical trials are needed to ensure a consistent performance of the drug formulation and the delivery device, although patient compliance and the ambient conditions, such as humidity and temperature, can significantly reduce the consistency of the delivered dose. There is an undisputed need for a rapid technology to measure the delivered dose on an actuation-by-actuation basis and in-line with a patient.

This thesis has developed and principally evaluated one of emerging technologies for an in-line, real-time assessment of the efficiency of pulmonary drug delivery.

The development aim was to bring the advantages of optical sensors, such as their non-invasive nature and ease of use, to the problem of a rapid and in-line assessment of the pulmonary drug delivery. The developed technology, the VariDose, exploits the phenomenon of light scattering by small particles. The unique relationship between the scattering cross-section and the particle size allows the finding of experimental conditions in which the fine particles of the pulmonary delivery cause the majority of the light obscuration in comparison to the other aerosol components.

The theoretical model calculates for the first time the optical density of a small cloud sample using the Lambert-Beer law and the Mie theory. The size of the sample is defined by the geometry of the sensor: the diameter of the light beam, the length of the light path in the cloud, the frequency of the measurement and the velocity of the cloud propagation. It has been shown that the temporal profile of the light obscuration, measured perpendicular to the direction of the cloud propagation, is indicative of the particle distribution in the cloud. In any given case, taking into account additionally available information, such as a nominated mass of the drug formulation and the cloud length (measured by VariDose), it is possible to find a single-number indicator for the fine particle dose.

To utilise the VariDose technology a novel prototype device has been built and a number of evaluating experiments have been performed. The experimental results show a strong correlation between the VariDose measurements and the conventional *in-vitro* data. The simultaneous measurements on a Bricanyl® Turbohaler® by VariDose and a Twin Cascade Impinger (TSI) have resulted in the correlation coefficient of 0.94 and $p < 0.0001$ for the assessments of the fine particle doses.

It is also has been shown that the VariDose system can operate as a stand-alone technology for a statistical assessment of the inhaler performance, as an example, the test performed on the Bricanyl® Turbohaler® was compared with published data. The coefficient of variation was 23.9% for the VariDose assessment of the delivered doses. This is in good agreement with the 25% reported by Meakin (Meakin *et al.*, 1995) for the coefficient of variation of the fine particle doses. The Kolmogorov-Smirnov test, KS-test (Kanji, 1999), has established with a high degree of certainty that the data of these two datasets (VariDose and Meakin's study) are similarly distributed.

This research has proved that a relatively simple optical sensor is able to provide a scaled indicator for how well the drug formulation is dispersed during pulmonary delivery and therefore may rapidly measure the delivered dose in-line with a patient. This technology can also be used for rapid assessment of iterative steps in innovating drug formulations and delivery devices. The main advantages are single actuation and real-time measurements. VariDose requires only a few seconds (up to one minute, taking into account the inhaler preparation time) to assess a single dose actuation, instead of the two hours required for a measurement by a cascade impactor. Additionally, the proposed technology offers a novel area of research, investigating how the aerosol cloud is changing along the propagation path.

5.2. Suggestions for future research.

The main purpose of the current investigation was to prove the principle of the VariDose technology, that a simple optical sensor can offer a rapid and an informative assessment of the efficiency of the pulmonary delivery. The future research could contribute to the following areas: 1) the device modernisation to improve its robustness; 2) the optimisation of measurement parameters such as the light wavelength, the light intensity and the rate of the data acquisition; and 3) case studies to develop routines for typical applications of the technology. Further interesting developments may arise through exploring the use of light sources of various wavelengths and multiple sensors.

5.2.1. Technology modernisation.

The white light source, fibre optic patches and miniature spectrometer of the current set-up are insufficiently robust for more general use. To improve the robustness of the method, the future VariDose device could be designed and built using light emitting diodes (LEDs) and semiconductor detectors. The use of LEDs allows a high rate of data acquisition, the acquisition rate can easily be 10kHz, this means that the moving cloud can be sampled every 100 μ sec. For the current design this rate would provide a sampling of 300 μ m along the cloud length at the flow rate of 60L/min. This high rate offers not only a high spatial resolution of the cloud, but also a high dynamic resolution for the multi-sensor applications.

The main challenge of using LEDs relates to the problem of creating a uniformly illuminating collimated beam of a small diameter and a relatively high intensity. Based on the current design, the requirements for the light beam can be summarised as follows. The total power of the illuminating light is $30\mu\text{W}$, the beam diameter is 1.8mm and the beam divergence angle (2Θ) is 3.5 degrees. Special care needs to be taken to ensure the homogeneous distribution of the light intensity over the cross section of the beam.

The wide range of available LEDs would allow the optimisation of the parameters of the illuminating beam, such as light power and wavelength. These also permit the exploration of the benefits of multi-wavelengths and multi-sensor measurements.

5.2.2. Technology applications.

The VariDose technology has been developed and intended for the assessment of the efficiency of the pulmonary delivery. There are many different applications in pharmacopoeias, where VariDose can provide significant benefits. The further investigation could evaluate these benefits for different applications through performing case studies.

The most straightforward studies relate to simultaneous measurements with the conventional pharmacopoeia methods such as inertial cascade impactors. Figure 5.1 shows, as an example, an experimental set-up for the simultaneous measurements using an Andersen impactor and two VariDose sensors. The VariDose sensor can be placed either (or both) between the inhaler's mouthpiece and the universal induction port (Figure 5.1, position A) and between the USP and the impactor entrance (Figure 5.1, position B). The main purpose of these studies would be to show that the VariDose data are strongly correlated with the impactor measurements for the entire variety of cases. The studies need also to prove that the VariDose sensor does not affect the impactor performance. As soon as this relation is established, VariDose can be used as a stand-alone technology and can lead to an effective and efficient design cycling, manufacturing and testing of the drug formulation and the delivery devices.

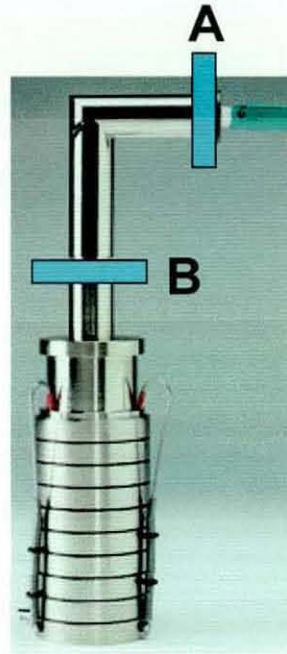


Figure 5.1. Experimental set-up for a simultaneous assessment of the inhaler performance by VariDose and Andersen impactor.

The other area of the study can exploit the VariDose's ability to operate in-line with a patient. Here, a breath-simulating machine can act as a robotic patient and VariDose would assess the performance of the drug delivery. The study can be designed to reproduce a clinical trial, which, for example, has been published. A statistical analysis would test that the outcomes of the clinical trial and the robotic trial are similar.

By varying the breathing parameters, a possible influence of the patient's inhalation effort on the outcome of the clinical trial can also be studied. The aim of these studies would be to show that the VariDose technology could serve as a rapid, inexpensive, pre-clinical test for the pulmonary delivery system. To prove the validity of this robotic trial would be of enormous benefit for the paediatric applications, where patients can breathe only spontaneously and cannot be trained for a special inhalation pattern.

5.2.3. Technology exploration.

The natural exploration of the VariDose technology is based on the use of multi-sensors. Multi-sensors along the path of the aerosol propagation would non-invasively assess a real-time cloud evolution. Currently, the aerosol evolution can be assessed using ultra fast imaging (Oxford Lasers, 2004), as we have discussed in section 1.4.2.a. This type of imaging can only be performed on an open aerosol, i.e. an aerosol, which propagates in an open space and not through a conduit. Therefore, ultra fast imaging of the aerosol evolution does not include two major factors that affect this evolution: the conduit's walls and the inhalation flow. On the contrary, the VariDose technology may allow the influence of the flow rate and the conduit diameter on the aerosol evolution to be studied.

Eventually, it would be possible to build a replica of the conducting zone of the human respiratory tract with strategically placed sensors. The replica may include only the oropharynx, larynx, trachea and segmental bronchus. The multi-sensors would allow the evolution of the cloud during the propagation towards the lung's respiratory zone to be investigated.

The other area of further research is more challenging and relates to the spectral behaviour of the light obscuration. It is well known, that for a single spherical particle the light extinction depends on the particle size and the light wavelength. For an aerosol cloud, an ensemble of particulates causes the light obscuration. The level of the obscured intensity depends on the amount of airborne matter and the particle size distribution in the cloud. The theoretical model, developed in this thesis, allows for the calculation of the light transmittance through a well-defined cloud, i.e. the particle amount and the particle distribution are known. There is a strong indication that if the majority of particles are in the range of $0.2\mu\text{m}$ to $0.8\mu\text{m}$ the blue light (450nm) is scattered more than the red light (650nm) and infra-red (800nm) (please refer to the section 2.4.1). The challenge is to find an experimental set-up for multi-wavelength (multi-colour) measurements, which would permit measuring the colour change between the transmitted light and the illuminating light. The aim is to distinguish between three classes of particle ranges, which are important for the pulmonary delivery: 1) the fine particles define the dose delivered to the deep lung,

the size ranges from 0.5 μm to 5 μm ; 2) the coarse particles contribute mainly to oropharyngeal absorption, the size ranges from 100 μm to 5 μm ; 3) the extra fine particles are normally exhaled and do not contribute to the delivered dose, the size range is smaller than 0.5 μm .

Multi-colour measurements on the same sample of the cloud may show which colour is scattered more than other colours, and therefore, it might indicate the size range of particles in the cloud sample. Introducing a colour parameter and measuring its temporal variation for the moving cloud might indicate, for example, the location of the fine particles in the cloud. It might be possible to remove, at least partly, the ambiguity of the light obscuration, i.e. it may be possible to distinguish between two situations, when the same obscuration is caused by the smaller amount of the fine particles or by the larger amount of the coarse particles.

References

- Adji, A.L., Gupta, P.K., 1997. Inhalation delivery of therapeutics peptides and proteins, New York.
- Asking, L., Nichols, S., 2003. Next generation pharmaceutical impactor (NGI)-EPAG collaborative study. Drug Delivery to the Lungs XIV, December 2003, London, The Aerosol Society, 33-36.
- Allen, T., 1997. Particle size measurement, Vol.1: Powder sampling and particle size measurement, London, Chapman & Hall, pp.439-442.
- Barnes, P.J., Pedersen, S., 1993. Efficacy and safety of inhaled steroids in asthma, *Am. Rev. Respir. Dis.* 148, S1-S26.
- Barnett, D.M., 2000. On multiple optical scattering in a scanning nephelometer, PhD Thesis, Loughborough University, UK.
- Bisgaard, H., Klug, B., Sumbly, B.S., Burnell, P.K.P., 1998. Fine particle mass from the diskus inhaler and turbuhaler inhaler in children with asthma, *Eur. Respir. J.* 11, 1111-1115.
- de Boer, A.H., Bolhuis, G.K., Gjaltema, D., Hagedoorn, P., 1997. Inhalation characteristics and their effects on in vitro drug delivery from dry powder inhalers. Part 3: The effect of flow increase rate on the in vitro drug release from the Pulmicort 200 Turbuhaler, *Int. J. Pharm.* 153(1), 67-77.
- de Boer, A.H., Gjaltema, D., Hagedoorn, P., Frijlink, H.W., 2002. Characterization of inhalation aerosols: a critical evaluation of cascade impactor analysis and laser diffraction technique, *Int. J. Pharm.* 249, 219-231.
- Bohren, C.F., Huffman, D.R., 1983. Absorption and scattering of light by small particles, John Wiley & Sons Inc.
- British Pharmacopoeia, 1993. Appendix XVII C.
- British Thoracic Society, 2003. British Thoracic Society guidelines on asthma management, *Thorax* 58 (Suppl. I).

- Burnell, P.K.P., Petchey, L., Prime, D., Sumbly, B.S., 1996. Patient inhalation profiles and dose emission characteristics from dry powder inhalers, *Respiratory Drug Delivery V*, 314-316.
- Burnell, P.K.P., Malton, A., Reavill, K., Ball, M.H.E., 1998. Design, validation and initial testing of the electronic lung device, *J. Aerosol Sci.* 29(8), 1011-1025.
- Chandrasekhar, S., 1960. Radiative transfer, Dover Publications, New York.
- Chavan, V., Dalby, R., 2000. Effect of rise in simulated inspiratory flow rate and carrier particle size on powder emptying from dry powder inhalers. *AAPS Pharmsci.* 2(2), article 10 (also at <http://www.pharmsci.org/>).
- Chavan, V., Dalby, R., 2002. Novel system to investigate the effects of inhaled volume and rates of rise in simulated inspiratory air flow on fine particle output from a dry powder inhaler. *AAPS Pharmsci.* 4(2), article 6 (also at <http://www.aapspharmsci.org>).
- Cheong, W.-F., Prahl, S.A., Welch, A.J., 1990. A review of the optical properties of biological tissues, *IEEE J. Quant. Elect.* 26(12), 2166-2185.
- Clark, A.R., Bailey, R., 1996. Inspiratory flow profiles in disease and their effects on the delivery characteristics of dry powder inhalers, *Respiratory Drug Delivery V*, 221-230.
- Crompton, G.K., 1982. Problems patients have using pressurised aerosol inhalers. *Eur. J. Respir. Dis.* 63 (Suppl. 119), 101-104.
- Dalby, R., Suman, J., 2003. Inhalation therapy: technological milestones in asthma treatment, *Advanced Drug Delivery Reviews* 55, 779-791.
- Dershwitz, M., Walsh, J.L., Morishige, R.J., Connors, P.M., Rubsamen, R.M., Shafer, S.L., Rosow, C.E., 2000. Pharmacokinetics and pharmacodynamics of inhaled versus intravenous morphine in healthy volunteers, *Anesthesiology* 93 (3), 619-628.
- Dunbar, C., Kataya, A., Tiangbe, T., 2005. Reducing bounce effects in the Andersen cascade impactor, *International Journal of Pharmaceutics* 301(1-2), 25-32.

- Dzubay, T.G., Hines, L.E., Stevens, R.K., 1976. Particle bounce errors in cascade impactors, *Atmospheric Environment* 10(3), 229-234.
- Everard, M.L., Devadason, S.G., Le Souef, P.N., 1997. Flow rate in the inspiratory manoeuvre affects the aerosol particle size distribution from a Turbuhaler, *Respir. Med.* 91, 624-628.
- Feddah, M.R., Brown, K.F., Gipp, E.M., Davies, N.M., 2000. In-vitro characterization of metered dose inhaler versus dry powder inhaler glucocorticoid products: influence of inspiratory flow rates, *J. Pharm. Pharmaceut. Sci.* 3(3), 317-324.
- Fleming, J.S., Conway, J.H., Holgate, S.T., Bailey, A.D., Martonen, T.B., 2000. Comparison of methods for deriving aerosol deposition by airway generation from three-dimensional radionuclide imaging, *J. Aerosol Sci.* 31(10), 1251-1259.
- Fleming, J.S., Conway, J.H., 2001. Three-dimensional imaging of aerosol deposition, *J. Aerosol Med.* 14(2), 147-153.
- Ganderton, D., 1997. General factors influencing drug delivery to the lung. *Respir. Med.* 91 (Suppl. A), 13-16.
- Geddes, D.M., 1992. Inhaled corticosteroids: benefits and risks, *Thorax* 47, 404-407.
- Hickey, A.J., 1990. Factors influencing aerosol deposition in inertial impactors and their effect on particle size characterization. *Pharm. Tech.* 14, 118-130.
- Hickey, J., Concessio, N., Platz, R., 1994. Factors influencing the dispersion of dry powders as aerosols. *Pharm. Tech.* 18, 58-64.
- Hilton, S., 1990. An audit of inhaler techniques among asthma patients of 34 general practitioners. *Br. J. Gen. Pract.* 40, 506-507.
- Hindle, M., Byron, P.R., 1995. Dose emissions from marketed dry powder inhalers. *Int. J. Pharm.* 116, 169-177.

-
- Holmes, C.E., Kippax, P.G., Newell, H.E., Southall, J.P., Ward, D.J., 2001. Simultaneous analysis of respirable aerosols via laser diffraction and cascade impaction, *Drug Delivery to the Lungs XII*, London, The Aerosol Society, 58-61.
- Hughes, J.M.B., 1999. *Lung Function Tests: physiological principles and clinical applications*. Saunders WBCO.
- van de Hulst, H.C., 1980. *Multiple Light scattering*, Academic, New York.
- van de Hulst, H.C., 1981. *Light Scattering by Small Particles*, Dover Publications, Inc., New York.
- Ishimaru, A., 1978. *Wave Propagation and Scattering in Random Media*, Academic press, Inc., New York.
- Kamin, W.E.S., Genz, T., Roeder, S., Scheuch, G., Trammer, T., Juenemann, R., Cloes, R.M., 2002. Mass output and particle size distribution of glucocorticosteroids emitted from different inhalation devices depending on various inspiratory parameters, *J. Aerosol Med.* 15(1), 65-73.
- Koglin, B., 1973. Methods for the determination of the degree of agglomeration in suspensions. *Proceed. 1st international conference on particle technology*, Chicago, 272-278.
- Koglin, B., 1977. Assessment of the degree of agglomeration in suspensions. *Powder Tchnology* 17, 219-227.
- Lipworth, B.J., 1992. Risks versus benefits of inhaled b_2 -agonists in the management of asthma, *Drug Safety* 7, 54-70.
- Meakin, B.J., Caine, J.M., Woodcock, P.M., 1995. Drug delivery characteristics of bricanyl turbohaler dry powder inhaler, *Int. J. Pharm.* 119, 91-102.
- Miller, R.G., 1997. *Beyond ANOVA: Basic of Applied Statistics*. Boca Raton, FL: Chapman & Hall.

-
- Muller, R.H., Schuhmann, R., 1996. Teilchengrossenmessung in der Laborpraxis. Wissenschaftliche Verlagsgesellschaft mbH, Stuttgart, Germany, 65-70.
- Newman, S.P., Johnson, M.A., Clarke, S.W., 1988. Effect of particle size of bronchodilator aerosols on lung distribution and pulmonary function in patients with chronic asthma. *Thorax* 43(2), 159.
- Niven, R., 1995. Delivery of biotherapeutics by inhalation aerosol, *Crit. Rev. Ther. Drug Carrier Syst.* 12, 151-231.
- Niven, R.W., 1996. Atomization and nebulisers, in: Hickey, A.J. (Ed.), *Inhalation Aerosols*, Vol. 94, Marcel Dekker, New York, 273-312.
- Olsson, B., Aiache, J.M., Bull, H., Ganderton, D., Haywood, P., Meakin, B.J., Schorn, P.J., Wright, P., 1996. The use of inertial impactors to measure the fine particle dose generated by inhalers. *PharmEuropa* 8, 291-298.
- Oxford Lasers, 2004. Applications brief, Drug delivery device characterization, <http://www.oxfordlasers.com/imaging/pdfs/appdrugs.pdf>.
- Pauwels, R., Newman, S., Borgstrom, L., 1997. Airway deposition and airway effects of antiasthma drugs delivered from metered-dose inhalers. *Eur. Respir. J.* 10, 2127-2138.
- Pedersen, S., 1995. Aerosols and other devices. In: Silverman, M., editor. *Childhood asthma and other wheezing disorders*. London, Chapman and Hall, 315-334.
- Prime, D., Atkins, P.J., Slater, A., Sumbly, B., 1997. Review of dry powder inhalers. *Advanced Drug Delivery Reviews* 26, 51-58.
- Puckhaber, M., Rothele, S., 1999. Laser diffraction: Millennium-link for particle size analysis. *Powder Handling & Processing* 11, 91-95.
- Rader, D.J., Marple, V.A., 1985. Effect of ultra-stokesian drag and particle interception on impaction characteristics. *Aerosol Sci. Tech.* 4, 141-156.
- Rudinger G., 1980. Fundamentals of gas-particle flow. *Handbook of powder technology*. Edited by J.C. Williams and T. Allen, Vol.2, 19-23.

-
- Sanderson, M.J., Sleight, M.A., 1981. Ciliary activity of cultured rabbit tracheal epithelium: beat pattern and metachrony, *J. Cell Sci.* 47, 331.
- Serra-Batlles, J., Plaza, V., Badiola, C., Morejon, E., 2002. Patient perception and acceptability of multidose dry powder inhalers: a randomized crossover of diskus/accuhaler with turbuhaler, *J. Aerosol Med.* 15(1), 59-64.
- Sherwood, L., 2001. *Human physiology: from cells to systems*. Fourth Edition, Brooks/Cole, USA, 437-461.
- Sigrist Process-Photometer, 1996. *ABC of Process Photometry: Potable water treatment*.
- Sigrist Process-Photometer, 1996. *ABC of Process Photometry: Power plants, thermal*.
- Sigrist Process-Photometer, 1996. *ABC of Process Photometry: Brewery*.
- Sigrist Process-Photometer, 1996. *ABC of Process Photometry: Spring water*.
- Sigrist Process-Photometer, 1996. *ABC of Process Photometry: Sand filtration*.
- Skoog, D.A., West, D.M., Holler, F.J., 1997. *Fundamentals of analytical chemistry*, 7th Edition, Harcourt College Publishers, 510-520.
- Turner, J.R., Hering, S.V., 1987. Greased and oiled substrates as bounce-free impaction surfaces, *Journal of Aerosol Science* 18(2), 215-224.
- United States Pharmacopeia, 2000. *Physical tests and determinations*, Chapter 601: Aerosols, Metered dose inhalers and dry powder inhalers, 24th edition, Supplement 1.
- Vidgren, M., 1994. Factors influencing lung deposition of inhaled aerosols, *Eur. Respir. Rev.* 4, 68-70.
- Warren, S., Taylor, G., Smith, J., Buck, H., Parry-Billings, M., 2002. Gamma scintigraphic evaluation of a novel budesonide dry powder inhaler using a validated radiolabeling technique, *J. Aerosol Med.* 15(1), 15-25.

Weibel, E.R., 1963. *Morphometry of the Human Lung*, Springer Verlag, Berlin.

Yu, J., Chien, Y.W., 1997. Pulmonary drug delivery: physiologic and mechanistic aspects, *Crit. Rev. Ther. Drug Carrier Syst.* 14(4), 395-453.

Appendix

Notation and Glossary

General abbreviations

p-MDI	pressurised metered dose inhaler
DPI	dry powder inhaler
F	flow rate
ΔP	pressure gradient
R	resistance to the flow

Lung Volume Definitions

TV	Tidal volume
IRV	Inspiratory reserve volume
ERV	Expiratory reserve volume
RV	Residual volume
FRC	Functional residual capacity
IC	Inspiratory capacity
VC	Vital capacity
TLC	Total lung capacity
FEV ₁	Forced expiratory volume in one second

In vitro assessment

MMAD	mass median aerodynamic diameter
GSD	geometric standard deviation
FPD	fine particle dose
FPF	fine particle fraction
ED	emitted dose
MD	metered dose
VD	varidose system

Inertial impaction systems

TSI	twin stage impinger
NGI	next generation pharmaceutical impactor

Particles

$d_{/a/g}$	particle diameter / aerodynamic/geometrical
r	particle radius
x	dimensionless particle size parameter
m	refractive index for the particle material
n_i	the number concentration for the i -type particles
ρ	material density of particles
v_{pi}	volume of a single i -type particle

Particle distribution

C_v, C_{vi}	volume concentration
f_i	fraction for the one type of particles in multi-species clouds
m_i	mass of the one type of particles
N_i	number of different types of particles
$N, N(z)$	particle number concentration
t	the time coordinate
z, z_0	spatial coordinate
z_d	coordinate of the sensor
ε_i, ϕ_i	characteristic parameters of Gaussian distribution for an individual type of particles
V_{cl}	cloud velocity

Model Notation

- a_n, b_n Mie coefficients
 ψ_n, χ_n, ζ_n Riccati-Bessel functions
 λ light wavelength
 L distance of the light propagation
 m_2 refractive index for the medium
 n integer from 1 to infinity
 n_c number for the Wiscombe criterion
 Q_{ext} extinction efficiency
 q_i extinction efficiency for one type of particles
 γ extinction coefficient
 I, I_0 radiation intensity
 T light transmittance
 Obs light obscuration

VariDose System

- d diameter of the collimated beam of light
 L diameter of the glass tube
 τ measurement period, detector's integration time
 V_{sample} volume of the measurement sample

Mathematical fitting procedure

- $y = y_1 + y_2$ fitting curve
 $A, a, \varepsilon, \xi, \alpha, R, b$ fitting parameters

Cloud characterisation

- H homogeneity
 Λ wall residue
 FWHM full width at the half maximum

